INTERSYMBOL INTERFERENCE AND ERROR PROBABILITY

FOR BANDLIMITED QPSK TRANSMISSION SYSTEMS

A Dissertation

Presented to

the Faculty of the Department of Electrical Engineering

University of Houston

In Partial Fulfillment

of the Requirements for the Degree

Doctor of Philosophy in Electrical Engineering

---

by

Bartus H. Batson

August 1972

ACKNOWLEDGEMENTS

I wish to acknowledge the encouragement, guidance, and counsel received from Dr. R. S. Simpson, chairman of my doctoral advisory committee. In addition, I feel a special debt to Drs. K. Tu and I. Korn, with whom I have had many stimulating discussions and who have made many valuable comments and criticisms.

Of considerable value was a thoughtful and detailed critical review of the entire manuscript by Dr. R. Cline. I wish to thank him for the time and effort he spent in performing this review.

Thanks are also due to L. Zwahlen and R. Rosencranz for their programming efforts, which provided most ot the numerical results presented herein.

I would like to express my appreciation to Mrs. C. Kunert for typing and retyping the manuscript according to an extremely difficult schedule.

Finally, I wish to express my gratitude to the National Aeronautics and Space Administration for its sponsorship and support, which made it possible for me to work in this field.

INTERSYMBOL INTERFERENCE AND ERROR PROBABILITY FOR BANDLIMITED QPSK TRANSMISSION SYSTEMS

An Abstract of a Dissertation

Presented to

the Faculty of the Department of Electrical Engineering

University of Houston

In Partial Fulfillment

of the Requirements for the Degree

Doctor of Philosophy in Electrical Engineering

---

by

Bartus H. Batson

August 1972

ABSTRACT

The effects of IF filtering on the error rate performance of QPSK transmission systems utilizing integrate-and-dump detectors are studied. It is assumed that (1) the QPSK demodulator reference signals are noise-free, (2) timing for the integrate-and-dump detectors is perfect, and (3) the channel noise is additive, white, and Gaussian, with zero mean. Two different filter types are considered: the ideal rectangular filter and a practical single-pole filter.

It is found that the bit error probability for bandlimited QPSK systems is affected by (1) a reduction in amplitude of the bit under detection, (2) intersymbol interference from adjacent bits in the same channel, and (3) crosstalk from the data stream in the quadrature channel. Computations of error probability are made for each filter type, using a series approximation method which can provide any desired degree of accuracy. For the cases considered, it was sufficient to assume that the effects of intersymbol interference and crosstalk were limited to 5 bits on either side of the bit under detection.

It is observed that the ideal filter provides superior performance in the noise-limited (low signal-to-noise ratio) region of operation. However, better performance is generally provided by the single-pole filter in the region of high signal-to-noise ratio where intersymbol interference and crosstalk become significant.

TABLE OF CONTENTS

LIST OF ILLUSTRATIONS

FIGURE PAGE

LIST OF TABLES

CHAPTER I

INTRODUCTION

Considerable interest has developed over the past several years in communications systems which transfer information in discrete or digital form. The digits which are transmitted may constitute information directly or they may represent approximations (usually in coded form) of *samples* of a continuous (analog) information signal. In the latter case, the transmission system must be designed such that no more than some acceptable level of *quantization* noise is introduced by the process of representing each sample of the analog signal by one of a finite number of possible amplitude levels. In general, quantization noise can be reduced by quantizing more finely (increasing the number of possible amplitude levels), but this requires a greater number of digits to identify (code) each level. As will subsequently be pointed out, transmission of a greater number of digits per second decreases the capability to make error-free decisions regarding the identity of each digit. Hence the advantage of quantization decreases as more stringent requirements are imposed on the signal-to-quantization-noise ratio. Assuming that an acceptable tradeoff has been achieved between quantization noise and transmission rate, the problem is essentially how to combat the effects of channel noise, which may be introduced anywhere between the transmitter and the detector.

Fig. 1.1 illustrates in block diagram form the basic components of a digital communications system. In general, each digit which is transmitted can assume one of m possible values, and the resulting system is called an

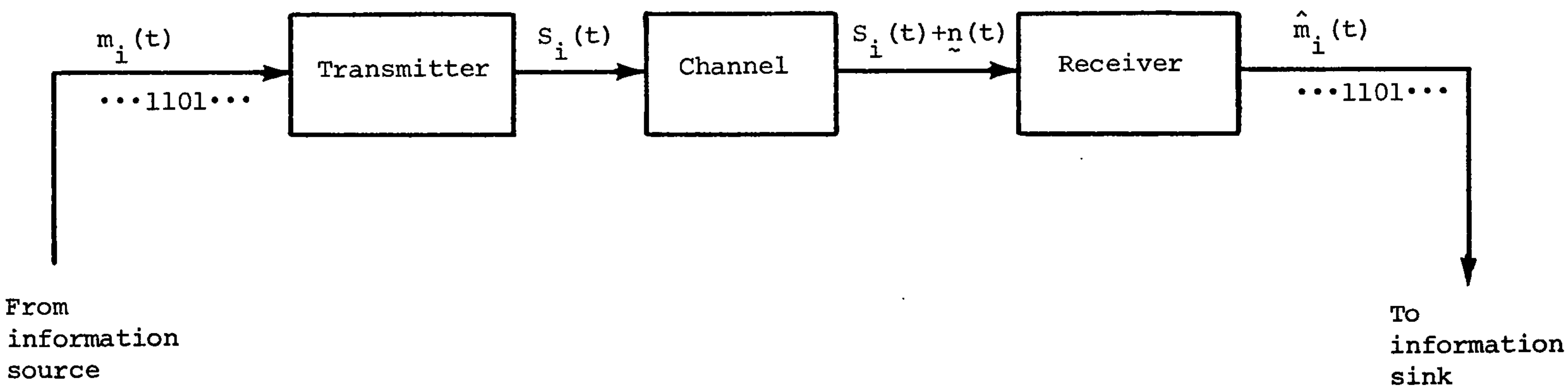

Fig. 1.1 - A binary communications system

m-ary system. Of special interest, and by far the most widely used, is the *binary* system, for which $m = 2$. This is the system illustrated in Fig. 1.1.

The *transmitter* has the task of assigning to each message digit $m_i(t)$ a waveform $S_i(t)$ which is suitable for transmission over the channel. For carrier systems, the transmitter thus must perform, in addition to other tasks such as power amplification, the process of *modulation*, in which each digit $m_i(t)$ is used to determine either the phase, frequency, or amplitude of $S_i(t)$.

The waveforms provided by the transmitter are passed through the *channel*, which can be a wire link or a radio link. It is during passage through the channel that the transmitted waveforms are invariably contaminated by noise. Most frequently this noise is assumed to be additive, white, and Gaussian; this is a particularly good assumption for certain classes of channels such as the space communications channel and a notably bad assumption for certain other channels such as many of the wire links in use today.

The task of the *receiver* is to consider each noisy waveform which it receives and to decide which message digit $m_i(t)$ most likely resulted in that particular received waveform. The receiver output is thus indicated in Fig. 1.1 as consisting of a sequence of estimated message digits $\hat{m}_i(t)$. The process of formulating the estimates $\hat{m}_i(t)$ is generally referred to as *bit detection*. For carrier systems, the operations performed by the receiver are sometimes identified separately as *carrier demodulation* and *bit detection*, where the latter is considered to be a baseband process.

In actuality, however, carrier demodulation can be visualized as being merely the first step of a multistep bit detection process.

Because of the presence of noise at the receiver input, the bit detector will occasionally make an erroneous decision. The *probability of error* associated with the estimated digits $\hat{m}_i(t)$ is a convenient and widely used criterion for evaluating the overall performance of any digital transmission system. For any given application, there will generally be a maximum allowable bit error probability. The optimum bit detector minimizes the signal-to-noise ratio required to provide operation at or below some designated error probability; alternately, the optimum detector minimizes the bit error probability for a given signal-to-noise ratio. For ideal binary communications over the additive, white, Gaussian noise channel, the optimum bit detector has been shown (see, for example, [1], [2], or [3]) to be a *correlation* detector or, equivalently, a *matched filter*. Fig. 1.2 illustrates these two embodiments of the optimum detector. It has also been shown [4] that the bit error probability which results when the optimum bit detector is used is given by

$$P_e = \frac{1}{2}\left[\frac{2}{\sqrt{\pi}}\int_{\sqrt{(1-\rho)E_b/2N_o}}^{\infty} e^{-\xi^2}\,d\xi\right]$$

$$= \frac{1}{2}\,\mathrm{erfc}\sqrt{\frac{(1-\rho)E_b}{2N_o}} \qquad (1\text{-}1)$$

where E_b is the average energy per signal bit

N_o is the single-sided noise spectral density

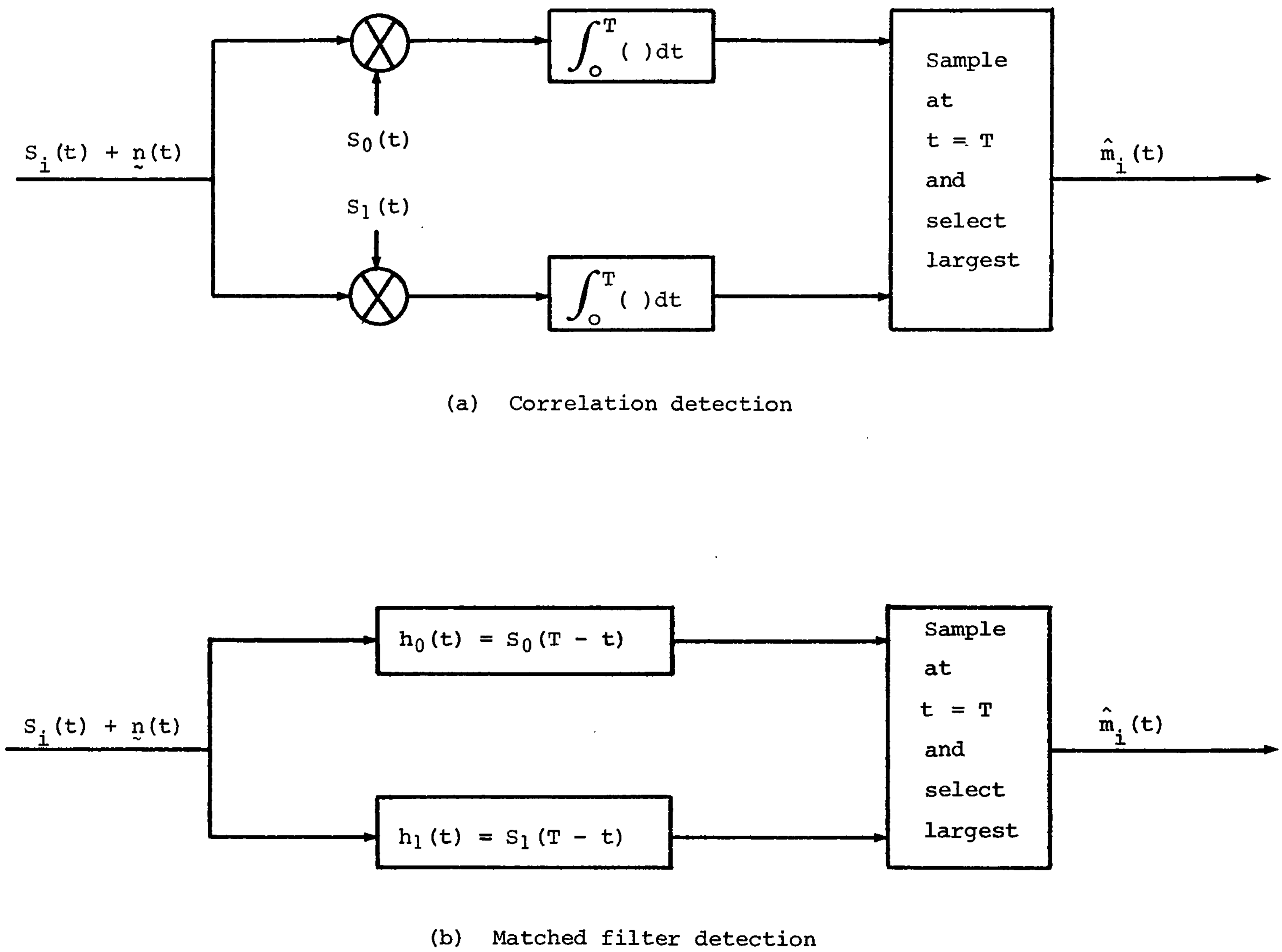

Fig. 1.2. - Optimum detection for binary transmission over the additive, white, Gaussian noise channel

and ρ is the correlation coefficient of the two waveforms $S_0(t)$ and $S_1(t)$

Note that so far there have been no restrictions placed on the waveforms $S_i(t)$. However, choice of a different set of waveforms does, in general, affect the correlation coefficient ρ and thus the error probability P_e. In addition to having an optimum bit detector for a given signaling set, it appears that there should also be an optimum signaling set. This is indeed the case, and the optimum set is that for which $\rho = -1$ and P_e is thereby minimized. The optimum waveforms for binary transmission over the additive, white, Gaussian noise channel are thus related by

$$S_0(t) = -S_1(t) \tag{1-2}$$

For baseband signaling, an optimum set of waveforms is the set of bipolar pulses shown in Fig. 1.3(a), while an optimum set of waveforms for carrier signaling is the set of phase-shift keyed (PSK) sinusoids shown in Fig. 1.3(b). When one of the optimum signaling sets is used, the structure of the correlation detector can be somewhat simplified. This is because the binary decision can now be based upon simply the *algebraic sign* of the received waveform. Fig. 1.4 illustrates these simplified correlation detection schemes. Note that the detection scheme for PSK requires a reference waveform accurate in both frequency and phase. This detection scheme is therefore sometimes referred to as a *coherent* detection scheme, and the multiplication process is sometimes called *coherent demodulation*.

By substituting (1-2) into (1-1), it is readily determined that the probability of error for the optimum binary signaling sets (using correlation detection) is given by

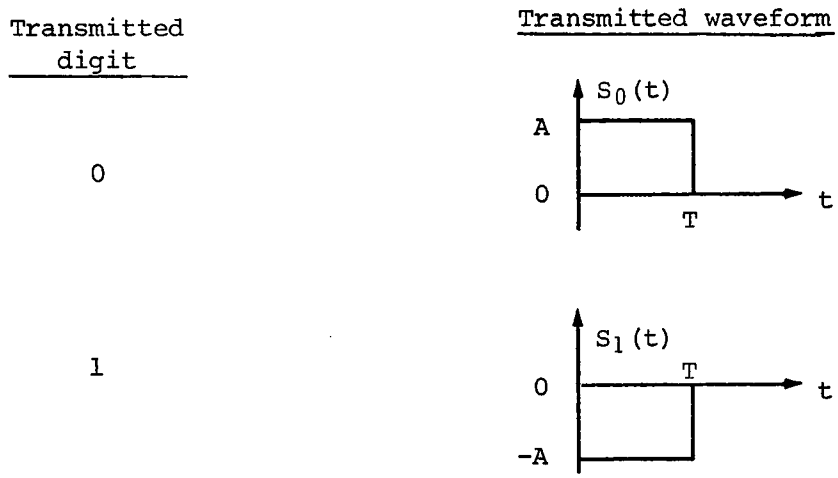

(a) Baseband signaling

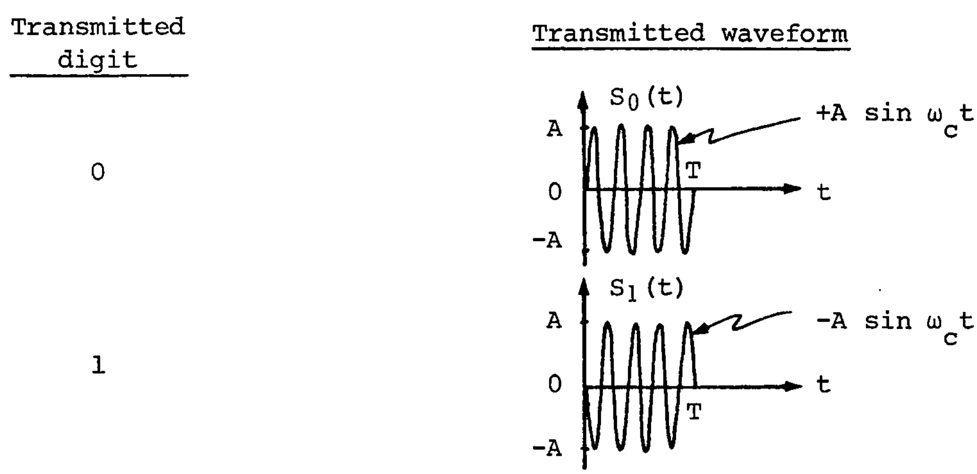

(b) Carrier signaling

Fig. 1.3. - Optimum waveforms for binary transmission over the additive, white, Gaussian noise channel

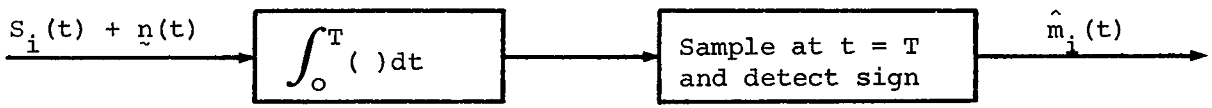

$$S_0(t) = \begin{cases} +A & \text{for } 0 \leq t \leq T \\ 0 & \text{otherwise} \end{cases}$$

$$S_1(t) = -S_0(t)$$

(a) Baseband signaling

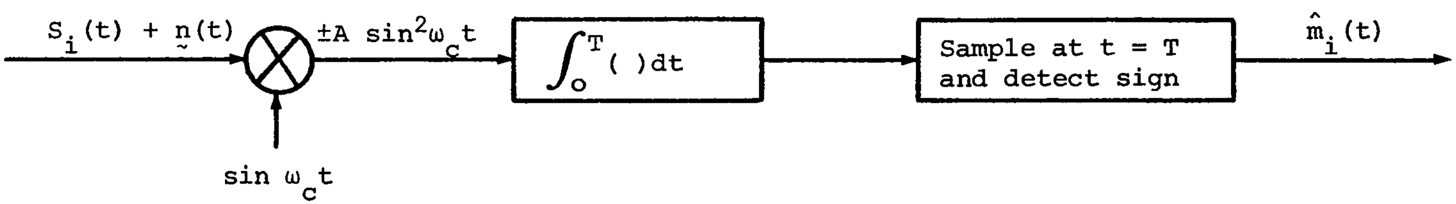

$$S_0(t) = \begin{cases} +A \sin \omega_c t & \text{for } 0 \leq t \leq T \\ 0 & \text{otherwise} \end{cases}$$

$$S_1(t) = -S_0(t)$$

(b) Carrier signaling (PSK)

Fig. 1.4. - Simplified correlation detection schemes for optimum binary signaling sets $\left(S_0(t) = -S_1(t)\right)$

$$P_e = \frac{1}{2} \operatorname{erfc} \sqrt{\frac{E_b}{N_o}} \tag{1-3}$$

The familiar plot of P_e vs. $\frac{E_b}{N_o}$, obtained using (1-3), is included for reference as Fig. 1.5. The ratio of signal energy per bit to single-sided noise spectral density, $\frac{E_b}{N_o}$, is sometimes referred to as *signal-to-noise ratio in the bit rate bandwidth* or, more simply, as *signal-to-noise ratio*. Justification for this terminology can be obtained by substituting the appropriate expression for E_b (this expression will always involve the bit transmission rate, $R = \frac{1}{T}$) and making a simple modification. Thus, for baseband signaling

$$\frac{E_b}{N_o} = \frac{A^2 T}{N_o} = \frac{A^2}{N_o\left(\frac{1}{T}\right)} = \frac{A^2}{N_o R} \tag{1-4}$$

and for PSK signaling,

$$\frac{E_b}{N_o} = \frac{A^2 T/2}{N_o} = \frac{A^2/2}{N_o\left(\frac{1}{T}\right)} = \frac{A^2/2}{N_o R} \tag{1-5}$$

For either class of signaling, it can be observed that $\frac{E_b}{N_o}$ is equivalent to signal power divided by the noise power in a (fictitious) bandwidth numerically equal to the bit rate R.

The digital transmission systems that have been described up to this point have been *idealized* systems, in the sense that performance (bit error probability) was assumed to be limited only by the noise encountered during transmission. In practice, however, signal distortion is frequently a significant factor in determining the overall performance of the system. Signal distortion can be introduced in a number of ways, including filtering, limiting, nonlinear amplification, and system phase

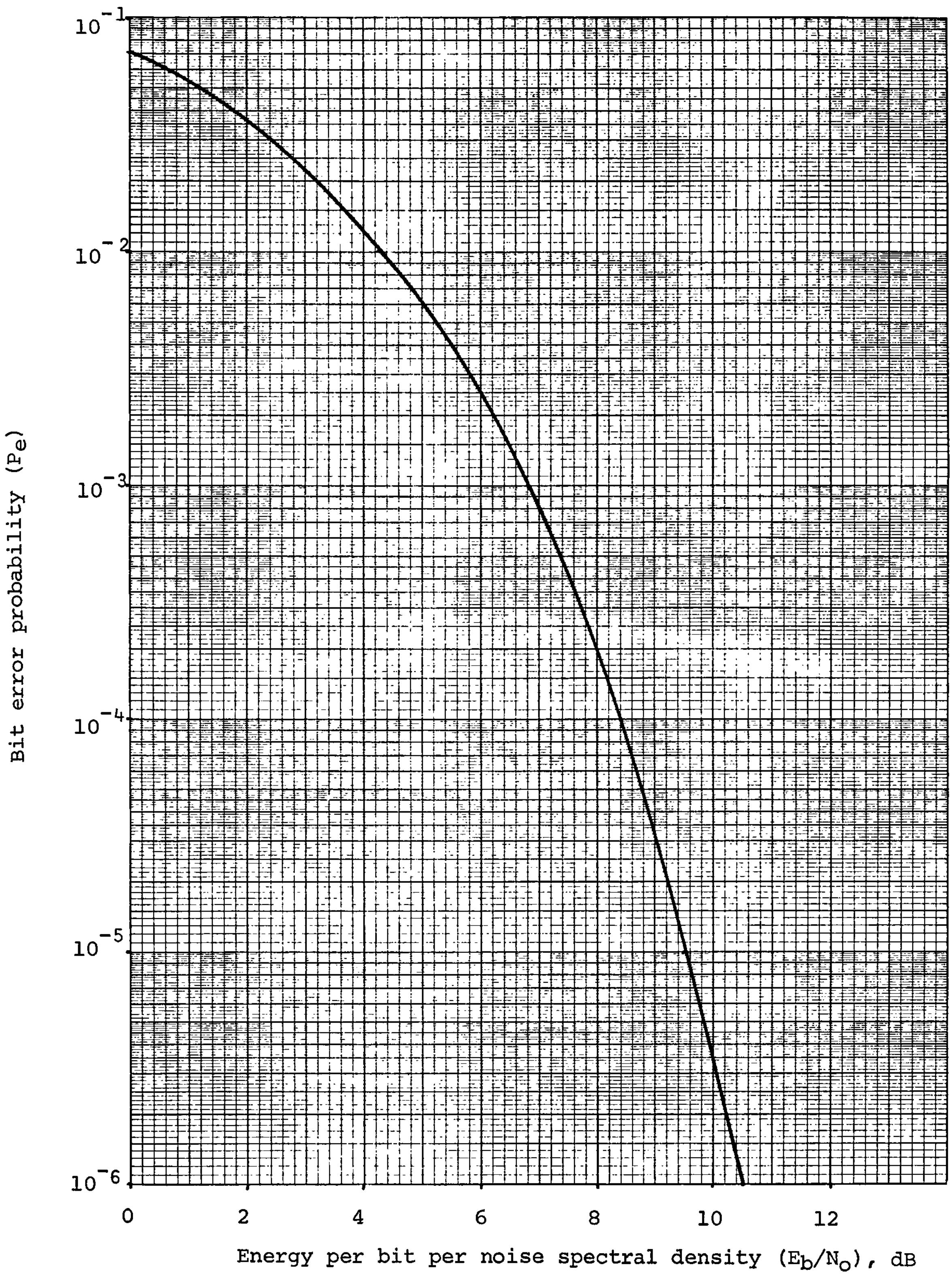

Fig. 1.5. - Probability of error for optimum binary signaling

instabilities. The effects of some of these sources of distortion can be made insignificant in many cases by careful system design. One major source of distortion, however, is inevitable in most systems. This is the result of restricted system bandwidth or of *filtering* in the transmitter, the channel, or the receiver. Bandwidth limiting will generally cause a reduction in energy per bit (E_b) and, more importantly, can cause a significant amount of *intersymbol interference* due to the smearing of waveforms in time.

The effects of filtering on digital signaling systems are discussed in more detail in Chapter II, and the results which have been obtained by previous researchers in their attempts to completely describe the effects of bandwidth limiting on bit error probability are summarized.

Ideal *quadriphase* signaling, which provides a 2:1 reduction in required channel bandwidth while transmitting information at the same rate (and at the same bit error probability) as PSK, is briefly described in Chapter III. Since quadriphase can theoretically double the information rate which can be transmitted over a fixed bandwidth channel, it is an important digital signaling technique. Unfortunately, the effects of signal distortion are even more severe in quadriphase systems than in PSK systems.

The central problem of this dissertation is, simply, *how is the bit error rate of a quadriphase transmission system affected by bandwidth limiting?* Chapter IV treats this problem in detail and shows that bandwidth limiting results in (1) a reduction in energy per bit, (2) intersymbol interference, and (3) *crosstalk* between the two quadrature channels associated with a quadriphase signal. Performance curves

$\left(P_e \text{ vs. } \frac{E_b}{N_o}\right)$ are obtained for quadriphase systems containing (1) an ideal rectangular bandpass filter and (2) a practical (single-pole) bandpass filter.

CHAPTER II

EFFECTS OF BANDLIMITING ON DIGITAL SIGNALING

As discussed in the previous chapter, optimum systems for transmission of binary information over the additive, white, Gaussian noise channel utilize either a set of bipolar pulses (for baseband transmission) or a set of PSK sinusoids (for carrier transmission). An optimum detector for baseband signaling consists of an integrate-and-dump circuit [Fig. 1.4(a)], and for carrier signaling consists of an integrate-and-dump circuit preceded by a product device [Fig. 1.4(b)]. The bandwidth of the transmission system has been assumed to be infinite.

For *finite* transmission bandwidth, the detectors shown in Fig. 1.4 are no longer optimum. This is because bandlimiting alters the shapes of the received waveforms, such that the inputs to the integrate-and-dump circuits are no longer rectangular pulses. The integrate-and-dump circuits are true matched filters (and are therefore optimum) for rectangular pulses, but are not true matched filters for bandlimited pulses. In practice, however, the relative simplicity of the integrate-and-dump circuit frequently dictates its use in the detection process for bandlimited signals. Considerable research has been performed to relate the system error probability (using the integrate-and-dump circuit) to the transmission bandwidth. As transmission bandwidth decreases, of course, the waveforms become more distorted, the integrate-and-dump circuit becomes less optimum, and the error probability increases.

There are actually two effects introduced by bandlimiting a binary signal, each of which tends to increase error probability. First, the energy per bit (E_b) seen by the integrate-and-dump circuit is decreased. Fig. 2.1, which shows the response of an ideal (rectangular) lowpass filter to a rectangular pulse, illustrates this reduction in E_b with decreasing bandwidth.

The second effect of bandlimiting, also evident from Fig. 2.1, is due to the "smearing" of each bit in time. That is, after bandlimiting, each bit occupies more than a single time slot. The result of this time-smearing of bits is that the energy per bit seen by the integrate-and-dump circuit is affected not only by the bit to be detected (the current bit), but also by adjacent bits. Fig. 2.2 provides an example of this *intersymbol interference* by applying superposition to determine the response of an ideal lowpass filter to a rectangular pulse train. It can be observed that the energy of the second bit (the shaded area between T and 2T) is greater than that of the fourth bit (the shaded area between 3T and 4T). The energy of any particular bit of a bandlimited pulse train is, in fact, determined by the state of that bit and by the states of some number of adjacent bits.

Depending on the pattern which exists around a certain bit, its energy may be greater than, less than, or equal to its energy prior to bandlimiting. It has been argued [5] that for a random pulse train (since the *average energy per bit* is the same as the energy of a single filtered bit without intersymbol interference), the *average error probability* for the filtered pulse train is the same as for a single filtered bit. However, as was pointed out in [6], this argument is in error because the relationship

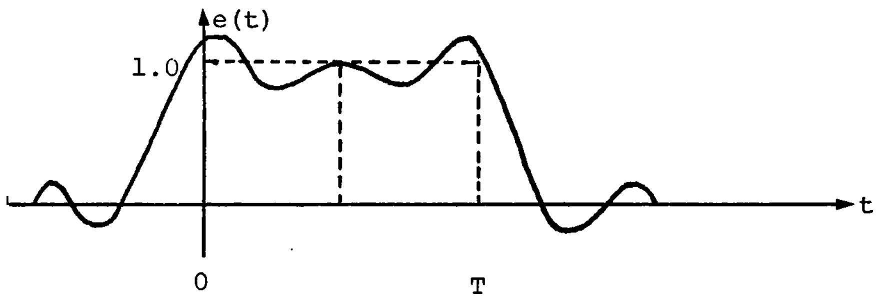

(a) Filter bandwidth > 1/T

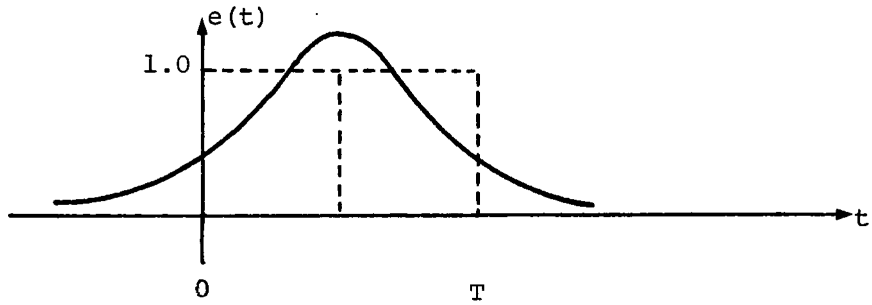

(b) Filter bandwidth = 1/T

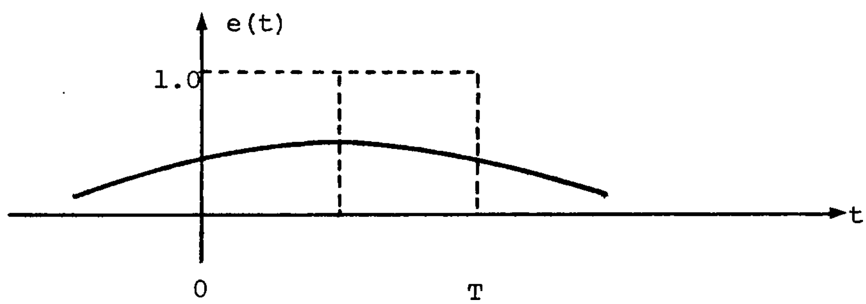

(c) Filter bandwidth = 0.5/T

Fig. 2.1. - Response of ideal lowpass filter to a rectangular pulse

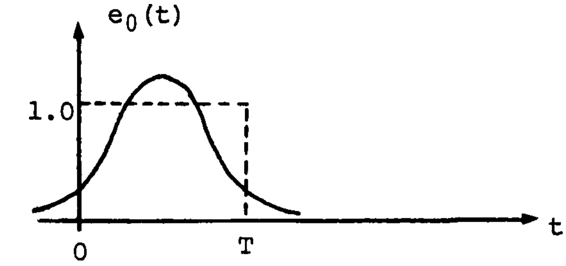

(a) Response to a single positive pulse (a *zero*)

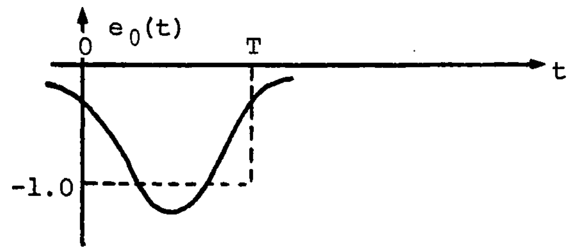

(b) Response to a single negative pulse (a *one*)

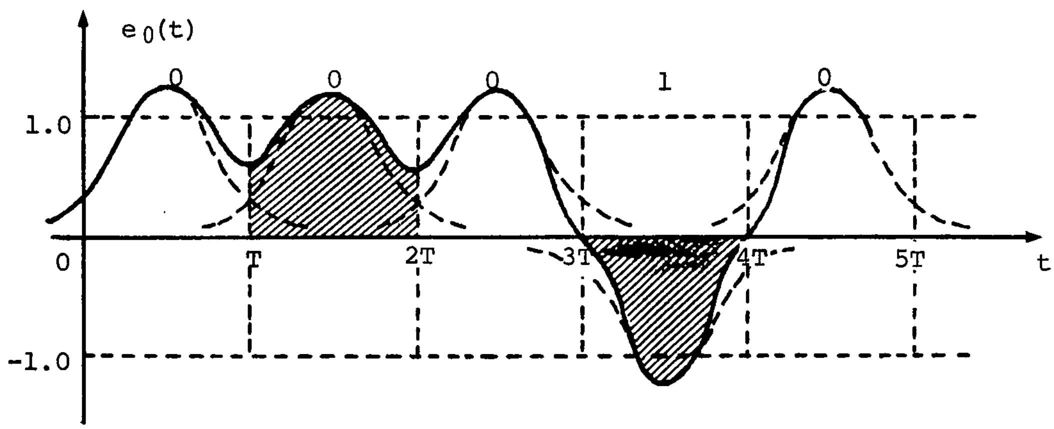

(c) Response to a pulse train (00010...)

Fig. 2.2. - Illustration of intersymbol interference for ideal lowpass filtering of rectangular pulses (filter bandwidth = 1/T)

between error probability and energy per bit is not a linear one. Thus the average error probability does not correspond to the average energy per bit and, consequently, the effects of intersymbol interference *cannot* be neglected. In fact, intersymbol interference is frequently the most significant factor in determining the performance of a given transmission system.

Determination of error probability for the bandlimited digital system is considerably more difficult than for the ideal (infinite bandwidth) system. One possible analytical approach involves the convolution of the probability density of the intersymbol interference with that of the noise. As noted by Saltzberg [7], however, this can be very difficult, since the probability density of the intersymbol interference is itself typically highly complex and irregular and hence difficult to compute. Approximations to this density by simpler functions may lead to gross misinterpretation.

An approximation to the error probability for a bandlimited digital system can be obtained by first assuming that the intersymbol interference is limited to a finite number (N) of symbols preceding and following the symbol under detection. The conditional error probabilities are computed for each of the truncated pulse sequences and then averaged with respect to the probability of occurrence of these sequences. This approach gives good results if the intersymbol interference is limited to only a few adjacent symbols, but the computational effort becomes prohibitive as N becomes large. Martindes and Reijns [8] applied the averaging method to a 40-bit periodic sequence and assumed that the intersymbol interference was limited to only the two nearest bits on either side of the bit under detection. Tu [9] applied the averaging method to a random sequence and assumed that the intersymbol interference was limited to the five nearest bits on either side of the bit under detection. Excellent agreement was obtained between these two investigations for lowpass filter bandwidths greater than the bit rate. However, for smaller bandwidths, Tu showed that Martinides' results were optimistic.

Because of the difficulties associated with the purely analytical approach involving convolution of the probability densities of intersymbol interference and noise and because of the computational problems associated with the averaging method, several researchers have made attempts to obtain bounds on the average error probability for bandlimited digital systems. The effects of intersymbol interference have frequently been bounded by means of the *eye pattern* [10]. The eye pattern is the superposition of all possible signals presented to the integrate-and-dump circuit and can be determined analytically or experimentally. The experimental determination involves exciting an oscilloscope with a random binary pulse train and synchronizing to the bit rate. A typical eye pattern is shown in Fig. 2.3. In the absence of intersymbol interference, the eye is open (rectangular). The two worst-case transmitted sequences (which are negatives of each other) result in the inner boundaries of the eye; hence, the size of the open portion of the eye pattern is a measure of the margin against intersymbol interference for the most adverse message sequence. As pointed out by Saltzberg [7], however, to use the eye opening to bound error probabilities is, in many instances, to be exceedingly pessimistic. A system with a completely closed eye pattern (and therefore a worst-case error probability of 0.5) can have a very low average bit error probability.

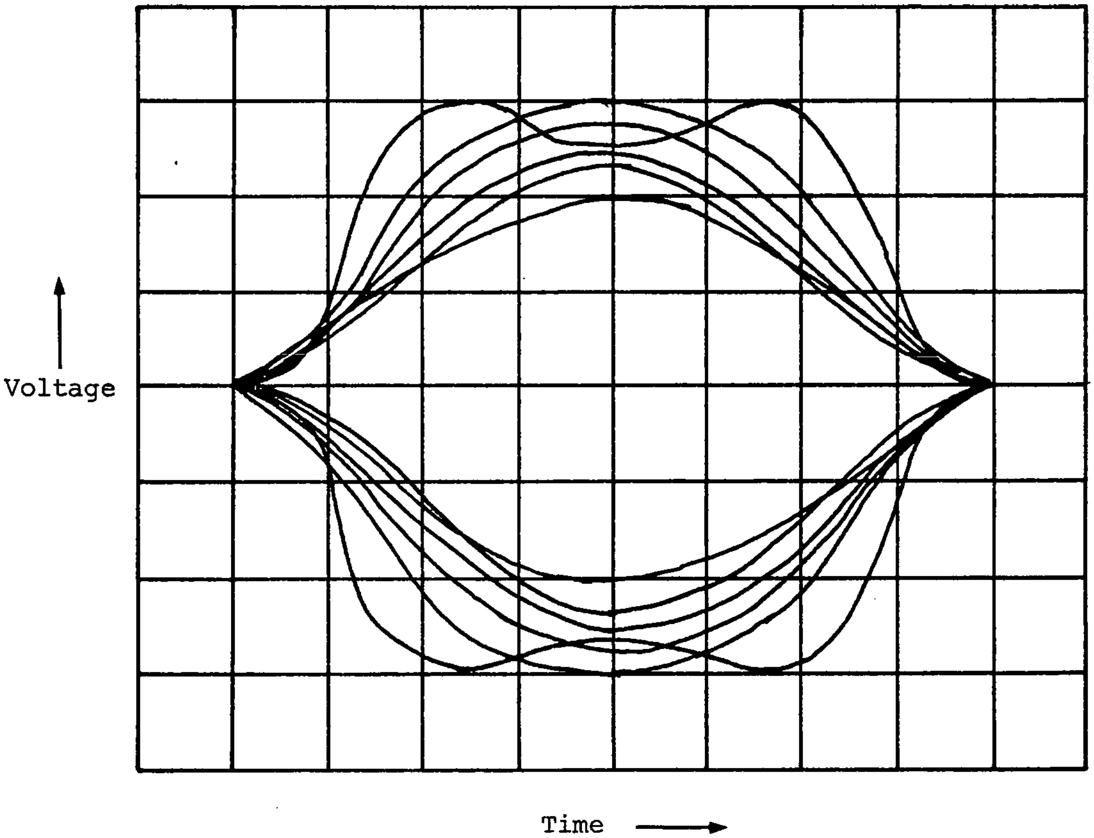

Fig 2.3 - Typical eye pattern

Hartmann [11] analyzed the bandlimited PSK system by applying a numerical method to find the worst-case probability of error and using this value as an upper bound. Hartmann's bound suffers from the same problem as the eye pattern analysis, namely that it can be overly pessimistic. Lugannani [12] obtained an improved upper bound (which never exceeds the worst-case upper bound) by applying the Chernoff inequality. Unfortunately, evaluation of the parameters of Lugannani's bound poses a computational problem about equal in magnitude to the problem of applying the averaging method to obtain an approximate solution.

Saltzberg [7] obtained an improved upper bound for error probability by separating intersymbol interference terms into two sets, one set containing larger components which subtract from the signal amplitude and another set containing smaller components which add to the noise power.

A very important result was recently obtained by Shimbo and Celebiler [13], in which an exact expression was obtained for the probability of error of a binary system having intersymbol interference and additive Gaussian noise. The procedure involves multiplying the characteristic functions of the noise and the intersymbol interference, which proves to be a considerably easier task than convolving the probability densities. Tu [9] applied the method of Shimbo and Celebiler to obtain numerical results for the error probabilities of several practical baseband and carrier binary systems. The computational effort required was orders of magnitude less than was required for obtaining the same results using the averaging method. Figs. 2.4 through 2.6 summarize the results obtained by Tu for the case of ideal bandpass filtering (rectangular filter characteristic) of a random binary PSK signal. The $f_c T$ product represents the number of cycles

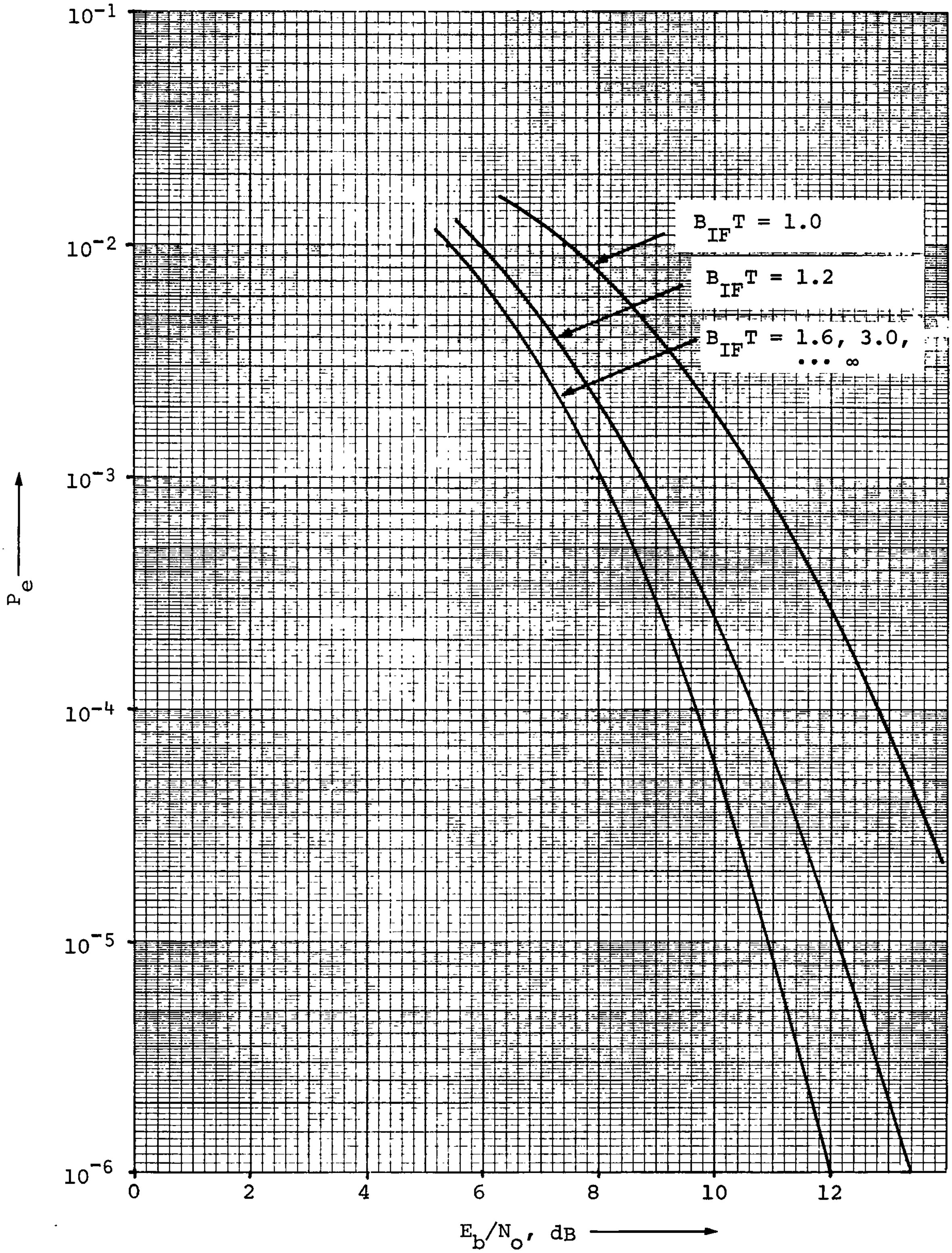

Fig. 2.4. - P_e vs. E_b/N_o for ideal bandlimited PSK with $f_cT = 1$

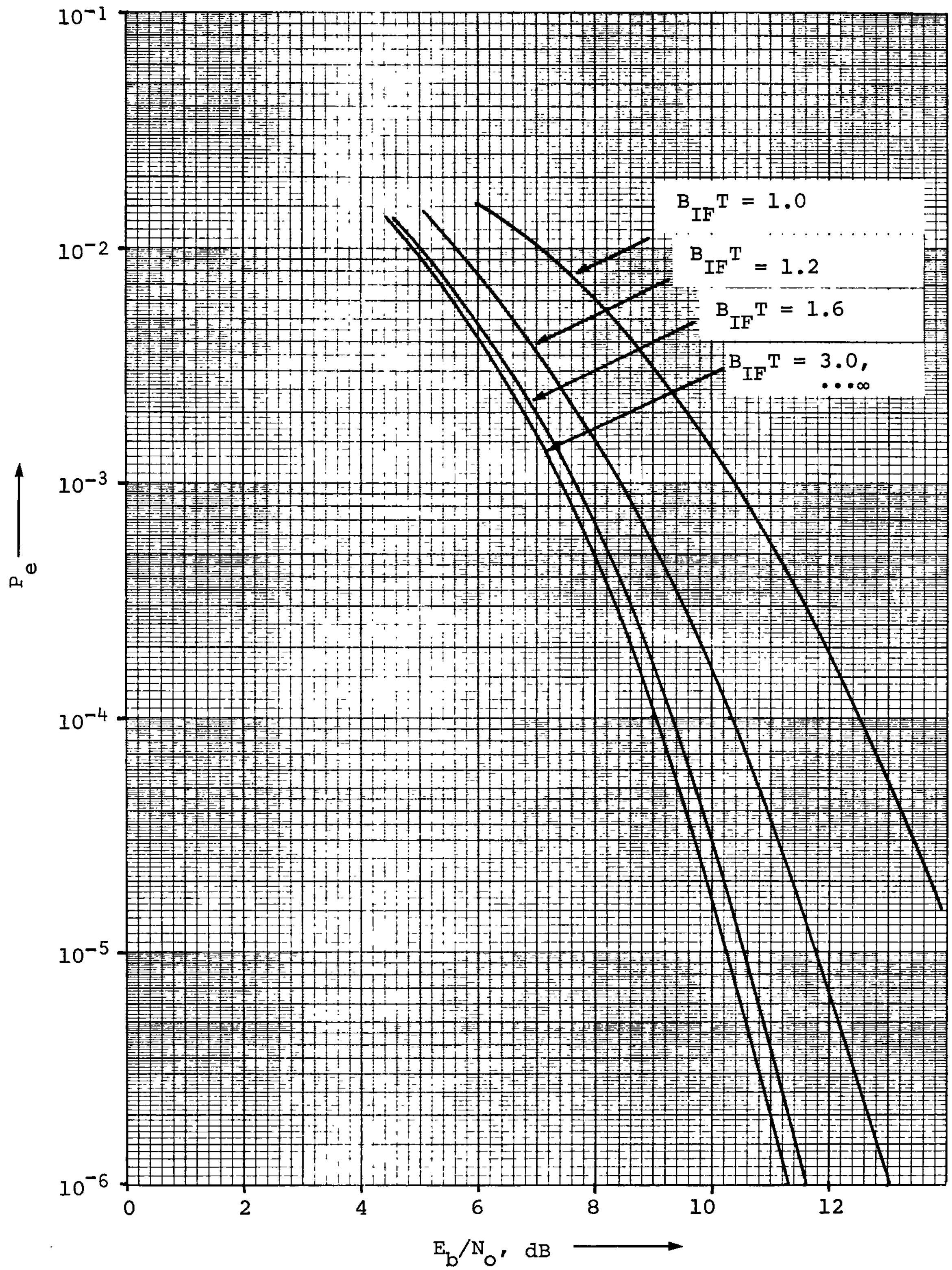

Fig. 2.5. - P_e vs. E_b/N_o for ideal bandlimited PSK with $f_cT = 2$

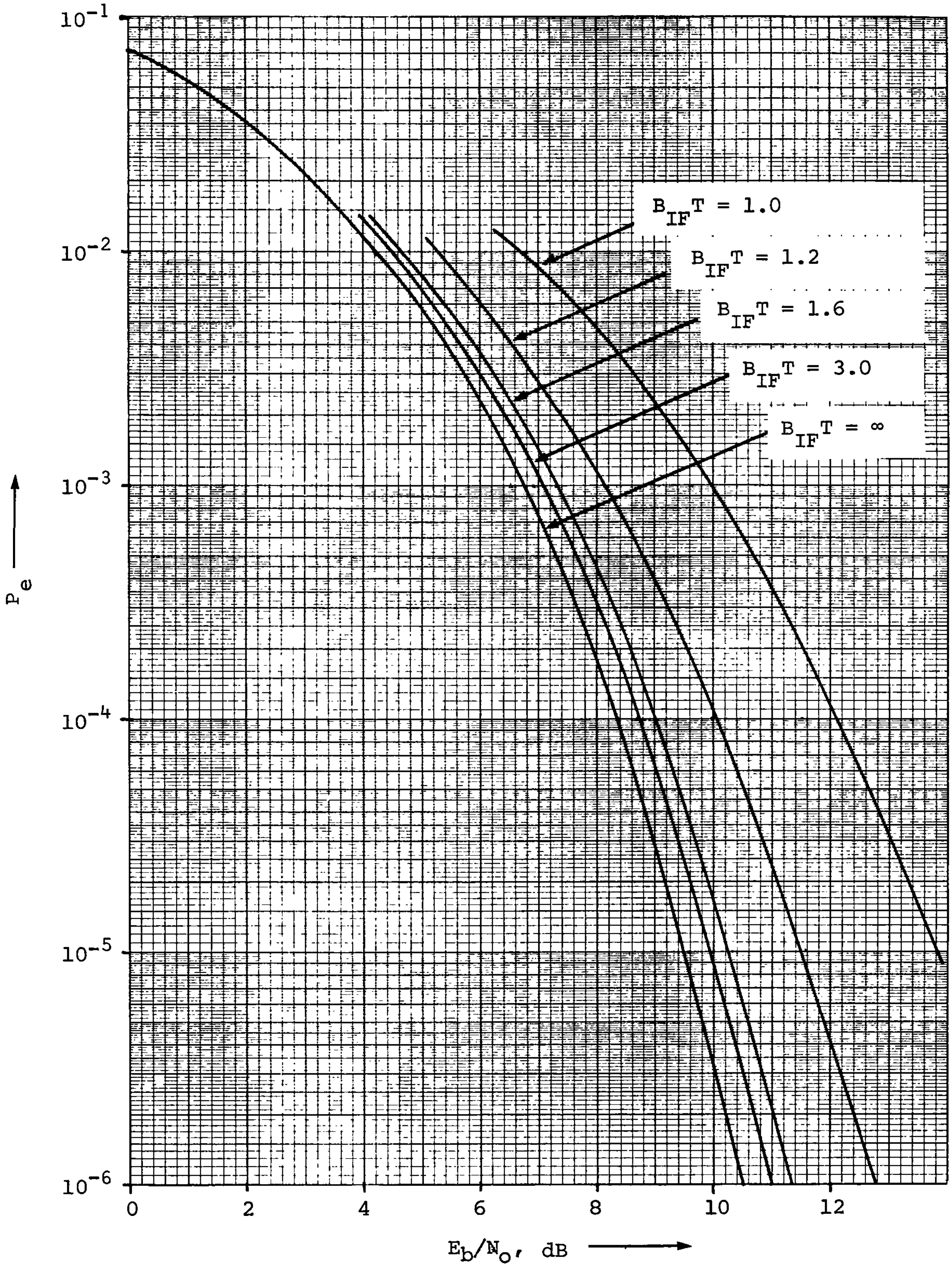

Fig. 2.6. - P_e vs. E_b/N_o for ideal bandlimited PSK with $f_cT = \infty$

of the carrier (f_c = carrier frequency) per bit of data (T = bit period, or $1/T$ = bit rate). The $B_{IF}T$ product represents the ratio of filter bandwidth (B_{IF}) to bit rate. Note that, for any particular value of f_cT, P_e increases as $B_{IF}T$ decreases. This is, of course, due to the increased intersymbol interference which results when the filter bandwidth is decreased. Also note that, for a constant value of $B_{IF}T$, P_e increases as f_cT decreases. This is because of the *aliasing* effect due to finite carrier frequency. Finally note from Fig. 2.6 that when $f_cT = \infty$ and $B_{IF}T = \infty$, the curve previously shown in Fig. 1.5 for optimum binary signaling results.

CHAPTER III

IDEAL QUADRIPHASE SIGNALING

The discussion in Chapters I and II was primarily directed towards ideal (infinite bandwidth) and non-ideal (finite bandwidth) *binary* transmission systems. The remainder of this dissertation will be concerned with a signaling scheme known as *quadriphase* or *QPSK*, which theoretically allows a 2:1 reduction in the bandwidth required for transmission of a given information rate. For ideal systems, PSK and QPSK signals provide equivalent performance (the same bit error probability for the same power levels) although the actual bandwidth occupied by the QPSK signal is only one-half that occupied by the PSK signal. QPSK offers a real advantage when the system is bandlimited and when it is desired to reduce the error probability which is achievable for a given transmitted or received power level.

A QPSK signal may be generated in several ways, as illustrated in Fig. 3.1. These methods of generation are different in terms of the hardware required for mechanization, but equivalent in terms of the four-phase signal that results. The signal $S_1(t)$ that is generated in the manner shown in Fig. 3.1(a) is given by

$$\begin{aligned} S_1(t) &= A_1 \cos[\omega_c t + A a_n(t)] + A_2 \sin[\omega_c t + B b_n(t)] \\ &= A_1 \cos(\omega_c t)\cos[A a_n(t)] - A_1 \sin(\omega_c t)\sin[A a_n(t)] \\ &\quad + A_2 \sin(\omega_c t)\cos[B b_n(t)] + A_2 \cos(\omega_c t)\sin[B b_n(t)] \end{aligned} \tag{3-1}$$

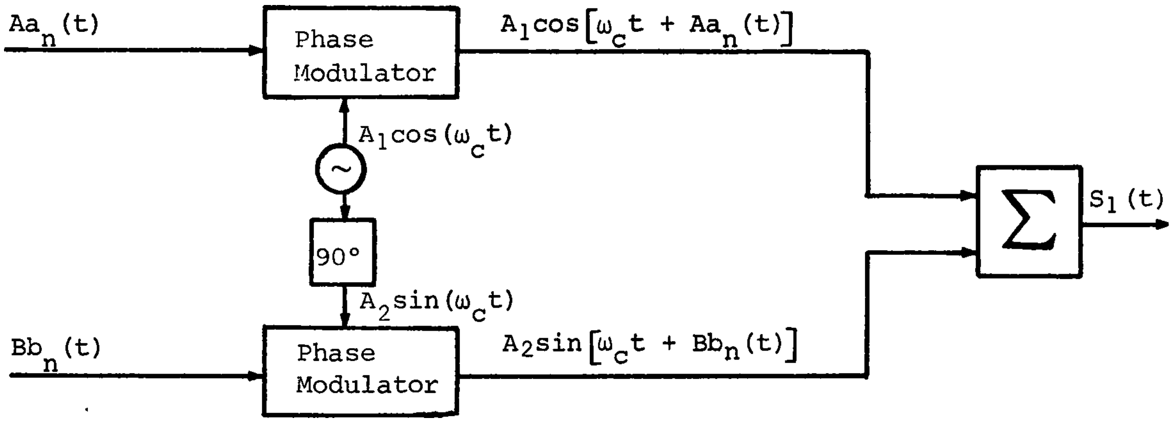

(a) Addition of phase-modulated quadrature carriers $[a_n(t) = \pm 1,\ b_n(t) = \pm 1]$

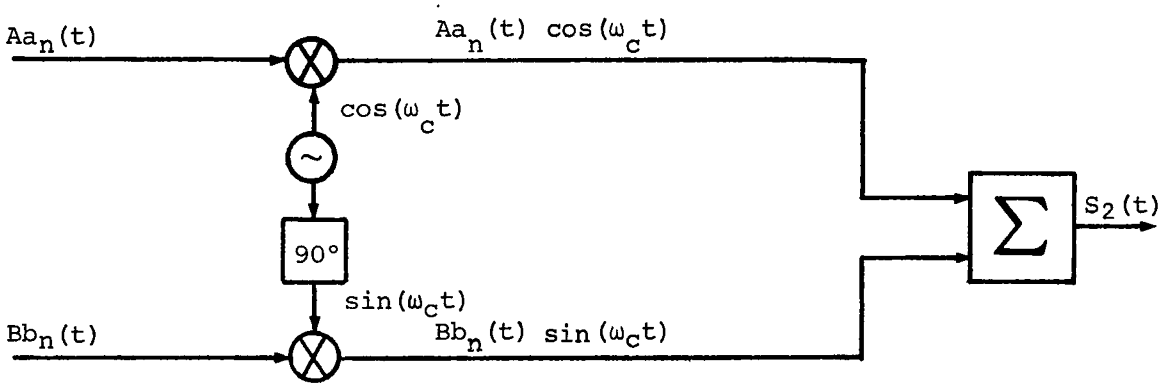

(b) Addition of DSB-modulated quadrature carriers $[a_n(t) = \pm 1,\ b_n(t) = \pm 1]$

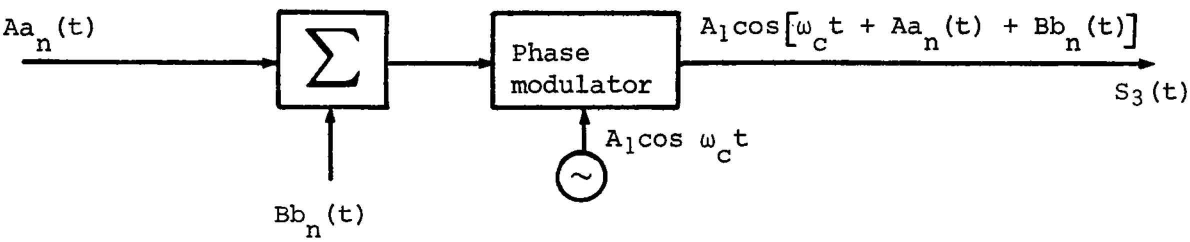

(c) Phase modulation of a single carrier by a quaternary (four-level) signal $[Aa_n(t) + Bb_n(t)$ is four-level for $a_n(t) = \pm 1,\ b_n(t) = \pm 1,$ and $A \neq B]$

Fig. 3.1. - Generation of QPSK signals

Substituting $a_n(t) = \pm 1$ and $b_n(t) = \pm 1$ into (3-1), the output signal reduces to

$$S_1(t) = \left[A_1 \cos A + A_2 b_n(t) \sin B\right] \cos(\omega_c t) + \left[A_2 \cos B - A_1 a_n(t) \sin A\right] \sin(\omega_c t) \tag{3-2}$$

Using the relationship

$$\alpha \cos x + \beta \sin x = \sqrt{\alpha^2 + \beta^2} \cos(x - \theta) \tag{3-3}$$

$$\text{where} \quad \theta = \tan^{-1}\left(\frac{\beta}{\alpha}\right)$$

the signal $S_1(t)$ can be represented by

$$S_1(t) = \sqrt{\left[A_1 \cos A + A_2 b_n(t) \sin B\right]^2 + \left[A_2 \cos B - A_1 a_n(t) \sin A\right]^2} \cos(\omega_c t - \theta) \tag{3-4}$$

$$\text{where} \quad \theta = \tan^{-1}\left[\frac{A_2 \cos B - A_1 a_n(t) \sin A}{A_1 \cos A + A_2 b_n(t) \sin B}\right]$$

From (3-4), it can be seen that $S_1(t)$ has, in general, four possible amplitude states and four possible phase states corresponding to the possible combinations of $a_n(t)$ and $b_n(t)$. For $A = B = \frac{\pi}{2}$, $S_1(t)$ becomes

$$S_1(t) = \sqrt{A_2^2 + A_1^2} \cos\left\{\omega_c t - \tan^{-1}\left[\frac{-A_1 a_n(t)}{A_2 b_n(t)}\right]\right\} \tag{3-5}$$

which is a signal having only one amplitude and four phase states. Further, for $A_1 = A_2$ (equal power in each quadrature carrier), the four phase states are exactly 90° apart. This condition will henceforth be referred to as *balanced quadriphase*. The condition for which the phase states are not 90° apart will be referred to as *unbalanced quadriphase*.

The signal $S_2(t)$ that is generated in the manner shown in Fig. 3.1(b), by adding two PSK signals which are in phase quadrature, is given by

$$S_2(t) = A a_n(t) \cos(\omega_c t) + B b_n(t) \sin(\omega_c t)$$
$$= \sqrt{A^2 + B^2} \cos\left\{\omega_c t - \tan^{-1}\left[\frac{B b_n(t)}{A a_n(t)}\right]\right\} \qquad (3\text{-}6)$$

which is equivalent to the expression given by (3-5) in that four phase states and a single amplitude state results.

The signal $S_3(t)$ that is generated in the manner shown in Fig. 3.1(c) is given by

$$S_3(t) = A_1 \cos\left[\omega_c t + A a_n(t) + B b_n(t)\right] \qquad (3\text{-}7)$$

This signal has a single amplitude state and four possible phase states (A+B, A-B, -A+B, -A-B). For $A = \frac{\pi}{2}$ and $B = \frac{\pi}{4}$, or for $A = \frac{\pi}{4}$ and $B = \frac{\pi}{2}$, these four phase states are 90° apart.

As discussed in the preceding paragraphs, several methods are available for generating a quadriphase signal. Each of the methods illustrated utilizes two bipolar (±1) signals $a_n(t)$ and $b_n(t)$. As no restrictions were imposed upon $a_n(t)$ and $b_n(t)$, they could be obtained either from separate, independent sources or from a single source (by means of a serial to parallel conversion device which converts a signal of rate R bits/second to two parallel signals each of rate $\frac{R}{2}$ bits/second). The latter case will be referred to as *single-channel* operation, while the former case will be referred to as *dual-channel* operation.

Regardless of the method used to generate the quadriphase signal, the quadrature detection scheme shown in Fig. 3.2 is the optimum means of recovering the two signal components $a_n(t)$ and $b_n(t)$. This is because for the ideal case, no crosstalk occurs between the two quadrature channels and each signal component is recovered using a correlation detector. Using the quadriphase representation given by (3-6), the input to the upper integrate-and-dump circuit is

$$\begin{aligned} e_1(t) &= [A a_n(t)\cos(\omega_c t) + B b_n(t)\sin(\omega_c t)]\, A_o \cos(\omega_c t + \phi) \\ &= [A a_n(t)\cos(\omega_c t) + B b_n(t)\sin(\omega_c t)][A_o \cos(\omega_c t)\cos\phi - A_o \sin(\omega_c t)\sin\phi] \\ &= \frac{A A_o a_n(t)\cos\phi - B A_o b_n(t)\sin\phi}{2} \\ &\quad + \frac{B A_o b_n(t)\cos\phi - A A_o a_n(t)\sin\phi}{2}\sin(2\omega_c t) \\ &\quad + \frac{A A_o a_n(t)\cos\phi + B A_o b_n(t)\sin\phi}{2}\cos(2\omega_c t) \end{aligned} \tag{3-8}$$

Assuming that the double-frequency terms make no contribution to the output of the integrate-and-dump circuit, and assuming $\phi = 0$ (the ideal case), the effective signal input to the upper integrate-and-dump circuit is given by

$$e_{1,eff}(t) = \frac{A_o A a_n(t)}{2} = K_1 a_n(t) \tag{3-9}$$

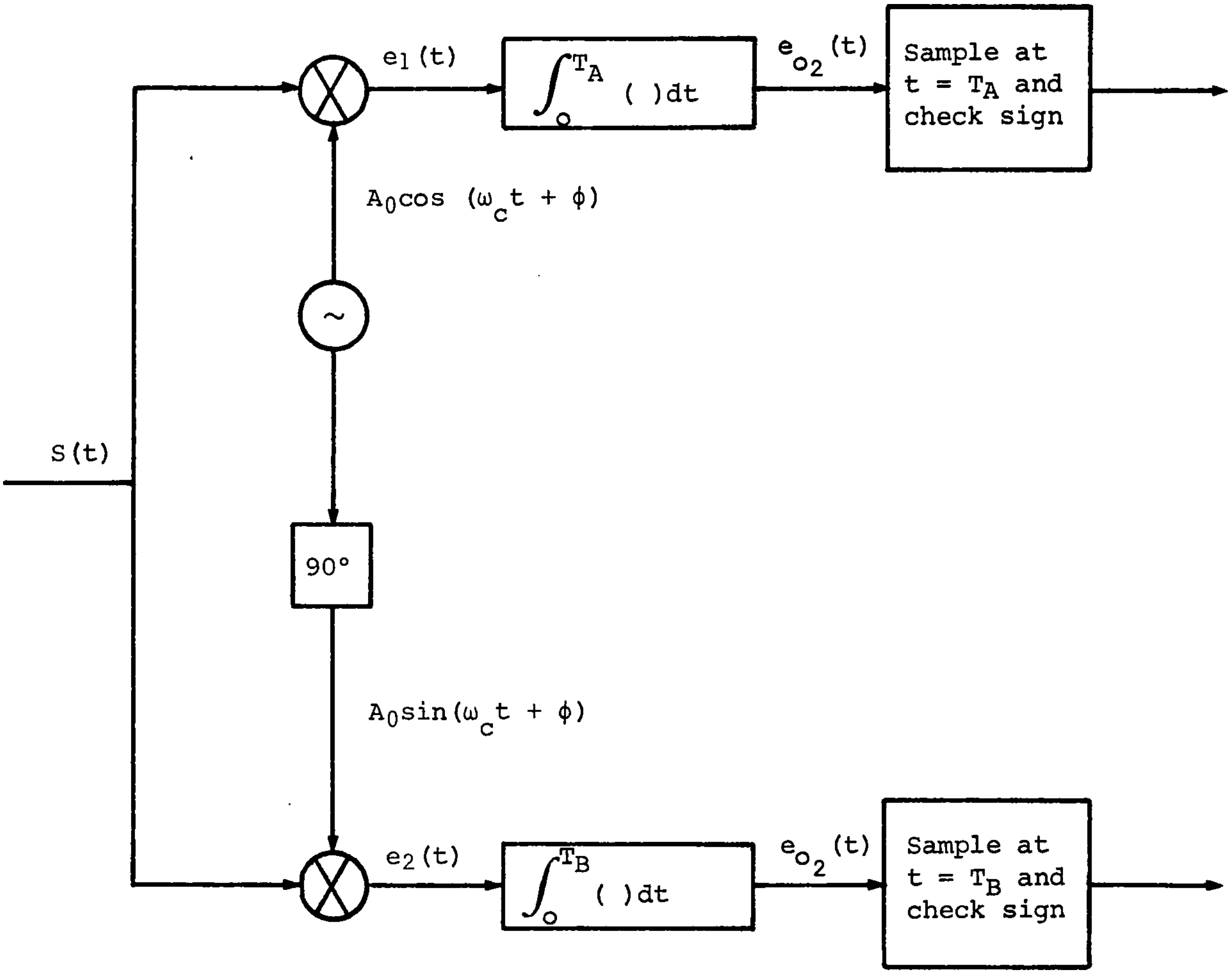

Fig. 3.2. - Detection of a QPSK signal

Likewise, it is easily shown that the effective signal input to the lower integrate-and-dump circuit is

$$e_{2,eff}(t) = \frac{A_o B\, b_n(t)}{2} = K_2\, b_n(t) \tag{3-10}$$

Therefore, for the ideal case in which the reference phase error $\phi = 0$, the upper half of the quadriphase detector is a correlation detector for $a_n(t)$ and the lower half is a correlation detector for $b_n(t)$. In the event that $\phi \neq 0$, an undesirable *crosstalk* terms appears in each quadrature channel. The problem of recovering a good phase reference will not be treated here, so it will be assumed throughout that $\phi = 0$.

Since the detection of a quadriphase signal has been shown to consist of two separate correlation detection processes, the probability of error associated with each of these processes is the same as previously given by (1-1):

$$P_e = \frac{1}{2} \operatorname{erfc} \sqrt{\frac{(1-\rho) E_b}{2N_o}} \tag{3-11}$$

For each of the two correlation detection processes, $\rho = -1$ and the energy per bit is given by

$$E_b = \text{channel power} \div \text{rate}$$

$$= \begin{cases} \dfrac{P_A}{R_A} & \text{for upper channel} \\[2ex] \dfrac{P_B}{R_B} & \text{for lower channel} \end{cases} \tag{3-12}$$

In order to meaningfully compare the performance of quadriphase transmission to that of biphase transmission, the same total information rate should be assumed for each scheme. For quadriphase signaling, the error probability in the upper channel can be expressed as

$$P_{e_A} = \frac{1}{2}\,\mathrm{erfc}\sqrt{\frac{E_{bA}}{N_o}}$$

$$= \frac{1}{2}\,\mathrm{erfc}\sqrt{\frac{P_A}{N_o R_A}} \tag{3-13}$$

Similarly, the error probability in the lower channel can be expressed as

$$P_{e_B} = \frac{1}{2}\,\mathrm{erfc}\sqrt{\frac{E_{bB}}{N_o}}$$

$$= \frac{1}{2}\,\mathrm{erfc}\sqrt{\frac{P_B}{N_o R_B}} \tag{3-14}$$

The error probabilities P_{e_A} and P_{e_B} can be compared with the error probability for PSK transmission of the same information rate ($R_A + R_B$ bits/second) at the same total power level ($P_A + P_B$ watts), as given by

$$P_e = \frac{1}{2}\,\mathrm{erfc}\sqrt{\frac{E_b}{N_o}}$$

$$= \frac{1}{2}\,\mathrm{erfc}\sqrt{\frac{P_A + P_B}{N_o (R_A + R_B)}} \tag{3-15}$$

For balanced QPSK operation, half of the total power is allocated to each of the two quadrature channels, or

$$P_A = P_B = \frac{P_T}{2} \tag{3-16}$$

Also, for balanced QPSK operation, the individual transmission rates are equal, or

$$R_A = R_B = \frac{R}{2} \tag{3-17}$$

The QPSK energy per bit is thus given by

$$E_b = \begin{cases} \dfrac{\frac{P_T}{2}}{\frac{R}{2}} = \dfrac{P_T}{R} & \text{for upper channel} \\[2ex] \dfrac{\frac{P_T}{2}}{\frac{R}{2}} = \dfrac{P_T}{R} & \text{for lower channel} \end{cases} \tag{3-18}$$

The resulting error probability for QPSK transmission of R bits/second is therefore

$$P_{eA} = P_{eB} = \frac{1}{2}\,\mathrm{erfc}\sqrt{\frac{P_T}{N_o R}} \tag{3-19}$$

and is the same as for PSK transmission of R bits/second (with the same total power). Note, however, that the bandwidth occupied by each quadrature channel (corresponding to a rate R/2) is only one-half that occupied by the equivalent PSK channel.

For unequal bit rates in the two quadrature channels, it is necessary to divide the channel powers unevenly in order to maintain equal error probabilities. That is, more of the total transmit power must be allocated to the higher rate channel in order to equalize the energy per bit in the two channels. For this case, $A \neq B$ and unbalanced operation results. For equal error probabilities

$$P_A / R_A = P_B / R_B \tag{3-20}$$

and

$$P_{eA} = P_{eB} = \frac{1}{2}\,\mathrm{erfc}\sqrt{\frac{P_A}{N_o R_A}} \tag{3-21}$$

For PSK transmission of $R_A + R_B$ bits/second with a power level of $P_A + P_B$ watts, the error probability is given by

$$P_e = \frac{1}{2}\,\text{erfc}\sqrt{\frac{P_A + P_B}{N_o(R_A + R_B)}}$$

$$= \frac{1}{2}\,\text{erfc}\sqrt{\frac{P_A + \dfrac{P_A R_B}{R_A}}{N_o(R_A + R_B)}}$$

$$= \frac{1}{2}\,\text{erfc}\sqrt{\frac{P_A}{N_o R_A}} \qquad (3\text{-}22)$$

which is again the same as for QPSK.

The preceding discussion establishes the error rate performance of ideal (infinite bandwidth) QPSK signaling with a perfect phase reference. Since QPSK is very attractive for bandlimited applications, however, it is important to determine the error rate performance of non-ideal QPSK systems. This problem is investigated in considerable detail in the next chapter.

CHAPTER IV

PERFORMANCE OF BANDLIMITED QUADRIPHASE SYSTEMS

This chapter is concerned with the error rate performance of bandlimited QPSK systems. The more significant assumptions which will be made for this analysis are as follows:

- The demodulator reference signals are noise-free.
- Timing for the integrate-and-dump detectors is perfect (no jitter).
- The channel noise is additive, white, Gaussian, zero-mean, and has single-sided noise spectral density N_o.

The system model which will be used for this investigation is shown in Fig. 4.1. The effects of bandpass (RF or IF) filtering will be considered, but it will be sometimes convenient to include lowpass (baseband) filters prior to the bit detectors. Baseband filtering alone (either prior to modulation or subsequent to demodulation) need not be considered here because the results previously obtained [9] for baseband filtering of PSK signals are directly applicable to each of the two quadrature channels of the QPSK system. As will be shown, however, bandpass filtering of a QPSK signal results in the generation of crosstalk which (along with a reduction in energy per bit and the generation of intersymbol interference) contributes to the degradation in bit error rate performance. The results previously obtained for bandpass filtering of PSK signals do not account for this crosstalk and, therefore, are not applicable to QPSK systems.

The QPSK modulator of Fig. 4.1 could be any of the three types discussed in the previous chapter and depicted in Fig. 3.1. The QPSK

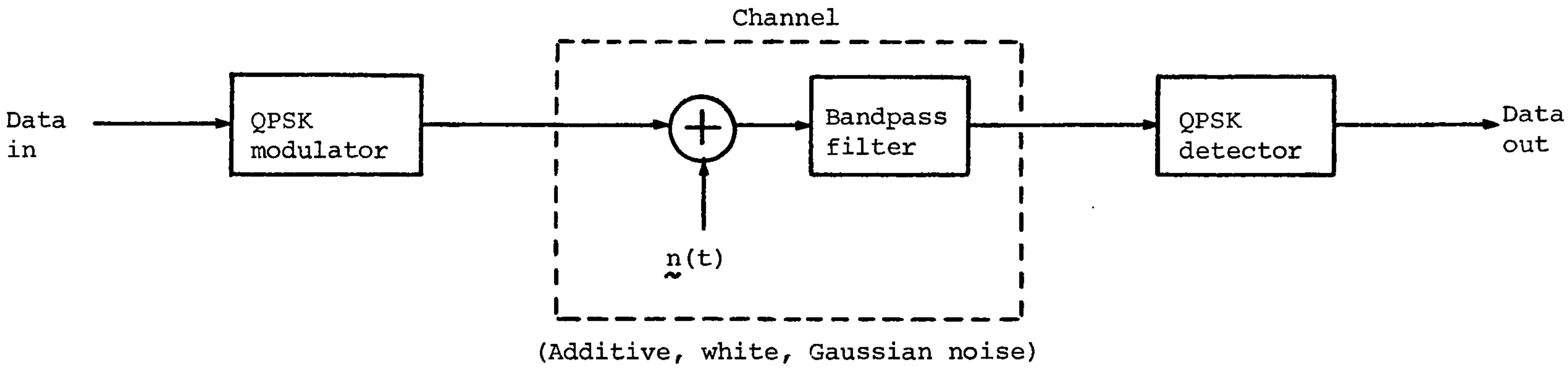

Fig. 4.1. - Bandlimited QPSK model

detector is the correlation detector (for ideal QPSK signals) shown in Fig. 3.2. Two different types of bandpass filters will be considered in this analysis. A filter with the ideal rectangular characteristic will first be assumed, and attention will then be directed to a more practical filter, the bandpass equivalent of the single-pole Butterworth.

IDEAL RECTANGULAR FILTERING

The ideal rectangular filter will first be assumed as the device which limits the bandwidth of the QPSK signal. As shown in Fig. 4.2, the magnitude of the filter characteristic H(f) for this filter is equal to a constant value (normalized to unity) for frequencies within the passband and is zero elsewhere. The characteristic for the ideal rectangular filter is actually given by

$$H(f) = |H(f)|\, e^{-j2\pi f t_o} \tag{4-1}$$

where t_o represents the constant time delay introduced by the filter. Without loss of generality, t_o can be assumed to be zero. (The impact of this assumption is that the period of integration for the QPSK integrate-and-dump circuits will be 0 to T, rather than t_o to $t_o + T$).

The QPSK signal present at the input to the bandpass filter can be expressed as the sum of the two infinite sequences

$$s(t) = \sum_{m=-\infty}^{\infty} a_m(t)\cos(\omega_c t) + \sum_{n=-\infty}^{\infty} b_n(t)\sin(\omega_c t) \tag{4-2}$$

where

$$a_m(t) = \begin{cases} A_m = +A \text{ or } -A & \text{for } mT_A \le t \le (m+1)T_A \\ 0 & \text{elsewhere} \end{cases}$$

and

$$b_n(t) = \begin{cases} B_n = +B \text{ or } -B & \text{for } nT_B \le t \le (n+1)T_B \\ 0 & \text{elsewhere} \end{cases}$$

The sequence $\sum_{m=-\infty}^{\infty} a_m(t)$ is the desired output signal from the upper (in-phase) channel of the QPSK detector of Fig. 3.2. This in-phase

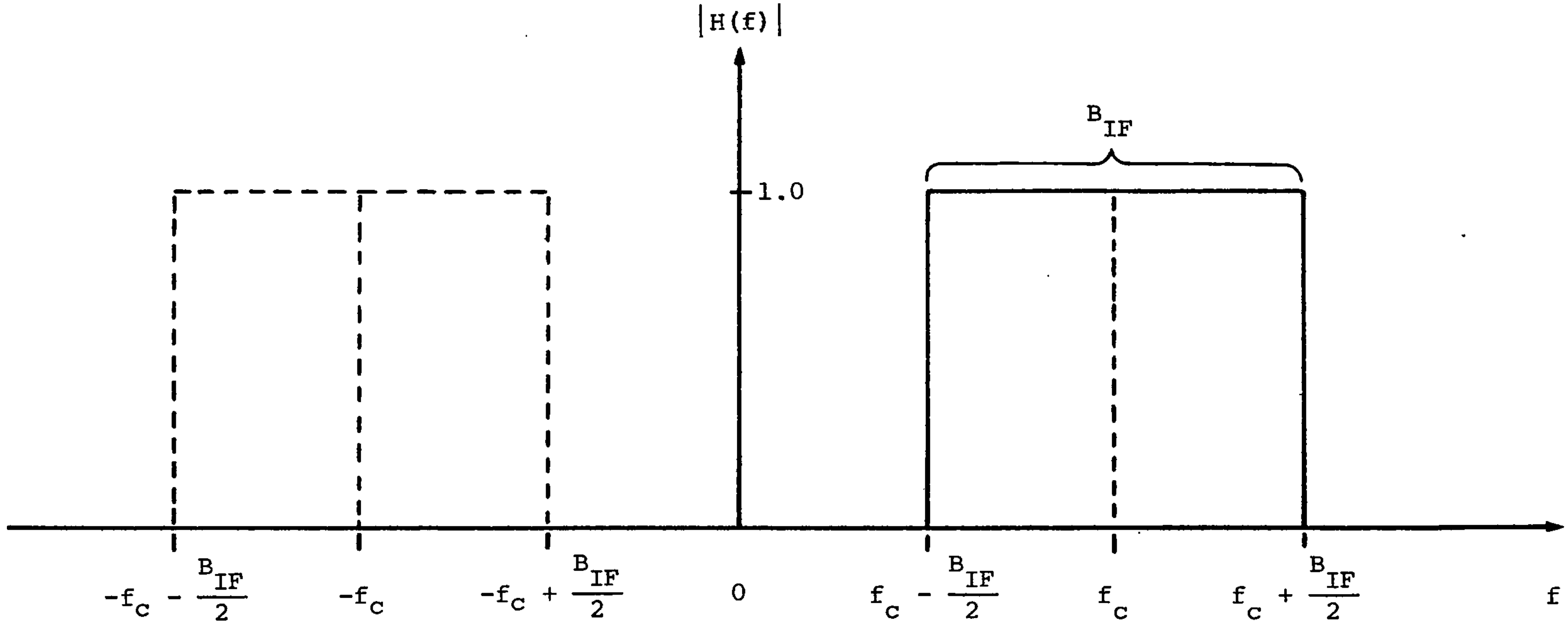

Fig. 4.2 - Bandpass filter characteristic for ideal rectangular filter

channel will henceforth be referred to as *Channel A*. Likewise, the sequence $\sum_{n=-\infty}^{\infty} b_n(t)$ is the desired output signal from the lower (quadrature) channel, which will be referred to as *Channel B*. Fig. 4.3 defines the detection model which will be used in this portion of the analysis. As discussed in Chapter III, the sequences $\sum_{m=-\infty}^{\infty} a_m(t)$ and $\sum_{n=-\infty}^{\infty} b_n(t)$ are either derived from a single source (single-channel operation), in which case $T_A = T_B$, or from two independent sources, in which case (in general) $T_A \neq T_B$.

To determine the effects of ideal rectangular filtering, a frequency domain (rather than a time domain) approach will be used initially. This is because the mathamatics associated with the ideal filter are much simpler in the frequency domain. Consequently, the Fourier transform of the m^{th} bit of Channel A (at the filter input) is

$$
\begin{aligned}
A_m(f) &= \int_{mT_A}^{(m+1)T_A} [a_m(t)\cos(\omega_c t)]\, e^{-j2\pi f t}\, dt \\
&= \int_{mT_A}^{(m+1)T_A} A_m \frac{e^{j2\pi f_c t} + e^{-j2\pi f_c t}}{2}\, e^{-j2\pi f t}\, dt \\
&= \frac{A_m \sin[\pi(f-f_c)T_A]\, e^{-j\pi(f-f_c)(1+2m)T_A}}{2\pi(f-f_c)} \\
&\quad + \frac{A_m \sin[\pi(f+f_c)T_A]\, e^{-j\pi(f+f_c)(1+2m)T_A}}{2\pi(f+f_c)}
\end{aligned}
\tag{4-3}
$$

This expression can be simplified by making the assumption that $f_c T_A$ is an integer, or that an integral number of cycles of the carrier frequency f_c occurs in each bit period T_A of Channel A. This assumption is not unreasonable, as the bit timing for many practical systems is derived

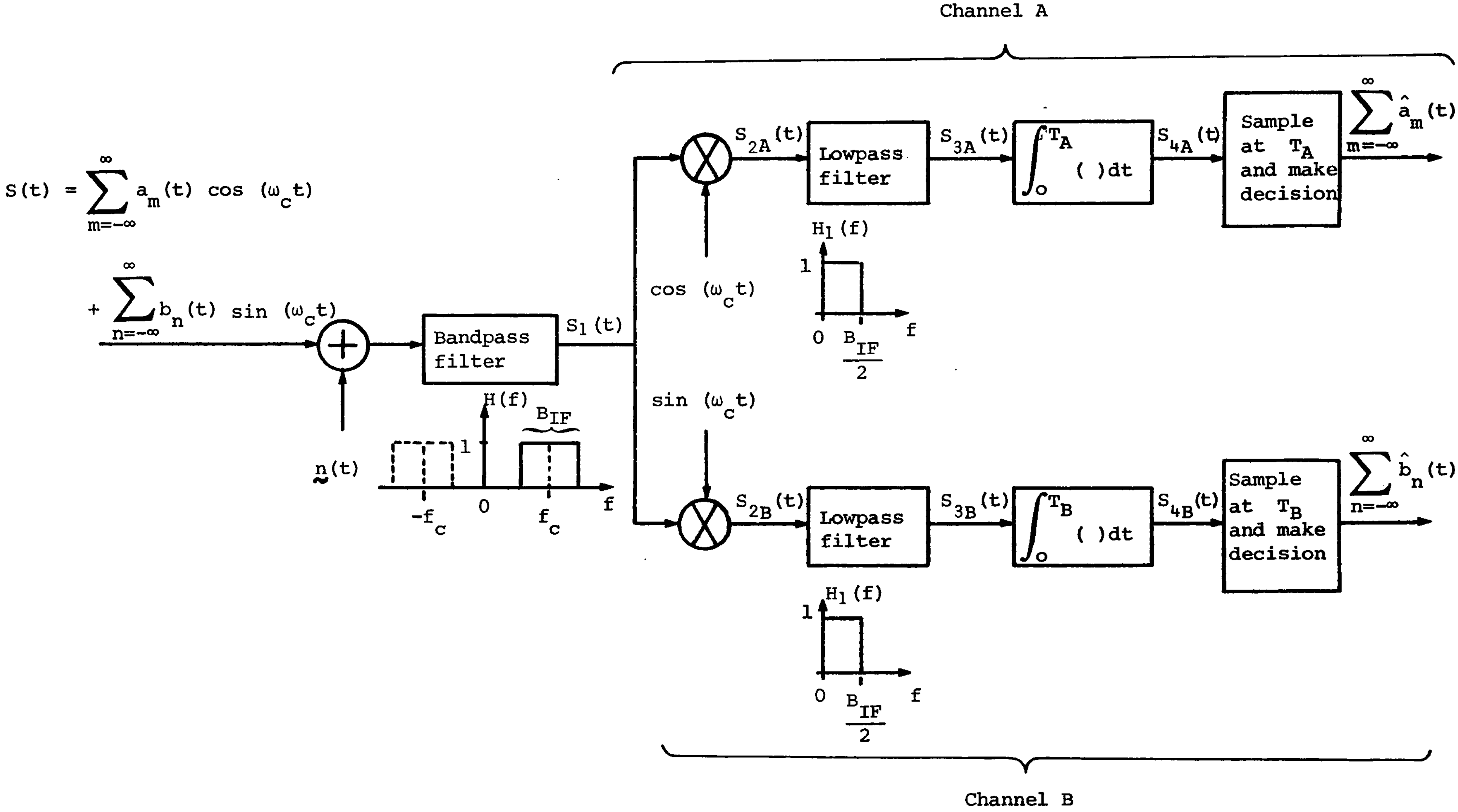

Fig. 4.3. - QPSK detection model for ideal rectangular filtering

from the same source as the carrier frequency. Making this assumption and simplifying accordingly, (4-3) reduces to

$$A_m(f) = \frac{A_m f \sin(\pi f T_A)}{\pi(f^2 - f_c^2)} e^{-j\pi f(1+2m)T_A} \tag{4-4}$$

The output of the bandpass filter corresponding to the m^{th} bit of Channel A can be expressed in the frequency domain as

$$S_{1A}(f) = \begin{cases} A_m(f) & \text{for } f_c - \frac{B_{IF}}{2} \le f \le f_c + \frac{B_{IF}}{2} \\ A_m(f) & \text{for } -f_c - \frac{B_{IF}}{2} \le f \le -f_c + \frac{B_{IF}}{2} \\ 0 & \text{otherwise} \end{cases} \tag{4-5}$$

The time domain response of the filter to the m^{th} bit of Channel A is determined by taking the inverse Fourier transform of (4-5).

$$\begin{aligned} s_{1A}(t) &= \mathcal{F}^{-1}\left[S_{1A}(f)\right] \\ &= \int_{-\infty}^{\infty} S_{1A}(f)\, e^{+j2\pi f t}\, df \\ &= \int_{-f_c - \frac{B_{IF}}{2}}^{-f_c + \frac{B_{IF}}{2}} \frac{A_m f \sin(\pi f T_A)}{\pi(f^2 - f_c^2)} e^{-j\pi f(1+2m)T_A} e^{+j2\pi f t}\, df \\ &\quad + \int_{f_c - \frac{B_{IF}}{2}}^{f_c + \frac{B_{IF}}{2}} \frac{A_m f \sin(\pi f T_A)}{\pi(f^2 - f_c^2)} e^{-j\pi f(1+2m)T_A} e^{+j2\pi f t}\, df \end{aligned} \tag{4-6}$$

As shown in Appendix A, (4-6) can be reduced to

$$\begin{aligned} s_{1A}(t) &= \frac{2A_m}{\pi}\left\{\int_0^{\frac{\pi B_{IF} T_A}{2}} \frac{\left[2y^2 - (2\pi f_c T_A)^2\right]\sin y}{y\left[y^2 - (2\pi f_c T_A)^2\right]} \cos\left\{\left[2\left(\frac{t}{T_A}\right) - (1+2m)\right]y\right\} dy\right\} \cos(2\pi f_c t) \\ &\quad + \frac{2A_m}{\pi}\left\{\int_0^{\frac{\pi B_{IF} T_A}{2}} \frac{2\pi f_c T_A \sin y}{y^2 - (2\pi f_c T_A)^2} \sin\left\{\left[2\left(\frac{t}{T_A}\right) - (1+2m)\right]y\right\} dy\right\} \sin(2\pi f_c t) \end{aligned} \tag{4-7}$$

Following the same procedure for Channel B and making the assumption that $f_c T_B$ is an integer, the Fourier transform of the n^{th} bit of Channel B is easily found to be

$$B_n(f) = \frac{-j B_n f_c \sin(\pi f T_B)}{\pi(f^2 - f_c^2)} e^{-j\pi f(1+2n)T_B} \tag{4-8}$$

The time-domain response of the bandpass filter corresponding to the n^{th} bit of Channel B is

$$s_{1B}(t) = \int_{-f_c-\frac{B_{IF}}{2}}^{-f_c+\frac{B_{IF}}{2}} \frac{-j B_n f_c \sin(\pi f T_B)}{\pi(f^2-f_c^2)} e^{-j\pi f(1+2n)T_B} e^{+j2\pi f t} df + \int_{f_c-\frac{B_{IF}}{2}}^{f_c+\frac{B_{IF}}{2}} \frac{-j B_n f_c \sin(\pi f T_B)}{\pi(f^2-f_c^2)} e^{-j\pi f(1+2n)T_B} e^{+j2\pi f t} df \tag{4-9}$$

which, as shown in Appendix A, can be reduced to

$$\begin{aligned} s_{1B}(t) = {} & 2B_n f_c T_B \left\{ \int_0^{\frac{\pi B_{IF} T_B}{2}} \frac{2 \sin y}{y^2 - (2\pi f_c T_B)^2} \sin\left\{\left[2\left(\frac{t}{T_B}\right) - (1+2n)\right] y\right\} dy \right\} \cos(2\pi f_c t) \\ & - 2B_n f_c T_B \left\{ \int_0^{\frac{\pi B_{IF} T_B}{2}} \frac{4\pi f_c T_B \sin y}{y[y^2 - (2\pi f_c T_B)^2]} \cos\left\{\left[2\left(\frac{t}{T_B}\right) - (1+2n)\right] y\right\} dy \right\} \sin(2\pi f_c t) \end{aligned} \tag{4-10}$$

An interesting observation can be made from (4-7) and (4-10). The response of the bandpass filter to the m^{th} bit of CHannel A contains both in-phase ($\cos 2\pi f_c t$) and quadrature ($\sin 2\pi f_c t$) terms. Likewise, the filter response to the n^{th} bit of Channel B contains both $\cos 2\pi f_c t$ and $\sin 2\pi f_c t$ terms. This means that the output of the Channel A demodulator will depend on $\sum_{n=-\infty}^{\infty} b_n(t)$ as well as on $\sum_{m=-\infty}^{\infty} a_m(t)$, with the same phenomenon occurring at the output of the Channel B demodulator. One effect of the bandpass filter then, is the introduction of *crosstalk* between the two QPSK channels. The ultimate effect of this crosstalk will be an increased error rate in each channel.

Combining (4-7) and (4-10), rearranging terms, and summing the response to all m bits of Channel A and all n bits of Channel B yields

$$
\begin{aligned}
s_1(t) &= \sum_{m=-\infty}^{\infty} s_{1A}(t) + \sum_{n=-\infty}^{\infty} s_{1B}(t) \\
&= \Bigg\{ \sum_{m=-\infty}^{\infty} \frac{2A_m}{\pi} \int_0^{\frac{\pi B_{IF} T_A}{2}} \frac{[2y^2-(2\pi f_c T_A)^2]\sin y}{y[y^2-(2\pi f_c T_A)^2]} \cos\left\{\left[2\left(\frac{t}{T_A}\right)-(1+2m)\right]y\right\} dy \\
&\quad + \sum_{n=-\infty}^{\infty} 2B_n f_c T_B \int_0^{\frac{\pi B_{IF} T_B}{2}} \frac{2\sin y}{y^2-(2\pi f_c T_B)^2} \sin\left\{\left[2\left(\frac{t}{T_B}\right)-(1+2n)\right]y\right\} dy \Bigg\} \cos(2\pi f_c t) \\
&\quad + \Bigg\{ \sum_{m=-\infty}^{\infty} \frac{2A_m}{\pi} \int_0^{\frac{\pi B_{IF} T_A}{2}} \frac{2\pi f_c T_A \sin y}{y^2-(2\pi f_c T_A)^2} \sin\left\{\left[2\left(\frac{t}{T_A}\right)-(1+2m)\right]y\right\} dy \\
&\quad - \sum_{n=-\infty}^{\infty} 2B_n f_c T_B \int_0^{\frac{\pi B_{IF} T_B}{2}} \frac{4\pi f_c T_B \sin y}{y[y^2-(2\pi f_c T_B)^2]} \cos\left\{\left[2\left(\frac{t}{T_B}\right)-(1+2n)\right]y\right\} dy \Bigg\} \sin(2\pi f_c t) \\
&= s_{1I}(t)\cos(2\pi f_c t) + s_{1Q}(t)\sin(2\pi f_c t)
\end{aligned}
\tag{4-11}
$$

As illustrated in Fig. 4.3, the signal $s_1(t)$ is applied to the Channel A and Channel B demodulators. The signal output from the Channel A multiplier is given by

$$
\begin{aligned}
s_{2A}(t) &= \left[s_{1I}(t)\cos(2\pi f_c t) + s_{1Q}(t)\sin(2\pi f_c t)\right]\cos(2\pi f_c t) \\
&= \frac{s_{1I}(t)}{2}\left[1+\cos(4\pi f_c t)\right] + \frac{s_{1Q}(t)}{2}\sin(4\pi f_c t)
\end{aligned}
\tag{4-12}
$$

Since the double-frequency terms will not appear at the output of the lowpass filter, the signal output of the Channel A lowpass filter is

$$
s_{3A}(t) = \frac{s_{1I}(t)}{2} \tag{4-13}
$$

Likewise, the signal output from the Channel B lowpass filter is

$$S_{3B}(t) = \frac{S_{1Q}(t)}{2} \tag{4-14}$$

The output of the Channel A integrator (at the sampling instant T_A) resulting from all m bits of Channel A and all n bits of Channel B is given by

$$\begin{aligned}
S_{4A}(T_A) &= \int_0^{T_A} S_{3A}(t)\,dt \\
&= \int_0^{T_A} \left\{ \sum_{m=-\infty}^{\infty} \frac{A_m}{\pi} \int_0^{\frac{\pi B_{IF} T_A}{2}} \frac{[2y^2 - (2\pi f_c T_A)^2] \sin y}{y[y^2 - (2\pi f_c T_A)^2} \cos\left\{\left[2\left(\tfrac{t}{T_A}\right) - (1+2m)\right] y\right\} dy \right\} dt \\
&+ \int_0^{T_A} \left\{ \sum_{n=-\infty}^{\infty} B_n f_c T_B \int_0^{\frac{\pi B_{IF} T_B}{2}} \frac{2 \sin y}{y^2 - (2\pi f_c T_B)^2} \sin\left\{\left[2\left(\tfrac{t}{T_B}\right) - (1+2n)\right] y\right\} dy \right\} dt \\
&= \sum_{m=-\infty}^{\infty} \frac{A_m}{\pi} \int_0^{\frac{\pi B_{IF} T_A}{2}} \frac{[2y^2 - (2\pi f_c T_A)^2] \sin y}{y[y^2 - (2\pi f_c T_A)^2]} \left\{ \int_0^{T_A} \cos\left\{\left[2\left(\tfrac{t}{T_A}\right) - (1+2m)\right] y\right\} dt \right\} dy \\
&+ \sum_{n=-\infty}^{\infty} B_n f_c T_B \int_0^{\frac{\pi B_{IF} T_B}{2}} \frac{2 \sin y}{y^2 - (2\pi f_c T_B)^2} \left\{ \int_0^{T_A} \sin\left\{\left[2\left(\tfrac{t}{T_B}\right) - (1+2n)\right] y\right\} dt \right\} dy \\
&= \sum_{m=-\infty}^{\infty} \frac{A_m T_A}{\pi} \int_0^{\frac{\pi B_{IF} T_A}{2}} \frac{[2y^2 - (2\pi f_c T_A)^2] \sin(y) \sin(y) \cos(2my)}{y^2[y^2 - (2\pi f_c T_A)^2]} dy \\
&- \sum_{n=-\infty}^{\infty} 2 B_n f_c T_B^2 \int_0^{\frac{\pi B_{IF} T_B}{2}} \frac{\sin(y) \sin\left[\left(\frac{T_A}{T_B}\right) y\right] \sin\left[\left(1 - \frac{T_A}{T_B} + 2n\right) y\right]}{y[y^2 - (2\pi f_c T_B)^2]} dy
\end{aligned} \tag{4-15}$$

The signal output of the Channel B integrator at the sampling instant T_B is similarly given by

$$\begin{aligned}
S_{4B}(T_B) &= \int_0^{T_B} S_{3B}(t)\,dt \\
&= \int_0^{T_B} \left\{ \sum_{m=-\infty}^{\infty} \frac{A_m}{\pi} \int_0^{\frac{\pi B_{IF} T_A}{2}} \frac{2\pi f_c T_A \sin y}{y^2 - (2\pi f_c T_A)^2} \sin\left\{\left[2\left(\tfrac{t}{T_A}\right) - (1+2m)\right] y\right\} dy \right\} dt \\
&- \int_0^{T_B} \left\{ \sum_{n=-\infty}^{\infty} B_n f_c T_B \int_0^{\frac{\pi B_{IF} T_B}{2}} \frac{4\pi f_c T_B \sin y}{y[y^2 - (2\pi f_c T_B)^2]} \cos\left\{\left[2\left(\tfrac{t}{T_B}\right) - (1+2n)\right] y\right\} dy \right\} dt
\end{aligned}$$

$$= \sum_{m=-\infty}^{\infty} \frac{A_m}{\pi} \int_0^{\frac{\pi B_{IF} T_A}{2}} \frac{2\pi f_c T_A \sin y}{y^2 - (2\pi f_c T_A)^2} \left\{ \int_0^{T_B} \sin\left\{\left[2\left(\frac{t}{T_A}\right) - (1+2m)\right] y\right\} dt \right\} dy$$

$$- \sum_{n=-\infty}^{\infty} B_n f_c T_B \int_0^{\frac{\pi B_{IF} T_B}{2}} \frac{4\pi f_c T_B \sin y}{y\left[y^2 - (2\pi f_c T_B)^2\right]} \left\{ \int_0^{T_B} \cos\left\{\left[2\left(\frac{t}{T_B}\right) - (1+2n)\right] y\right\} dt \right\} dy$$

$$= -\sum_{m=-\infty}^{\infty} 2A_m f_c T_A^2 \int_0^{\frac{\pi B_{IF} T_A}{2}} \frac{\sin(y) \sin\left[\left(\frac{T_B}{T_A}\right) y\right] \sin\left[\left(1 - \frac{T_B}{T_A} + 2m\right) y\right]}{y\left[y^2 - (2\pi f_c T_B)^2\right]} dy$$

$$+ \sum_{n=-\infty}^{\infty} \frac{B_n T_B}{\pi} \int_0^{\frac{\pi B_{IF} T_B}{2}} \frac{\left[-(2\pi f_c T_B)^2\right] \sin(y) \sin(y) \cos(2my)}{y^2\left[y^2 - (2\pi f_c T_B)^2\right]} dy \qquad (4\text{-}16)$$

Inspection of (4-15) and (4-16) reveals the presence of both a desired signal term and an undesired crosstalk term at the output of each integrator. As could be expected, the signal terms in Channels A and B are identical in form, as are the crosstalk terms. The computation of error probability, therefore, is identical for each channel. Consequently, these computations wll be made only for Channel A.

From (4-15), the signal voltage for Channel A is seen to be

$$S_{4A,signal}(T_A) = \sum_{m=-\infty}^{\infty} \frac{A_m T_A}{\pi} \int_0^{\frac{\pi B_{IF} T_A}{2}} \frac{\left[2y^2 - (2\pi f_c T_A)^2\right] \sin(y) \sin(y) \cos(2my)}{y^2\left[y^2 - (2\pi f_c T_A)^2\right]} dy \qquad (4\text{-}17)$$

and the crosstalk voltage is seen to be

$$S_{4A,crosstalk}(T_A) = -\sum_{n=-\infty}^{\infty} 2B_n f_c T_B^2 \int_0^{\frac{\pi B_{IF} T_B}{2}} \frac{\sin(y) \sin\left[\left(\frac{T_A}{T_B}\right) y\right] \sin\left[\left(1 - \frac{T_A}{T_B} + 2n\right) y\right]}{y\left[y^2 - (2\pi f_c T_B)^2\right]} dy \qquad (4\text{-}18)$$

Appendix B shows that the signal voltage can be reduced to

$$S_{4A,signal}(T_A) = \sum_{m=-\infty}^{\infty} \frac{A_m T_A}{2} \left[\Psi_{I1}(m) - \Psi_{I2}(m)\right] \qquad (4\text{-}19)$$

where

$$\Psi_{I1}(m) = \frac{2}{\pi}\int_0^{\frac{\pi B_{IF}T_A}{2}} \frac{\sin^2(y)\cos(2my)}{y^2}\,dy$$

and

$$\Psi_{I2}(m) = \frac{2}{\pi}\int_0^{\frac{\pi B_{IF}T_A}{2}} \frac{\sin^2(y)\cos(2my)}{(2\pi f_c T_A)^2 - y^2}\,dy$$

The expression for the Channel A output signal given by (4-19) is identical to that derived in [9] for bandlimited PSK transmission. The $\Psi_{I_1}(o)$ term indicates an amplitude reduction in the bit being detected (o^{th} bit) while the $\Psi_{I_1}(m)$ terms for $m \neq 0$ define the intersymbol interference (contributions due to all previous and subsequent bits). The $\Psi_{I_2}(m)$ terms result because of *aliasing* or because the ratio of carrier frequency (f_c) to bit rate ($1/T_A$) is not infinite.

Appendix B also shows that the crosstalk voltage at the output of Channel A can be reduced to

$$s_{4A,\,crosstalk}(T_A) = \sum_{n=-\infty}^{\infty} \frac{B_n T_B}{2}\left(\frac{1}{2\pi f_c T_B}\right)\left[\Psi_{I3}(n) - \Psi_{I4}(n)\right] \tag{4-20}$$

where

$$\Psi_{I3}(n) = \frac{2}{\pi}\int_0^{\frac{\pi B_{IF}T_B}{2}} \frac{\sin(y)\sin\left[\left(\frac{T_A}{T_B}\right)y\right]\sin\left[\left(1-\frac{T_A}{T_B}+2n\right)y\right]}{y}\,dy$$

and

$$\Psi_{I4}(n) = \frac{2}{\pi}\int_0^{\frac{\pi B_{IF}T_B}{2}} \frac{y\sin(y)\sin\left[\left(\frac{T_A}{T_B}\right)y\right]\sin\left[\left(1-\frac{T_A}{T_B}+2n\right)y\right]}{y^2-(2\pi f_c T_B)^2}\,dy$$

The total voltage at the output of Channel A (at the sampling instant T_A) is

$$e_{4A}(T_A) = \sum_{m=-\infty}^{\infty} \frac{A_m T_A}{2}\left[\Psi_{I_1}(m) - \Psi_{I2}(m)\right] + \sum_{n=-\infty}^{\infty} \frac{B_n T_B}{2}\left(\frac{1}{2\pi f_c T_B}\right)\left[\Psi_{I3}(n) - \Psi_{I4}(n)\right] + \underset{\sim}{n}_{out}(T_A) \tag{4-21}$$

The signal and crosstalk terms are deterministic and can be evaluated directly for specific sequences of bits in Channel A and Channel B. As discussed in Chapter II, if all possible sequences of finite length are considered, an averaging method could be applied to obtain a solution for error probability. The noise voltage $\underset{\sim}{n}_{out}(T_A)$ is a random variable, however, and only certain of its statistical properties can be determined. As shown in Appendix C, the noise *power* at the output of Channel A is given by

$$\sigma_n^2 = \frac{N_o T_A}{4} \Psi_{I_1}(o) \tag{4-22}$$

where $\Psi_{I_1}(o)$ is as previously defined.

Although error probability could be determined in a straightforward manner using an averaging method, it was previously noted that such an approach has the disadvantage of requiring excessive computational time, even when a very high-speed computer is used. To overcome this disadvantage, a series expansion procedure similar to that followed by Shimbo and Celebiler [13] and later by Tu [9] for PSK systems will be applied here. The details of this approach are contained in Appendix D. The resultant expression for the bit error probability is

$$P_e = \frac{1}{2}\left\{ 1 - \operatorname{erf}\sqrt{\frac{A^2T_A}{2N_0}\,\frac{\left[\Psi_{I_1}(0) - \Psi_{I_2}(0)\right]^2}{\Psi_{I_1}(0)}} - \sum_{i=1}^{\infty} 2b_{2i}(-1)^i G_{2i-1} - \sum_{k=1}^{\infty} 2h_{2k}(-1)^k G_{2k-1} - \sum_{i=1}^{\infty}\sum_{k=1}^{\infty} 2b_{2i}h_{2k}(-1)^{i+k} G_{2i+2k-1} \right\} \qquad (4\text{-}23)$$

where the b_{2i} are defined by (D-27), the h_{2k} are defined by (D-28), and the G_j are defined by (D-36). In order to compute the error probability for a given value of $A^2T_A/2N_o$ (the Channel A energy per bit per single-sided noise spectral density), the recursive relationships for b_{2i}, h_{2k}, and G_j given by (D-44), (D-51), and (D-37), respectively, must be used.

It should be noted that the expression for bit error probability given by (4-23) is actually valid only for Channel A. However, it was previously observed that the error probability computation for Channel B is identical to that for Channel A. Thus if such a computation is to be made for Channel B, the $A^2T_A/2N_o$ term in (4-23) can simply be replaced by $B^2T_B/2N_o$. Since $\Psi_{I_1}(m)$ and $\Psi_{I_2}(m)$, and therefore b_{2i} and G_j, were originally defined in terms of the parameters m, A, and T_A, it is also necessary to substitute the parameters n, B, and T_B into the appropriate expressions. Likewise, since the h_{2k} were originally defined in terms of $\Psi_{I_3}(n)$ and $\Psi_{I_4}(n)$ which, in turn, were dependent on the parameters n, B/A, and T_B/T_A, it is necessary to substitute m, A/B, and T_A/T_B into the appropriate expressions.

It is convenient at this point to express (4-23) in the form

$$P_e = P_{e1} + P_{e2} + P_{e3} + P_{e4} \qquad (4\text{-}24)$$

where

$$P_{e_1} = \frac{1}{2}\left\{1 - \operatorname{erf}\sqrt{\frac{A^2 T_A}{2N_0}\,\frac{[\Psi_{I1}(0) - \Psi_{I2}(0)]^2}{\Psi_{I1}(0)}}\right\}$$

$$P_{e2} = \sum_{i=1}^{\infty} 2\,b_{2i}\,(-1)^{i+1} G_{2i-1}$$

$$P_{e3} = \sum_{k=1}^{\infty} 2\,h_{2k}\,(-1)^{k+1} G_{2k-1}$$

$$P_{e4} = \sum_{i=1}^{\infty}\sum_{k=1}^{\infty} 2\,b_{2i}\,h_{2k}\,(-1)^{i+k+1} G_{2i+2k-1}$$

The first term (P_{e_1}) in (4-24) represents the contribution to the total probability of error due to the bit being detected. It can be observed that the energy per bit per single-sided noise spectral density for the bit under detection is degraded by the factor $\frac{[\Psi_{I_1}(o) - \Psi_{I_2}(o)]^2}{\Psi_{I_1}(o)}$, which results from bandlimiting the signal and noise. Recall that the term $\Psi_{I_1}(o)$ represents an amplitude reduction in the bit being detected ($m = 0$), and that the term $\Psi_{I_2}(o)$ represents an additional degradation which results because of aliasing. For a large value of $f_c T_A$, the $\Psi_{I_2}(o)$ term is very small, and the energy per bit per single sided noise spectral density for the bit under detection is degraded only by the factor $\Psi_{I_1}(o)$.

A review of the derivations outlined in Appendix D reveals that the second term (P_{e_2}) in (4-24) represents the contribution to the total probability of error due to intersymbol interference (and aliasing) on the bit under detection. Equation (D-37) shows that the G_{2i-1} terms in the expression for P_{e_2} are affected only by $\left[\Psi_{I_1}(0) - \Psi_{I_2}(o)\right]$, but (D-41) and (D-44) indicate that the b_{2j} terms are dependent on $\left[\Psi_{I_1}(m) - \Psi_{I_2}(m)\right]$ for all m not equal to zero.

From Appendix D it can also be seen that the third term (P_{e_3}) in (4-24) represents the contribution to the total probability of error due to cross-talk from Channel B. The G_{2k-1} terms are still affected only by $\left[\Psi_{I_1}(o) - \Psi_{I_2}(o)\right]$, but (D-51) and (D-49) indicate that the h_{2k} terms are dependent on $\left[\Psi_{I_3}(n) - \Psi_{I_4}(n)\right]$ for all n.

The significance of the fourth term (P_{e_4}) in (4-24) is not intuitively obvious, since Appendix D shows it to result from a cross-product due to the multiplication of the characteristic functions of the intersymbol interference and crosstalk terms.

In order to obtain numerical results for bit error probability, it is necessary to assume that the effects of intersymbol interference and crosstalk are confined to a finite number of bits preceding and following the bit under detection. To assist in determining how many bits must be considered, numerical solutions for $\Psi_{I_1}(m)$, $\Psi_{I_2}(m)$, $\Psi_{I_3}(n)$, and $\Psi_{I_4}(n)$ were first obtained. Table 4.1 shows values of $\Psi_{I_1}(m)$ for various values of $B_{IF}T_A$ and for various bit positions. Note from (4-19) that the integrand of $\Psi_{I_1}(m)$ is an even function of m and therefore that computations need not be made for negative values of m.

The numbers presented in Table 4.1 satisfy previous observations regarding the significance of the $\Psi_{I_1}(m)$. The term $\Psi_{I_1}(o)$ represents the amplitude of the bit being detected, and a finite IF filter bandwidth should cause $\Psi_{I_1}(o)$ to be less than unity. Table 4.1 indicates that as the IF filter bandwidth increases ($B_{IF}T_A \to \infty$), $\Psi_{I_1}(o) \to 1$ and that as the filter bandwidth decreases ($B_{IF}T_A \to 1$), $\Psi_{I_1}(o)$ does become smaller. The $\Psi_{I_1}(m)$ for $m \neq 0$ represent intersymbol interference from bits preceding

Table 4.1. - Some values of $\Psi_{I_1}(m)$

$B_{IF}T_A$	$\Psi_{I_1}(0)$	$\Psi_{I_1}(1)$	$\Psi_{I_1}(2)$	$\Psi_{I_1}(3)$	$\Psi_{I_1}(4)$	$\Psi_{I_1}(5)$	$\Psi_{I_1}(6)$
1.0	0.7737	0.1291	-0.0222	0.0094	-0.0052	0.0033	-0.0023
1.2	0.8393	0.0673	0.0292	-0.0271	0.0152	-0.0028	-0.0063
1.6	0.8960	0.0433	0.0033	0.0054	0.0031	-0.0012	-0.0029
2.0	0.9028	0.0471	0.0012	0.0002	0.0001	0.0000	0.0000
2.4	0.9066	0.0493	0.0002	-0.0025	-0.0017	0.0004	0.0013
2.8	0.9218	0.0440	-0.0082	0.0051	-0.0023	0.0001	0.0014
3.0	0.9311	0.0353	-0.0011	0.0004	-0.0002	0.0001	0.0014
4.0	0.9499	0.0248	0.0002	0.0000	0.0000	0.0000	0.0000
5.0	0.9592	0.0206	-0.0003	0.0001	-0.0000	0.0000	0.0000

and following the bit under detection. Intuitively, the interference resulting from more remote bits ($|m| >> 0$) should be less than from bits closer to the bit being detected. Table 4.1 verifies this observation. Note that for any particular filter bandwidth, $|\Psi_{I_1}(m)|$ generally decreases with increasing m. Also note that for any particular value of m, $|\Psi_{I_1}(m)| \to 0$ as $B_{IF}T_A \to \infty$.

Table 4.2 shows values of $\Psi_{I_2}(m)$ for various values of f_cT_A, $B_{IF}T_A$, and for various bit positions. Since, from (4-19), the integrand of $\Psi_{I_2}(m)$ is an even function of m, computations need not be made for negative values of m. The $\Psi_{I_2}(m)$ terms represent signal degradations which result from aliasing. Note that for any particular values of m and $B_{IF}T_A$, $|\Psi_{I_2}(m)| \to 0$ as $f_cT_A \to \infty$. Also note that for any given values of f_cT_A and $B_{IF}T_A$, $|\Psi_{I_2}(m)|$ generally decreases with increasing m.

Values of $\Psi_{I_3}(n)$ are shown in Table 4.3 for various values of T_A/T_B, $B_{IF}T_B$, and n. Although values are shown only for positive values of n, it can be seen from (4-20) that it is actually necessary to compute $\Psi_{I_3}(n)$ for negative values as well. For the special case when $T_A = T_B$, $\Psi_{I_3}(n)$ is an odd function of n and values need not be computed for negative values of n.

As previously observed, the $\Psi_{I_3}(n)$ terms represent signal degradations which result because of crosstalk from the bit stream in Channel B. Table 4.3 shows that the $\Psi_{I_3}(n)$ are generally less significant for larger values of n. It is interesting to note that $\Psi_{I_3}(o)$ is always zero when $T_A = T_B$. That this should be the case is readily seen by substituting $T_A = T_B$ into the defining expression for $\Psi_{I_3}(n)$ given by (4-20).

Table 4.2. - Some values of $\Psi_{I_2}(m)$

f_cT_A	$B_{IF}T_A$	$\Psi_{I_2}(0)$	$\Psi_{I_2}(1)$	$\Psi_{I_2}(2)$	$\Psi_{I_2}(3)$	$\Psi_{I_2}(4)$	$\Psi_{I_2}(5)$	$\Psi_{I_2}(6)$
1	1.0	0.0131	-0.0067	0.0001	-0.0000	0.0000	-0.0000	0.0000
	1.2	0.0184	-0.0116	0.0042	-0.0028	0.0013	-0.0001	-0.0007
	1.6	0.0258	-0.0144	0.0003	0.0011	0.0007	-0.0002	-0.0006
	2.0	0.0273	-0.0135	-0.0001	-0.0000	-0.0000	-0.0000	-0.0000
	3.0	0.0511	-0.0267	0.0016	-0.0006	0.0003	-0.0002	0.0001
	5.0	0.0575	-0.0300	0.0016	-0.0006	0.0003	-0.0002	0.0001
2	1.0	0.0032	-0.0016	0.0000	-0.0000	0.0000	-0.0000	0.0000
	1.2	0.0044	-0.0028	0.0010	-0.0006	0.0003	-0.0000	-0.0002
	1.6	0.0061	-0.0034	0.0001	0.0002	0.0001	-0.0000	-0.0001
	2.0	0.0064	-0.0032	0.0000	-0.0000	-0.0000	-0.0000	-0.0000
	3.0	0.0100	-0.0050	0.0000	-0.0000	0.0000	-0.0000	0.0000
	5.0	0.0187	-0.0094	0.0001	-0.0000	0.0000	-0.0000	0.0000
3	1.0	0.0014	-0.0007	0.0000	-0.0000	0.0000	-0.0000	0.0000
	1.2	0.0020	-0.0012	0.0004	-0.0003	0.0001	-0.0000	-0.0001
	1.6	0.0027	-0.0015	0.0000	0.0001	0.0001	-0.0000	-0.0001
	2.0	0.0028	-0.0014	-0.0000	-0.0000	-0.0000	-0.0000	-0.0000
	3.0	0.0043	-0.0022	0.0000	-0.0000	0.0001	-0.0000	0.0000
	5.0	0.0075	-0.0038	0.0000	-0.0000	0.0000	-0.0000	0.0000
5	1.0	0.0005	-0.0003	0.0000	-0.0000	0.0000	-0.0000	0.0000
	1.2	0.0007	-0.0004	0.0002	-0.0001	0.0000	-0.0000	-0.0000
	1.6	0.0010	-0.0005	0.0000	0.0000	0.0000	-0.0000	-0.0000
	2.0	0.0010	-0.0005	-0.0000	-0.0000	-0.0000	-0.0000	-0.0000
	3.0	0.0015	-0.0008	0.0000	-0.0000	0.0000	-0.0000	0.0000
	5.0	0.0026	-0.0013	0.0000	-0.0000	0.0000	-0.0000	0.0000
10	1.0	0.0001	-0.0001	0.0000	-0.0000	0.0000	-0.0000	0.0000
	1.2	0.0002	-0.0001	0.0000	-0.0000	0.0000	-0.0000	-0.0000
	1.6	0.0002	-0.0001	0.0000	0.0000	0.0000	-0.0000	-0.0000
	2.0	0.0003	-0.0001	-0.0000	-0.0000	-0.0000	-0.0000	-0.0000
	3.0	0.0004	-0.0002	0.0000	-0.0000	0.0000	-0.0000	0.0000
	5.0	0.0006	-0.0003	0.0000	-0.0000	0.0000	-0.0000	0.0000

Table 4.3. - Some values of $\Psi_{I_3}(n)$

T_A/T_B	$B_{IF}T_B$	$\Psi_{I_3}(0)$	$\Psi_{I_3}(1)$	$\Psi_{I_3}(2)$	$\Psi_{I_3}(3)$	$\Psi_{I_3}(4)$	$\Psi_{I_3}(5)$	$\Psi_{I_3}(6)$
0.01	1.0	0.0050	0.0000	-0.0000	0.0000	-0.0000	0.0000	-0.0000
	1.2	0.0069	-0.0017	0.0013	-0.0007	0.0002	0.0001	-0.0004
	1.6	0.0095	-0.0011	-0.0008	-0.0001	0.0004	0.0002	-0.0001
	2.0	0.0100	-0.0000	-0.0000	-0.0000	-0.0000	-0.0000	-0.0000
	3.0	0.0150	0.0001	-0.0001	0.0000	-0.0000	0.0000	-0.0000
	5.0	0.0248	0.0002	-0.0001	0.0001	-0.0001	0.0000	-0.0000
0.10	1.0	0.0471	0.0039	-0.0021	0.0015	-0.0011	0.0009	-0.0008
	1.2	0.0666	-0.0142	0.0124	-0.0082	0.0035	0.0005	-0.0031
	1.6	0.0954	-0.0136	-0.0071	0.0008	0.0042	0.0018	-0.0018
	2.0	0.1030	-0.0027	-0.0008	-0.0004	-0.0002	-0.0002	-0.0001
	3.0	0.1353	-0.0110	-0.0060	0.0041	-0.0032	0.0026	-0.0022
	5.0	0.2073	-0.0161	-0.0087	0.0060	-0.0046	0.0038	-0.0032
1.00	1.0	0.0000	0.3638	-0.1099	0.0699	-0.0516	0.0410	-0.0341
	1.2	0.0000	0.3311	-0.0506	-0.0056	0.0277	-0.0307	0.0222
	1.6	0.0000	0.2283	-0.0230	0.0055	-0.0074	-0.0084	-0.0003
	2.0	0.0000	0.2139	0.0077	0.0020	0.0008	0.0004	0.0002
	3.0	0.0000	0.2915	-0.0390	0.0238	-0.0174	0.0138	-0.0114
	5.0	0.0000	0.2752	-0.0235	0.0143	-0.0105	0.0083	-0.0068

Table 4.4 shows values of $\Psi_{I_4}(n)$ for various values of f_cT_B, T_A/T_B, $B_{IF}T_B$, and n. As for the computation of $\Psi_{I_3}(n)$, it is actually necessary to compute $\Psi_{I_4}(n)$ for negative values of n except for the special case of $T_A = T_B$. Table 4.4 indicates that the $\Psi_{I_4}(n)$ are generally less significant for the larger values of n. Again, for the special case when $T_A = T_B$, it can be observed that $\Psi_{I_4}(o) = 0$ for all values of f_cT_B and $B_{IF}T_B$. It can also be observed that $|\Psi_{I_4}(n)|$ decreases for all n as f_cT_B increases.

Tables 4.1 through 4.4 indicate that $\Psi_{I_1}(m)$, $\Psi_{I_2}(m)$, $\Psi_{I_3}(n)$, and $\Psi_{I_4}(n)$ generally are negligibly small for values of m and n greater than about 5. Values of P_e were computed for several cases of interest, using $|m| \leq 5$ and $|n| \leq 5$. The effects of intersymbol interference and crosstalk were therefore assumed to be limited to the 10 bits closest to the bit under detection.

The results of these P_e calculations will now be summarized.

Single-Channel (Balanced Power) Results

As pointed out in Chapter III, *single-channel operation* refers to the case in which a serial to parallel device converts a signal of rate R bits/second to two parallel signals each of rate $R/2$ bits/second. These two parallel signals are then applied to the inputs of the two quadrature channels of the QPSK modulator. After QPSK demodulation and after independent bit detection processes have been performed, the two parallel signals are recombined to form an estimate of the original signal of rate R bits/second. If equal transmit powers are allocated to each of the two QPSK

Table 4.4. - Some values of $\Psi_{I_4}(n)$

f_cT_B	T_A/T_B	$B_{IF}T_B$	$\Psi_{I_4}(0)$	$\Psi_{I_4}(1)$	$\Psi_{I_4}(2)$	$\Psi_{I_4}(3)$	$\Psi_{I_4}(4)$	$\Psi_{I_4}(5)$	$\Psi_{I_4}(6)$
1	0.01	1.0	0.0050	0.0000	-0.0000	0.0000	-0.0000	0.0000	-0.0000
		1.2	0.0069	-0.0017	0.0013	-0.0007	0.0002	0.0001	-0.0004
		1.6	0.0095	-0.0011	-0.0008	-0.0001	0.0004	0.0002	-0.0001
		2.0	0.0100	-0.0000	-0.0000	-0.0000	-0.0000	-0.0000	-0.0000
		3.0	0.0149	0.0001	-0.0001	0.0000	-0.0000	0.0000	-0.0000
		5.0	0.0247	0.0002	-0.0001	0.0001	-0.0001	0.0000	-0.0000
	0.10	1.0	0.0360	0.0025	-0.0014	0.0010	-0.0007	0.0006	-0.0005
		1.2	0.0507	-0.0111	0.0094	-0.0062	0.0025	0.0005	- .0024
		1.6	0.0723	-0.0100	-0.0055	0.0004	0.0031	0.0015	-0.0013
		2.0	0.0778	-0.0017	-0.0005	-0.0003	-0.0002	-0.0001	-0.0001
		3.0	0.1046	0.0071	-0.0039	0.0027	-0.0021	0.0017	-0.0014
		5.0	0.1638	0.0106	-0.0058	0.0040	-0.0031	0.0025	-0.0021
	1.00	1.0	0.0000	-0.0082	0.0077	-0.0048	0.0035	-0.0028	0.0023
		1.2	0.0000	-0.0053	0.0026	0.0017	0.0032	0.0031	-0.0021
		1.6	0.0000	0.0086	-0.0059	-0.0016	0.0013	0.0017	0.0002
		2.0	0.0000	0.0117	-0.0024	-0.0007	-0.0003	-0.0001	-0.0001
		3.0	0.0000	-0.0479	0.0465	-0.0298	0.0221	-0.0176	0.0146
		5.0	0.0000	0.3139	-0.0615	0.0389	-0.0287	0.0228	-0.0189
2	0.01	1.0	0.0049	0.0000	-0.0000	0.0000	-0.0000	0.0000	-0.0000
		1.2	0.0068	-0.0017	0.0012	-0.0007	0.0002	0.0001	-0.0004
		1.6	0.0094	-0.0011	-0.0008	-0.0001	0.0004	0.0002	-0.0001
		2.0	0.0099	-0.0000	-0.0000	-0.0000	-0.0000	-0.0000	-0.0000
		3.0	0.0148	0.0001	-0.0001	0.0000	-0.0000	0.0000	-0.0000
		5.0	0.0246	0.0002	-0.0001	0.0001	-0.0001	0.0000	-0.0000
	0.10	1.0	0.0121	-0.0004	0.0002	-0.0002	0.0001	-0.0001	0.0001
		1.2	0.0167	-0.0043	0.0030	-0.0017	0.0004	0.0005	-0.0009
		1.6	0.0225	-0.0022	-0.0020	-0.0003	0.0009	9.0007	-0.0002
		2.0	0.0234	0.0003	0.0001	0.0000	0.0003	0.0002	0.0000
		3.0	0.0378	-0.0010	0.0005	-0.0004	0.0003	-0.0002	0.0002
		5.0	0.0678	-0.0008	0.0004	-0.0003	0.0002	-0.0002	0.0001
	1.00	1.0	0.0000	-0.0020	0.0019	-0.0011	0.0008	-0.0007	0.0005
		1.2	0.0000	-0.0013	0.0007	0.0004	-0.0007	0.0007	-0.0005
		1.6	0.0000	0.0018	-0.0013	-0.0003	0.0003	0.0004	0.0000
		2.0	0.0000	0.0025	-0.0006	-0.0001	-0.0001	-0.0000	-0.0000
		3.0	0.0000	-0.0068	0.0064	-0.0039	0.0029	-0.0023	0.0019
		5.0	0.0000	-0.0159	0.0149	-0.0092	0.0067	-0.0053	0.0044

Table 4.4. - Some values of $\Psi_{I_4}(n)$ (continued)

f_cT_B	T_A/T_B	$B_{IF}T_B$	$\Psi_{I_4}(0)$	$\Psi_{I_4}(1)$	$\Psi_{I_4}(2)$	$\Psi_{I_4}(3)$	$\Psi_{I_4}(4)$	$\Psi_{I_4}(5)$	$\Psi_{I_4}(6)$
5	0.01	1.0	0.0047	0.0000	-0.0000	0.0000	-0.0000	0.0000	-0.0000
		1.2	0.0065	-0.0016	0.0012	-0.0007	0.0002	0.0001	-0.0003
		1.6	0.0089	-0.0010	-0.0007	-0.0000	0.0004	0.0002	-0.0001
		2.0	0.0094	-0.0000	-0.0000	-0.0000	-0.0000	-0.0000	-0.0000
		3.0	0.0140	0.0001	-0.0001	0.0000	-0.0000	0.0000	-0.0000
		5.0	0.0232	0.0002	-0.0001	0.0001	-0.0001	0.0000	-0.0000
	0.10	1.0	-0.0001	0.0000	-0.0000	0.0000	0.0000	-0.0000	0.0000
		1.2	-0.0001	0.0000	-0.0000	0.0000	-0.0000	-0.0000	0.0000
		1.6	-0.0003	0.0001	0.0000	-0.0000	-0.0000	-0.0000	0.0000
		2.0	-0.0003	-0.0000	0.0000	0.0000	0.0000	0.0000	0.0000
		3.0	-0.0010	-0.0001	0.0001	-0.0001	0.0001	-0.0001	0.0000
		5.0	-0.0036	-0.0009	0.0005	-0.0004	0.0003	-0.0002	0.0002
	1.00	1.0	0.0000	-0.0003	0.0003	-0.0002	0.0001	-0.0001	0.0001
		1.2	0.0000	-0.0002	0.0001	0.0001	-0.0001	0.0001	-0.0001
		1.6	0.0000	0.0003	-0.0002	-0.0001	0.0000	0.0001	0.0000
		2.0	0.0000	0.0004	-0.0001	-0.0000	-0.0000	-0.0000	-0.0000
		3.0	0.0000	-0.0010	0.0009	-0.0006	0.0004	-0.0003	0.0003
		5.0	0.0000	-0.0017	0.0016	-0.0010	0.0007	-0.0006	0.0004
10	0.01	1.0	0.0038	0.0000	-0.0000	0.0000	-0.0000	0.0000	-0.0000
		1.2	0.0052	-0.0013	0.0010	-0.0006	0.0002	0.0001	-0.0003
		1.6	0.0072	-0.0008	-0.0006	-0.0000	0.0003	0.0002	-0.0001
		2.0	0.0076	-0.0000	-0.0000	-0.0000	-0.0000	-0.0000	-0.0000
		3.0	0.0113	0.0001	-0.0000	0.0000	-0.0000	0.0000	-0.0000
		5.0	0.0188	0.0001	-0.0001	0.0000	-0.0000	0.0000	-0.0000
	0.10	1.0	-0.0000	0.0000	-0.0000	0.0000	0.0000	-0.0000	0.0000
		1.2	-0.0000	0.0000	-0.0000	0.0000	-0.0000	-0.0000	0.0000
		1.6	-0.0001	0.0000	0.0000	-0.0000	-0.0000	-0.0000	0.0000
		2.0	-0.0001	-0.0000	0.0000	0.0000	0.0000	0.0000	0.0000
		3.0	-0.0002	-0.0000	0.0000	-0.0000	0.0000	-0.0000	0.0000
		5.0	-0.0009	-0.0002	0.0001	-0.0001	0.0001	-0.0001	0.0000
	1.00	1.0	0.0000	-0.0001	0.0001	-0.0000	0.0000	-0.0000	0.0000
		1.2	0.0000	-0.0001	0.0000	0.0000	-0.0000	0.0000	-0.0000
		1.6q	0.0000	0.0001	-0.0000	-0.0000	0.0000	0.0000	0.0000
		2.0	0.0000	0.0001	-0.0000	-0.0000	-0.0000	-0.0000	-0.0000
		3.0	0.0000	-0.0002	0.0002	-0.0001	0.0001	-0.0001	0.0001
		5.0	0.0000	-0.0004	0.0003	-0.0002	0.0002	-0.0001	0.0001

channels, the bit error probabilities will be the same for both channels. Computation of error probability thus need only be performed for one of the two channels.

Tables 4.5 through 4.7 show values of P_{e_1}, P_{e_2}, P_{e_3}, P_{e_4}, and total error probability, P_e, for various signal-to-noise ratios (E_{bA}/N_o) and for various values of $B_{IF}T_A$ and f_cT_A. From Table 4.5, it can be seen that when f_cT_A is high (corresponding to a large number of carrier cycles per bit) and $B_{IF}T_A$ is low, the QPSK transmission system is noise-limited (P_{e_1} dominates) at low signal-to-noise ratios and intersymbol interference-limited (P_{e_2} dominates) at high signal-to-noise ratios. However, Table 4.7 shows that when f_cT_A and $B_{IF}T_A$ are both low, crosstalk (P_{e_3} and P_{e_4} terms) becomes very significant at high signal-to-noise ratios.

Although it is very often assumed that the carrier frequency is much higher than the data rate, such an assumption is not always valid in practical situations. Even though the RF carrier frequency for a practical QPSK transmission system might be much higher than the data rate, hardware considerations would probably dictate that the QPSK demodulation process be performed at some intermediate frequency. This intermediate frequency could well be comparable to the data rate. The values of f_cT_A used in Tables 4.5 through 4.7 are therefore considered to be representative of practical transmission systems.

To provide additional insight into the performance of bandlimited QPSK systems, the results presented in Tables 4.5, 4.6, and 4.7 are plotted in Figs. 4.4, 4.5, and 4.6, respectively. It should be noted that the

Table 4.5. - Error probability results for single-channel QPSK transmission with ideal rectangular filtering ($f_c T_A = 10$)

$B_{IF}T_A$	$\frac{E_{bA}}{N_o}$ (dB)	P_{e_1}	P_{e_2}	P_{e_3}	P_{e_4}	P_e
1.0	0	1.068×10^{-1}	1.002×10^{-2}	2.352×10^{-5}	-1.498×10^{-6}	1.168×10^{-1}
	2	5.870×10^{-2}	1.282×10^{-2}	2.985×10^{-5}	-1.322×10^{-6}	7.155×10^{-2}
	4	2.435×10^{-2}	1.304×10^{-2}	2.909×10^{-5}	1.875×10^{-6}	3.742×10^{-2}
	6	6.540×10^{-3}	9.574×10^{-3}	1.864×10^{-5}	8.637×10^{-6}	1.614×10^{-2}
	8	8.917×10^{-4}	4.537×10^{-3}	6.148×10^{-6}	1.285×10^{-5}	5.448×10^{-3}
	10	4.196×10^{-5}	1.227×10^{-3}	7.087×10^{-7}	8.960×10^{-6}	1.278×10^{-3}
	12	3.689×10^{-7}	1.617×10^{-4}	1.547×10^{-8}	2.827×10^{-6}	1.649×10^{-4}
1.5	0	9.128×10^{-2}	9.976×10^{-4}	7.674×10^{-6}	-4.288×10^{-8}	9.228×10^{-2}
	2	4.667×10^{-2}	1.186×10^{-3}	9.107×10^{-6}	-1.306×10^{-8}	4.786×10^{-2}
	4	1.732×10^{-2}	1.045×10^{-3}	7.975×10^{-6}	1.302×10^{-7}	1.837×10^{-2}
	6	3.912×10^{-3}	5.773×10^{-4}	4.315×10^{-6}	3.166×10^{-7}	4.494×10^{-3}
	8	4.068×10^{-4}	1.543×10^{-4}	1.089×10^{-6}	2.669×10^{-7}	5.624×10^{-4}
	10	1.249×10^{-5}	1.354×10^{-5}	8.194×10^{-7}	6.529×10^{-8}	2.618×10^{-5}
2.0	0	8.958×10^{-2}	1.073×10^{-3}	5.585×10^{-6}	-3.302×10^{-8}	9.066×10^{-2}
	2	4.540×10^{-2}	1.265×10^{-3}	6.574×10^{-6}	-7.935×10^{-9}	4.667×10^{-2}
	4	1.662×10^{-2}	1.101×10^{-3}	5.683×10^{-6}	1.054×10^{-7}	1.773×10^{-2}
	6	3.677×10^{-3}	5.957×10^{-4}	3.013×10^{-6}	2.461×10^{-7}	4.276×10^{-3}
	8	3.700×10^{-4}	1.541×10^{-4}	7.3555×10^{-7}	1.997×10^{-7}	5.250×10^{-4}
	10	1.079×10^{-5}	1.280×10^{-5}	5.258×10^{-8}	4.621×10^{-8}	2.368×10^{-5}
5.0	0	8.316×10^{-2}	1.936×10^{-4}	8.621×10^{-6}	-8.544×10^{-9}	8.336×10^{-2}
	2	4.071×10^{-2}	2.206×10^{-4}	9.823×10^{-6}	4.724×10^{-10}	4.094×10^{-2}
	4	1.413×10^{-2}	1.814×10^{-4}	8.065×10^{-6}	3.340×10^{-8}	1.432×10^{-2}
	6	2.875×10^{-3}	8.898×10^{-5}	3.940×10^{-6}	6.626×10^{-8}	2.968×10^{-3}
	8	2.538×10^{-4}	1.931×10^{-5}	8.454×10^{-7}	4.466×10^{-8}	2.740×10^{-4}
	10	6.022×10^{-6}	1.159×10^{-6}	4.926×10^{-8}	7.532×10^{-9}	7.238×10^{-6}

Table 4.6. - Error probability results for single-channel QPSK transmission with ideal rectangular filtering $(f_c T_A = 5)$

$B_{IF}T_A$	$\frac{Eb_A}{N_o}$ (dB)	P_{e_1}	P_{e_2}	P_{e_3}	P_{e_4}	P_e
1.0	0	1.069×10^{-1}	1.005×10^{-2}	9.425×10^{-5}	-6.024×10^{-6}	1.171×10^{-1}
	2	5.879×10^{-2}	1.287×10^{-2}	1.197×10^{-4}	-5.341×10^{-6}	7.177×10^{-2}
	4	2.441×10^{-2}	1.309×10^{-2}	1.167×10^{-4}	7.461×10^{-6}	3.762×10^{-2}
	6	6.562×10^{-3}	9.626×10^{-3}	7.497×10^{-5}	3.463×10^{-5}	1.630×10^{-2}
	8	8.964×10^{-4}	4.371×10^{-3}	2.486×10^{-5}	5.172×10^{-5}	5.544×10^{-3}
	10	4.229×10^{-5}	1.240×10^{-3}	2.902×10^{-6}	3.634×10^{-5}	1.322×10^{-3}
	12	3.736×10^{-7}	1.644×10^{-4}	6.525×10^{-8}	1.163×10^{-5}	1.764×10^{-4}
	14	2.336×10^{-10}	8.138×10^{-6}	1.100×10^{-10}	1.391×10^{-6}	9.530×10^{-6}
1.5	0	9.145×10^{-2}	1.014×10^{-3}	3.069×10^{-5}	-1.746×10^{-7}	9.249×10^{-2}
	2	4.679×10^{-2}	1.207×10^{-3}	3.645×10^{-5}	-5.441×10^{-8}	4.804×10^{-2}
	4	1.739×10^{-2}	1.065×10^{-3}	3.197×10^{-5}	5.270×10^{-7}	1.849×10^{-2}
	6	3.936×10^{-3}	5.985×10^{-4}	1.734×10^{-5}	1.288×10^{-6}	4.546×10^{-3}
	8	4.106×10^{-4}	1.582×10^{-4}	4.393×10^{-6}	1.091×10^{-6}	5.743×10^{-4}
	10	1.267×10^{-5}	1.397×10^{-5}	3.336×10^{-7}	2.695×10^{-7}	2.725×10^{-5}
2.0	0	8.976×10^{-2}	1.091×10^{-3}	2.230×10^{-5}	-1.343×10^{-7}	9.087×10^{-2}
	2	4.554×10^{-2}	1.288×10^{-3}	2.627×10^{-5}	-3.331×10^{-8}	4.685×10^{-2}
	4	1.670×10^{-2}	1.122×10^{-3}	2.274×10^{-5}	4.260×10^{-7}	1.784×10^{-2}
	6	3.702×10^{-3}	6.088×10^{-4}	1.209×10^{-5}	9.995×10^{-7}	4.324×10^{-3}
	8	3.738×10^{-4}	1.581×10^{-4}	2.964×10^{-6}	8.154×10^{-7}	5.357×10^{-4}
	10	1.096×10^{-5}	1.324×10^{-5}	2.136×10^{-7}	1.905×10^{-7}	2.460×10^{-5}
5.0	0	8.359×10^{-2}	2.125×10^{-4}	3.491×10^{-5}	-3.818×10^{-8}	8.384×10^{-2}
	2	4.102×10^{-2}	2.427×10^{-4}	3.988×10^{-5}	1.277×10^{-9}	4.130×10^{-2}
	4	1.429×10^{-2}	2.003×10^{-4}	3.287×10^{-5}	1.473×10^{-7}	1.452×10^{-2}
	6	2.925×10^{-3}	9.885×10^{-5}	1.616×10^{-5}	2.954×10^{-7}	3.041×10^{-3}
	8	2.606×10^{-4}	2.167×10^{-5}	3.504×10^{-6}	2.016×10^{-7}	2.860×10^{-4}
	10	6.273×10^{-6}	1.323×10^{-6}	2.080×10^{-7}	3.472×10^{-8}	7.839×10^{-6}

Table 4.7. - Error probability results for single-channel QPSK transmission with ideal rectangular filtering $(f_c T_A = 1)$

$B_{IF}T_A$	$\frac{E_{bA}}{N_o}$ (dB)	P_{e_1}	P_{e_2}	P_{e_3}	P_{e_4}	P_e
1.0	0	1.107×10^{-1}	1.110×10^{-2}	2.500×10^{-3}	-1.804×10^{-4}	1.241×10^{-1}
	2	6.184×10^{-2}	1.441×10^{-2}	3.227×10^{-3}	-1.810×10^{-4}	7.930×10^{-2}
	4	2.630×10^{-2}	1.502×10^{-2}	3.247×10^{-3}	1.455×10^{-4}	4.473×10^{-2}
	6	7.345×10^{-3}	1.150×110^{-2}	2.253×10^{-2}	9.190×10^{-4}	2.202×10^{-2}
	8	1.064×10^{-3}	5.857×10^{-3}	8.821×10^{-4}	1.571×10^{-3}	9.374×10^{-3}
	10	5.510×10^{-5}	1.783×10^{-3}	1.502×10^{-4}	1.374×10^{-3}	3.362×10^{-3}
	12	5.634×10^{-7}	2.832×10^{-4}	7.968×10^{-6}	6.662×10^{-4}	9.580×10^{-4}
	14	4.443×10^{-10}	1.854×10^{-5}	8.821×10^{-8}	1.800×10^{4}	1.986×10^{-4}
1.5	0	9.741×10^{-2}	1.697×10^{-3}	7.552×10^{-4}	-7.591×10^{-6}	9.986×10^{-2}
	2	5.133×10^{-2}	2.076×10^{-3}	9.226×10^{-4}	-4.053×10^{-6}	5.432×10^{-2}
	4	1.995×10^{-2}	$1.918 \times 10-3$	8.482×10^{-4}	1.836×10^{-5}	2.274×10^{-2}
	6	4.845×10^{-3}	1.148×10^{-3}	4.990×10^{-4}	5.333×10^{-5}	6.544×10^{-3}
	8	5.640×10^{-4}	3.521×10^{-4}	1.461×10^{-4}	5.380×10^{-5}	1.116×10^{-3}
	10	2.070×10^{-5}	3.940×10^{-5}	1.451×10^{-5}	1.805×10^{-5}	9.266×10^{-5}
2.0	0	9.628×10^{-2}	1.804×10^{-3}	5.110×10^{-4}	5.406×10^{-6}	9.858×10^{-2}
	2	5.045×10^{-2}	2.195×10^{-3}	6.210×10^{-4}	2.676×10^{-6}	5.327×10^{-2}
	4	1.945×10^{-2}	2.013×10^{-3}	5.656×10^{-4}	1.365×10^{-5}	2.204×10^{-2}
	6	4.662×10^{-3}	1.190×10^{-3}	3.271×10^{-4}	3.385×10^{-5}	6.217×10^{-3}
	8	5.318×10^{-4}	3.588×10^{-4}	9.273×10^{-5}	3.752×10^{-5}	1.021×10^{-3}
	10	1.890×10^{-5}	3.903×10^{-5}	8.631×10^{-6}	1.194×10^{-5}	7.850×10^{-5}
5.0	0	9.646×10^{-2}	1.185×10^{-3}	5.279×10^{-5}	-3.673×10^{-7}	9.769×10^{-2}
	2	5.059×10^{-2}	1.443×10^{-3}	6.416×10^{-5}	-1.775×10^{-7}	5.210×10^{-2}
	4	1.953×10^{-2}	1.321×10^{-3}	5.837×10^{-5}	9.498×10^{-7}	2.091×10^{-2}
	6	4.690×10^{-3}	7.742×10^{-4}	3.357×10^{-5}	2.632×10^{-6}	5.501×10^{-3}
	8	5.368×10^{-4}	2.274×10^{-4}	9.339×10^{-6}	2.490×10^{-6}	7.761×10^{-4}
	10	1.917×10^{-5}	2.313×10^{-5}	8.243×10^{-7}	7.169×10^{-7}	4.385×10^{-5}

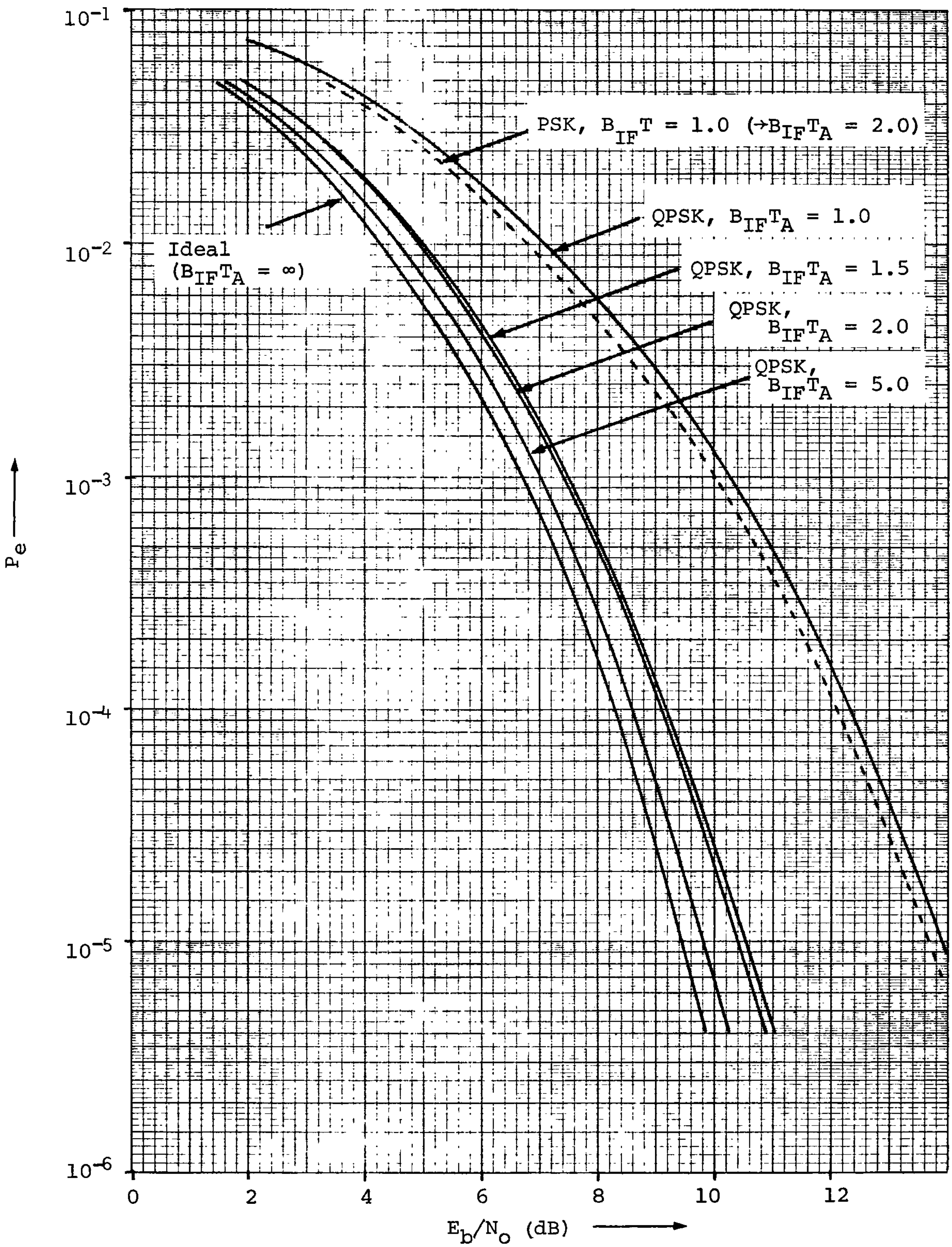

Fig. 4.4. - Error probability results for single-channel QPSK transmission with ideal rectangular filtering ($f_cT_A = 10$)

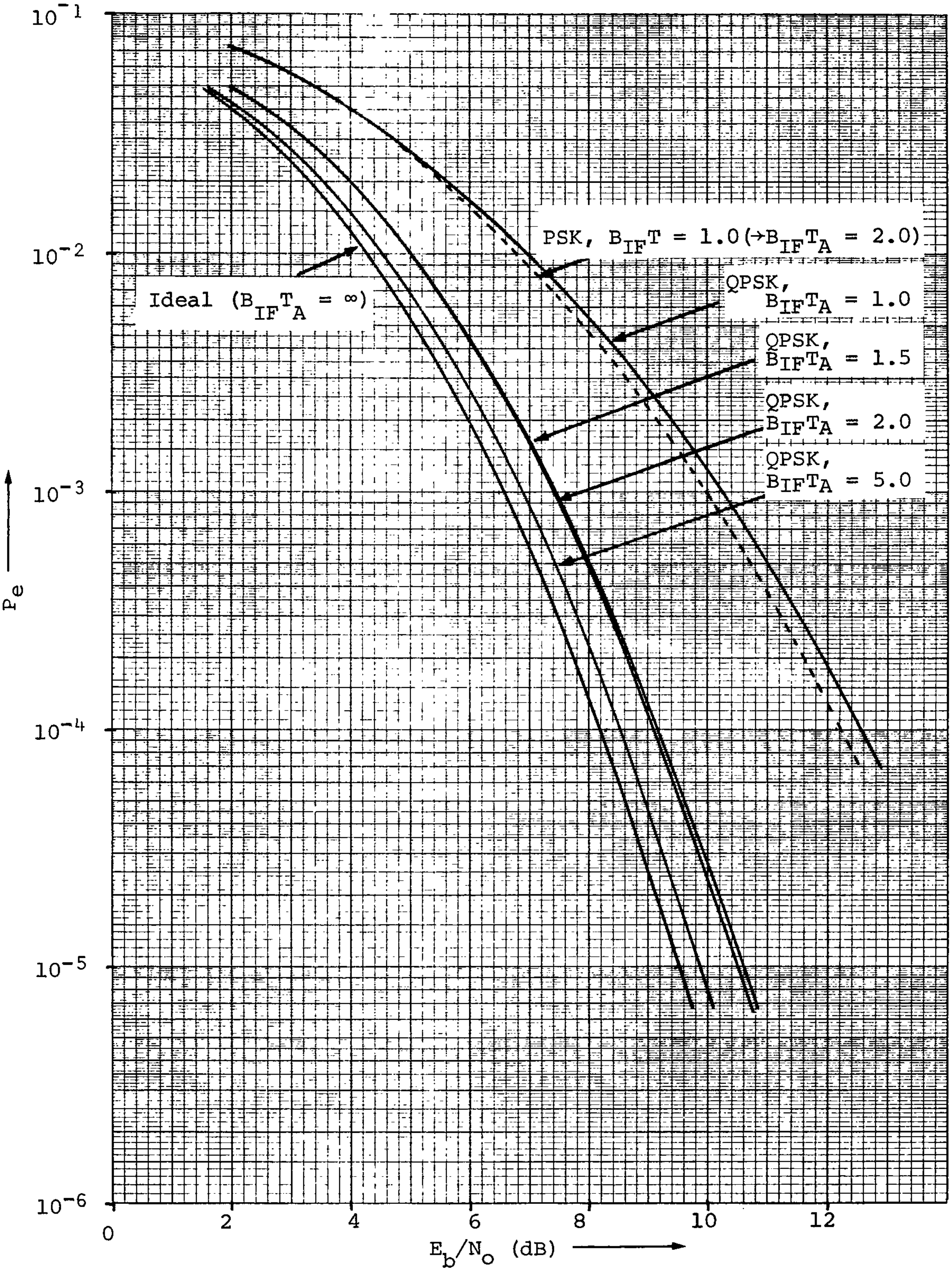

Fig. 4.5. - Error probability results for single-channel QPSK transmission with ideal rectangular filtering ($f_cT_A = 5$)

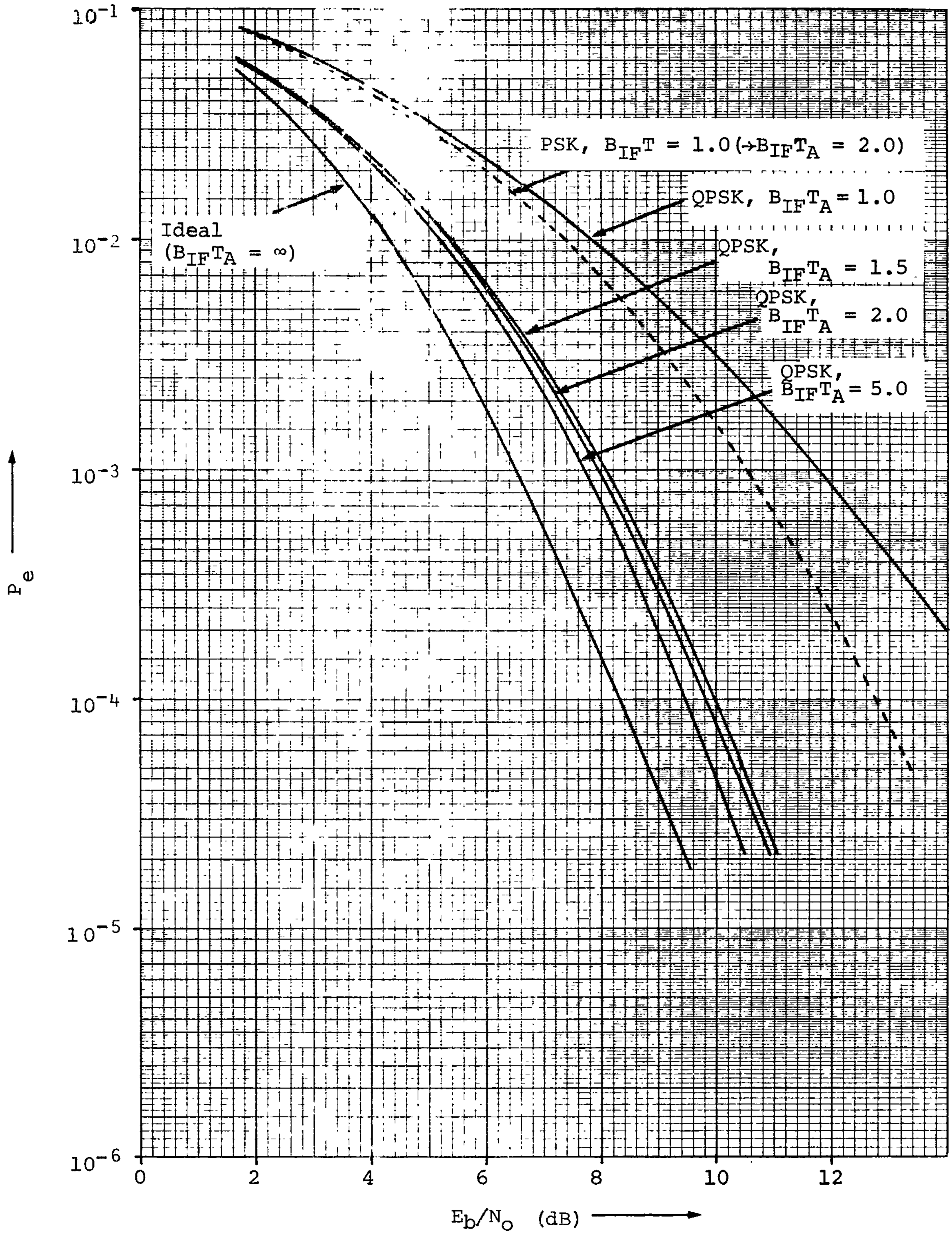

Fig. 4.6. - Error probability results for single-channel QPSK transmission with ideal rectangular filtering ($f_cT_A = 1$)

plots are versus E_b/N_o rather than the E_{bA}/N_o used in the tables. This is because the tables contained values of Channel A error probability corresponding to the energy per bit (in Channel A) per single-sided noise spectral density. In order to meaningfully assess the performance of a QPSK transmission system, however, the QPSK error probability should be compared with the error probability for PSK transmission of the same information rate ($R_A + R_B$ bits/second) at the same total power level ($P_A + P_B$ watts). Thus instead of plotting Channel A error probability versus E_{bA}/N_o, plots of Channel A and Channel B error probability versus E_b/N_o should be presented. For balanced, single-channel operation, the error probabilities are equal in Channel A and Channel B, so only one plot is required. Since (3-13), (3-18), and (3-19) show that $E_b/N_o = E_{bA}/N_o$, the preceding discussion is of little consequence for this case. However, for unbalanced, dual-channel operation, these points will be very significant.

To facilitate evaluation of the performance of bandlimited single-channel QPSK transmission, two additional curves are presented on each of the three figures. The bit error probability curve for ideal (infinite bandwidth) PSK transmission is included, along with a curve for bandlimited PSK transmission [9]. The curves for bandlimited PSK are for the case when the IF filter bandwidth is equal to the data rate, or when $B_{IF}T = 1$. These curves should be compared with the QPSK curves for $B_{IF}T_A = 2$, because the input to the IF filter consists of two parallel channels each of half the rate of the equivalent PSK channel. A comparison of the PSK curves with the appropriate QPSK curves indicates that the effects of a fixed bandwidth IF filter are not as severe in a QPSK transmission system.

This is an intuitively satisfying result and indeed provides justification for the additional complexity involved in implementing a QPSK system.

Dual-Channel (Unbalanced Power) Results

Dual-channel operation refers to the case in which the parallel inputs to the two quadrature channels of the QPSK modulator are obtained from separate, independent sources. After QPSK demodulation and after independent bit detection processes have been performed, the two parallel signals are routed to different points. Equation (3-20) shows that, for equal output error probabilities in the two channels,

$$P_A / R_A = P_B / R_B \tag{4-25}$$

For $R_A \neq R_B$, however, this relationship is valid only for the infinite bandwidth case. The reason for this is obvious if it is observed that a finite bandwidth filter will result in a more severe performance degradation in the high rate channel than in the low rate channel. It would appear, then, that if the bandwidth is limited and if it is desired to equalize the Channel A and Channel B error probabilities, the power in the high-rate channel will have to be somewhat greater than the value which satisfies (4-25).

Figs. 4.7 through 4.10 show Channel A and Channel B error probabilities for various signal-to-noise ratios (E_b/N_o) and for various values of $B_{IF}T_A$, T_A/T_B, and f_cT_A. No attempt has yet been made to equalize the Channel A and B error rates by properly unbalancing the power levels in the two channels. Rather, for the cases illustrated in Figs. 4.7 through 4.10, the ratio of amplitudes for the two channels was obtained using (4-25),

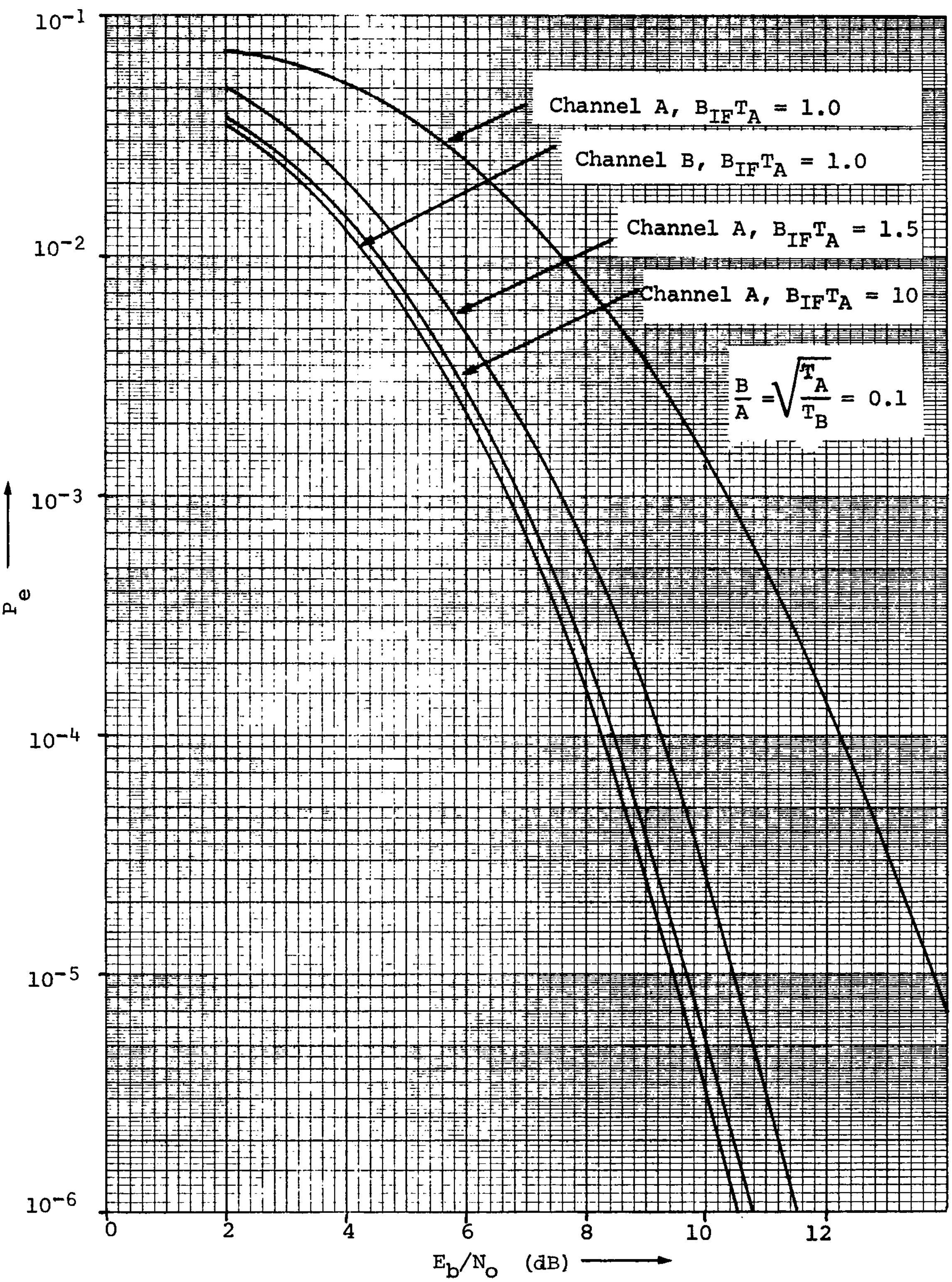

Fig. 4.7. - Error probability results for dual-channel QPSK transmission with ideal rectangular filtering ($f_cT_A = 10$, $T_A/T_B = 0.01$)

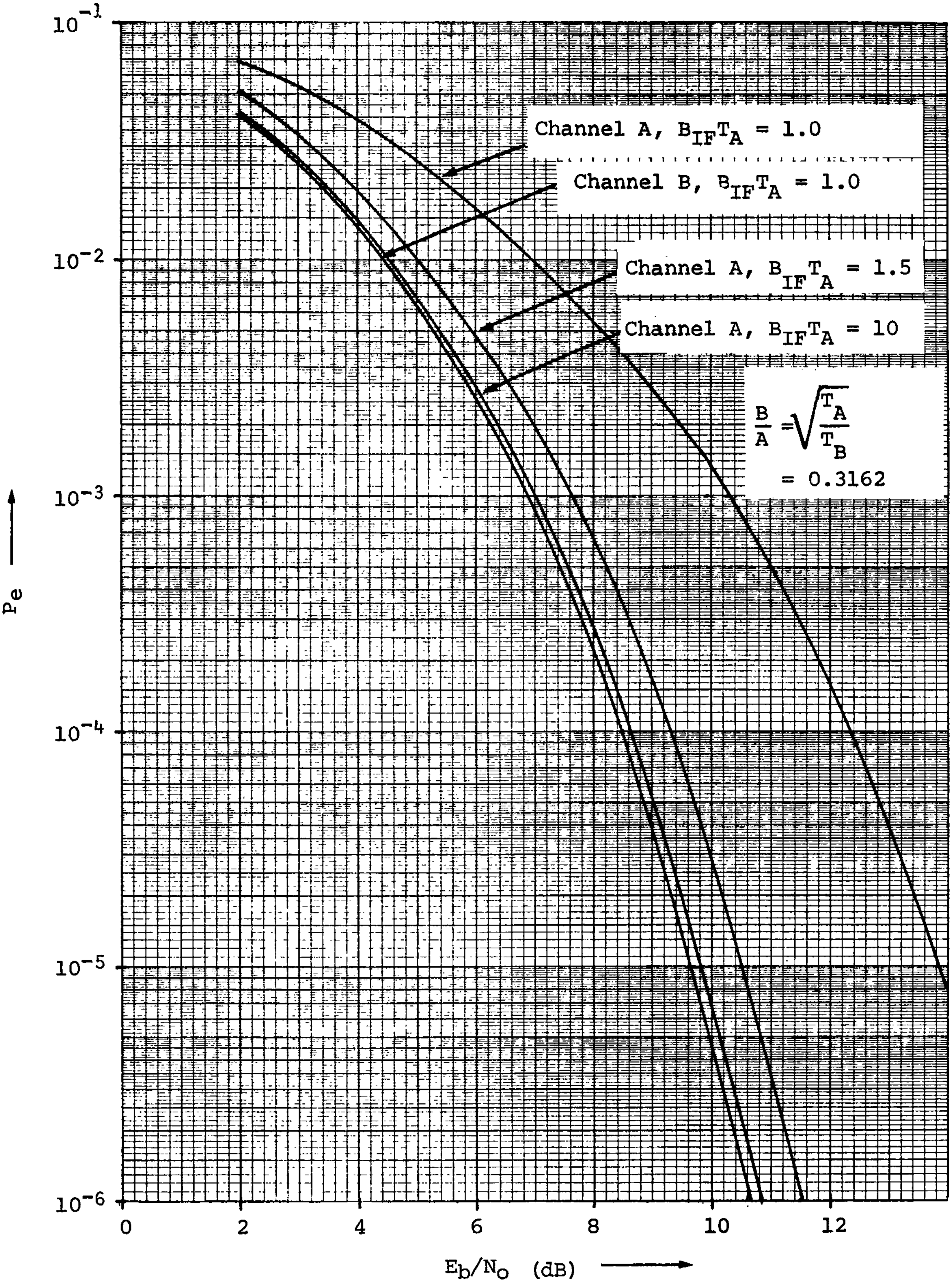

Fig. 4.8. - Error probability results for dual-channel QPSK transmission with ideal rectangular filtering ($f_cT_A = 10$, $T_A/T_B = 0.1$)

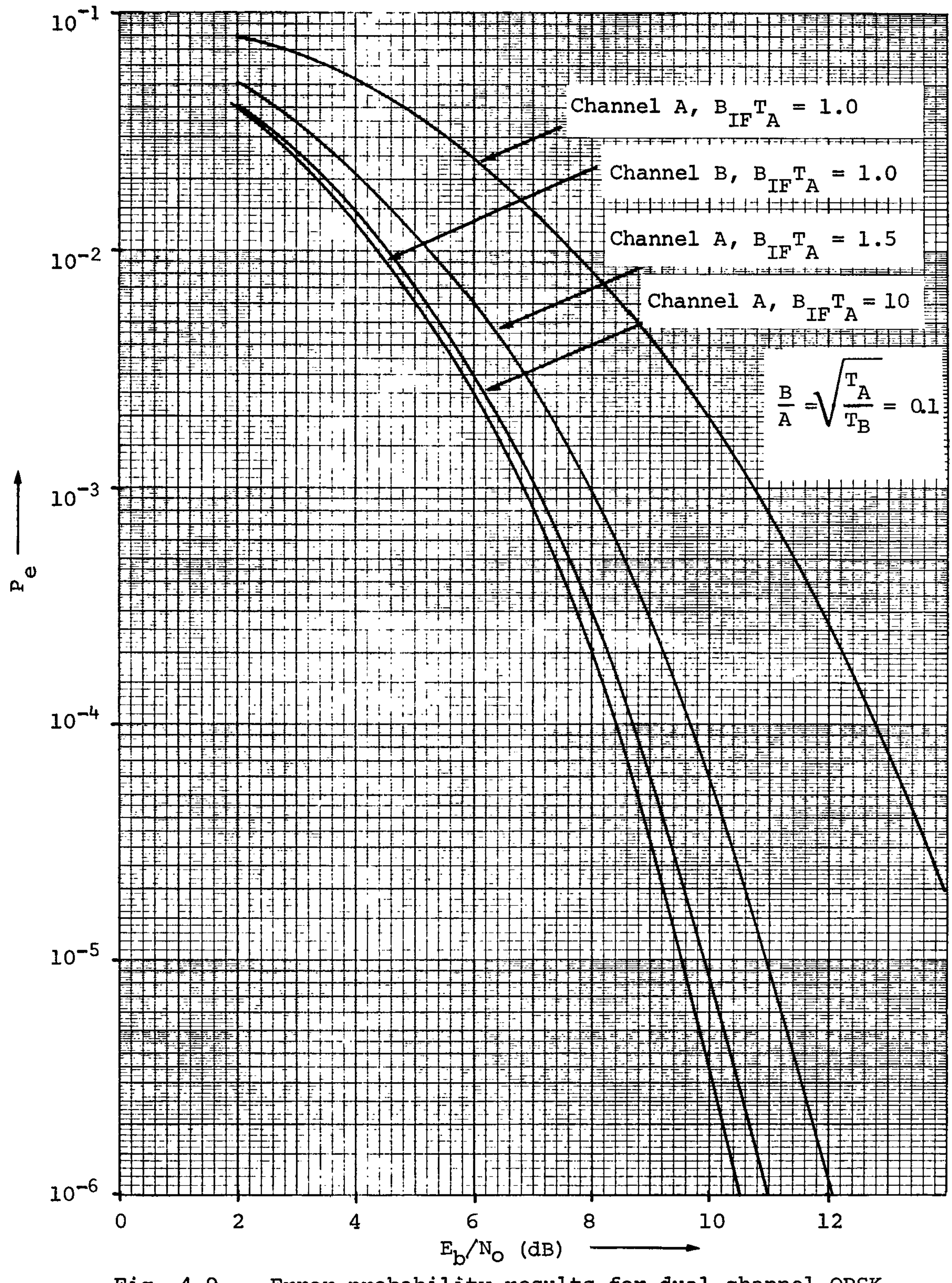

Fig. 4.9. - Error probability results for dual-channel QPSK transmission with ideal rectangular filtering ($f_cT_A = 1$, $T_A/T_B = 0.01$)

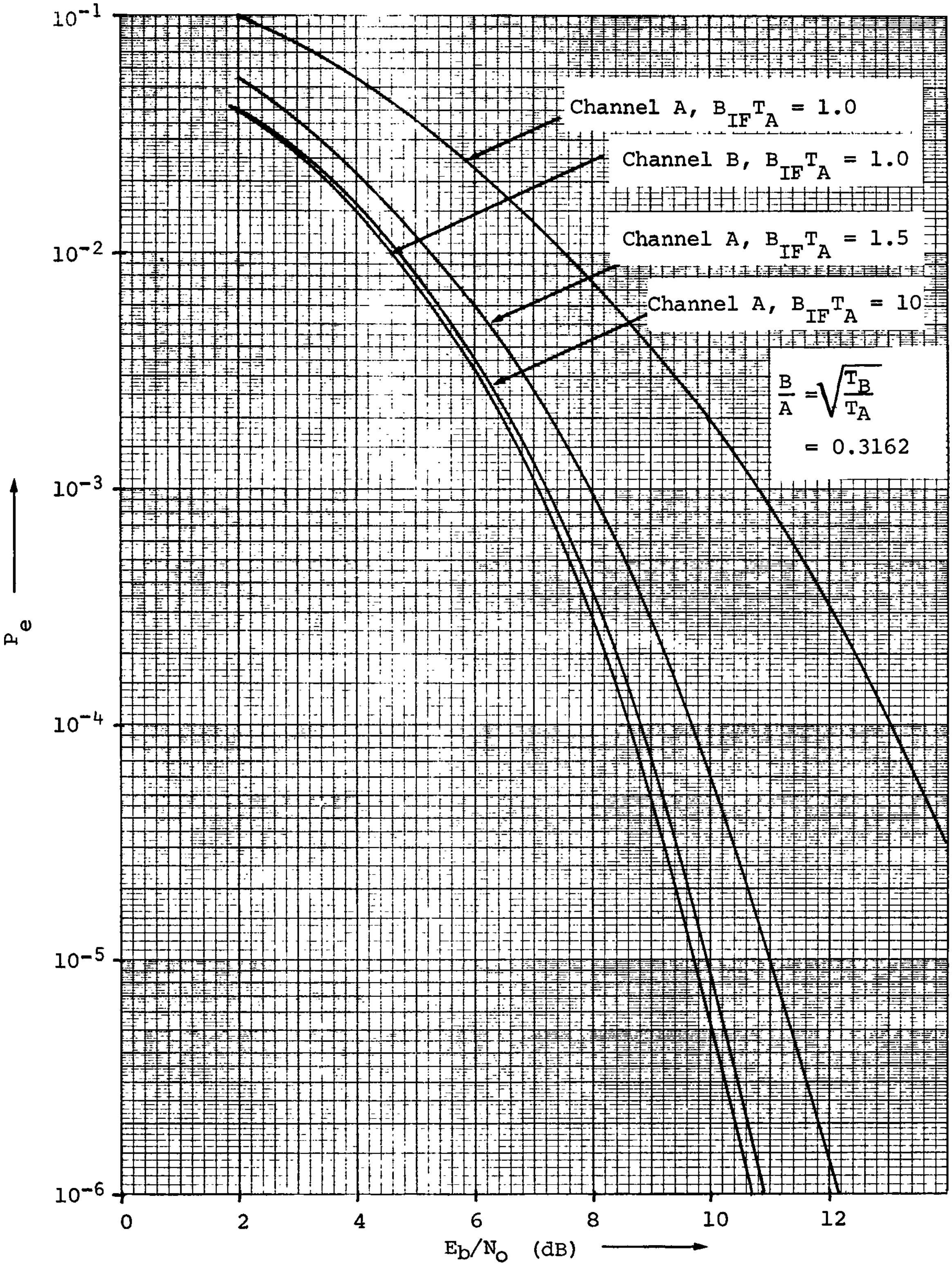

Fig. 4.10. - Error probability results for dual-channel QPSK transmission with ideal rectangular filtering ($f_cT_A = 1$, $T_A/T_B = 0.1$)

which assumes infinite bandwidth. Substituting

$$P_A = \frac{A^2}{2} \tag{4-26}$$

and

$$P_B = \frac{B^2}{2} \tag{4-27}$$

into (4-25) yields

$$\frac{A^2 T_A}{2} = \frac{B^2 T_B}{2} \tag{4-28}$$

or

$$\frac{B}{A} = \sqrt{\frac{T_A}{T_B}} \tag{4-29}$$

The signal-to-noise ratio, or energy per bit per single-sided noise spectral density (E_b/N_o), used in Figs. 4.7 through 4.10 is a *total* signal-to-noise ratio and is given by

$$\frac{E_b}{N_o} = \frac{P_A + P_B}{N_o(R_A + R_B)} \tag{4-30}$$

Substituting (4-26) and (4-27) into (4-30) gives

$$\frac{E_b}{N_o} = \frac{A^2 + B^2}{2N_o(1/T_A + 1/T_B)} \tag{4-31}$$

Using the ratio of amplitudes given by (4-29) gives

$$\frac{E_b}{N_o} = \frac{A^2(1 + T_A/T_B)}{2N_o(1/T_A + 1/T_B)} = \frac{A^2 T_A}{2N_o} \tag{4-32}$$

or

$$\frac{E_b}{N_o} = \frac{B^2(T_B/T_A + 1)}{2N_o(1/T_A + 1/T_B)} = \frac{B^2 T_B}{2N_o} \tag{4-33}$$

Thus the total signal-to-noise ratio used in Figs. 4.7 through 4.10 can be directly related to the individual signal-to-noise ratios in Channels A (SNR_A) and B (SNR_B).

Letting

$$SNR_A = \frac{A^2 T_A}{2N_o} \tag{4-34}$$

and

$$SNR_B = \frac{B^2 T_B}{2N_o} \tag{4-35}$$

it is seen that

$$SNR_B = SNR_A \left[\frac{(B/A)^2}{(T_A/T_B)} \right] \tag{4-36}$$

or

$$\frac{B}{A} = \sqrt{\frac{SNR_B}{SNR_A} \left(\frac{T_A}{T_B} \right)} \tag{4-37}$$

Equation (4-37) provides a means for determining that value of B/A which equalizes the probability of error in the two channels. It is not generally possible to make the Channel A and Channel B error probabilities everywhere equal, since one effect of filtering is to change the <u>shapes</u> of the error probability curves. However, suppose that it is desired to find the value of B/A which, for given values of f_cT_A, T_A/T_B, and $B_{IF}T_A$, equalizes the probability of error at, say, 10^{-4}. Using the appropriate curves, such as given by Figs. 4.7, 4.8, 4.9, or 4.10, the values of SNR_A and SNR_B required for a probability of error of 10^{-4} should be determined. These values, along with the T_A/T_B ratio being assumed, should be substituted into (4-37) to yield a new trial value of B/A. The process of determining the optimum B/A is necessarily iterative, since the probability of error for each of the two channels is affected by that ratio. Using the new value of B/A, the probability of error can be computed again for each of the two channels. This entire process can be repeated until the error probability curves *cross* at 10^{-4}. No more than two iterations were required to equalize error probabilities at 10^{-4} for the particular cases considered in this study. Figs. 4.11 through 4.14 illustrate the types of results provided by this iterative process for $B_{IF}T_A = 1$. The same process could be used to obtain results for other values of f_cT_A, T_A/T_B, and $B_{IF}T_A$, or to force the error probability curves to cross at any arbitrary point.

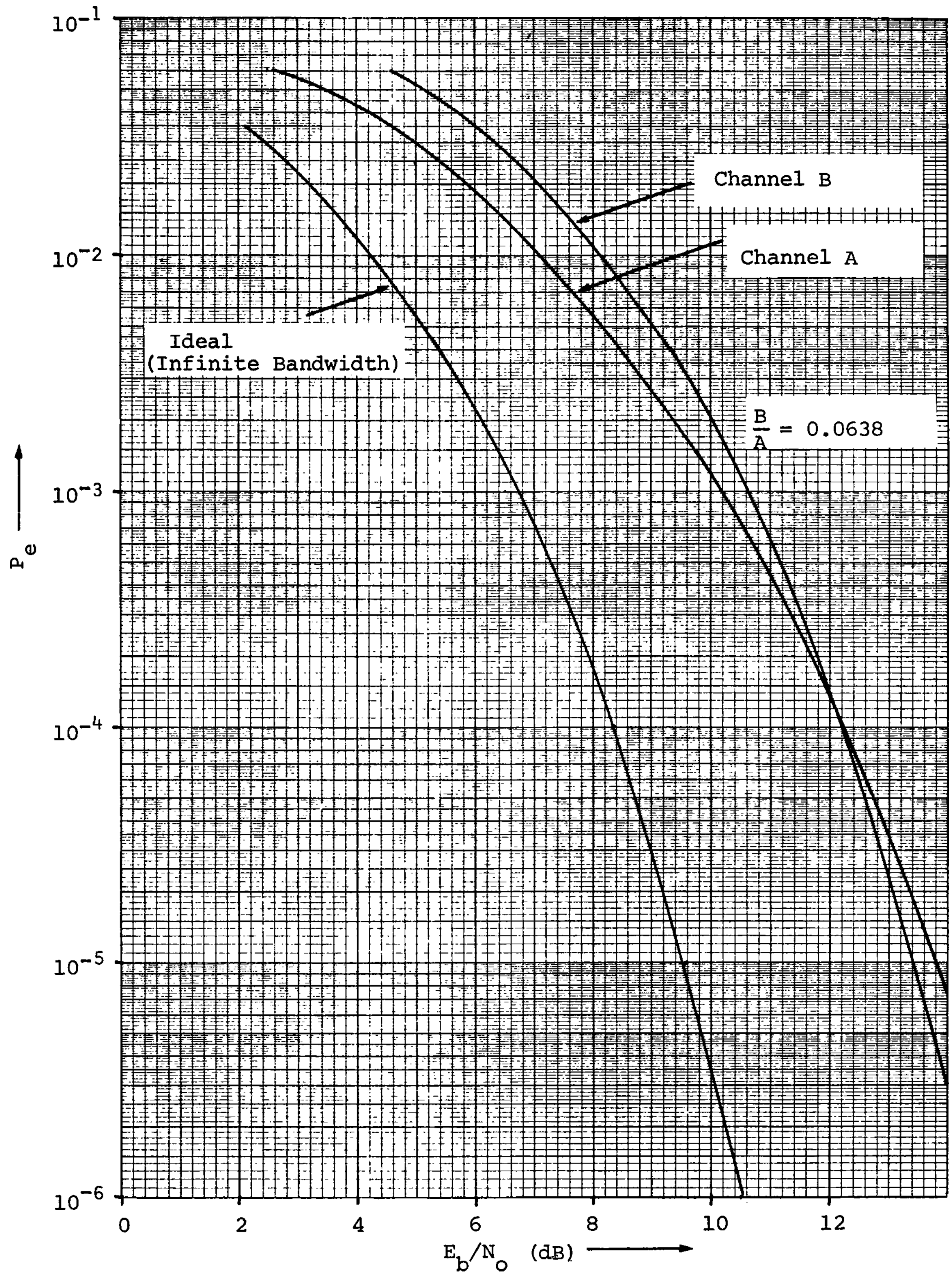

Fig. 4.11. - Iterated error probability results for dual-channel QPSK transmission with ideal rectangular filtering ($f_cT_A = 10$, $T_A/T_B = 0.01$, $B_{IF}T_A = 1$)

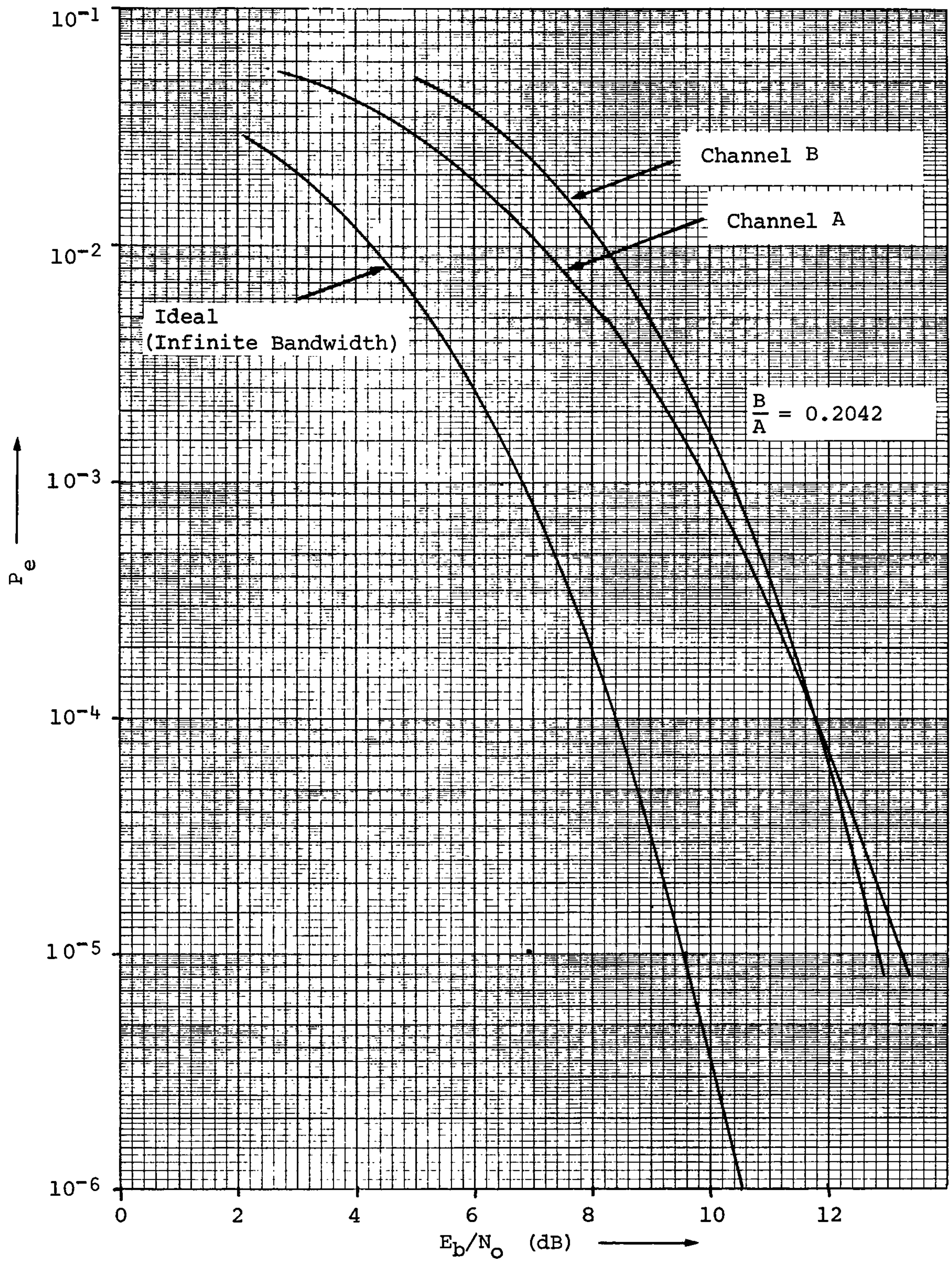

Fig. 4.12. - Iterated error probability results for dual-channel QPSK transmission with ideal rectangular filtering ($f_cT_A = 10$, $T_A/T_B = 0.1$, $B_{IF}T_A = 1$)

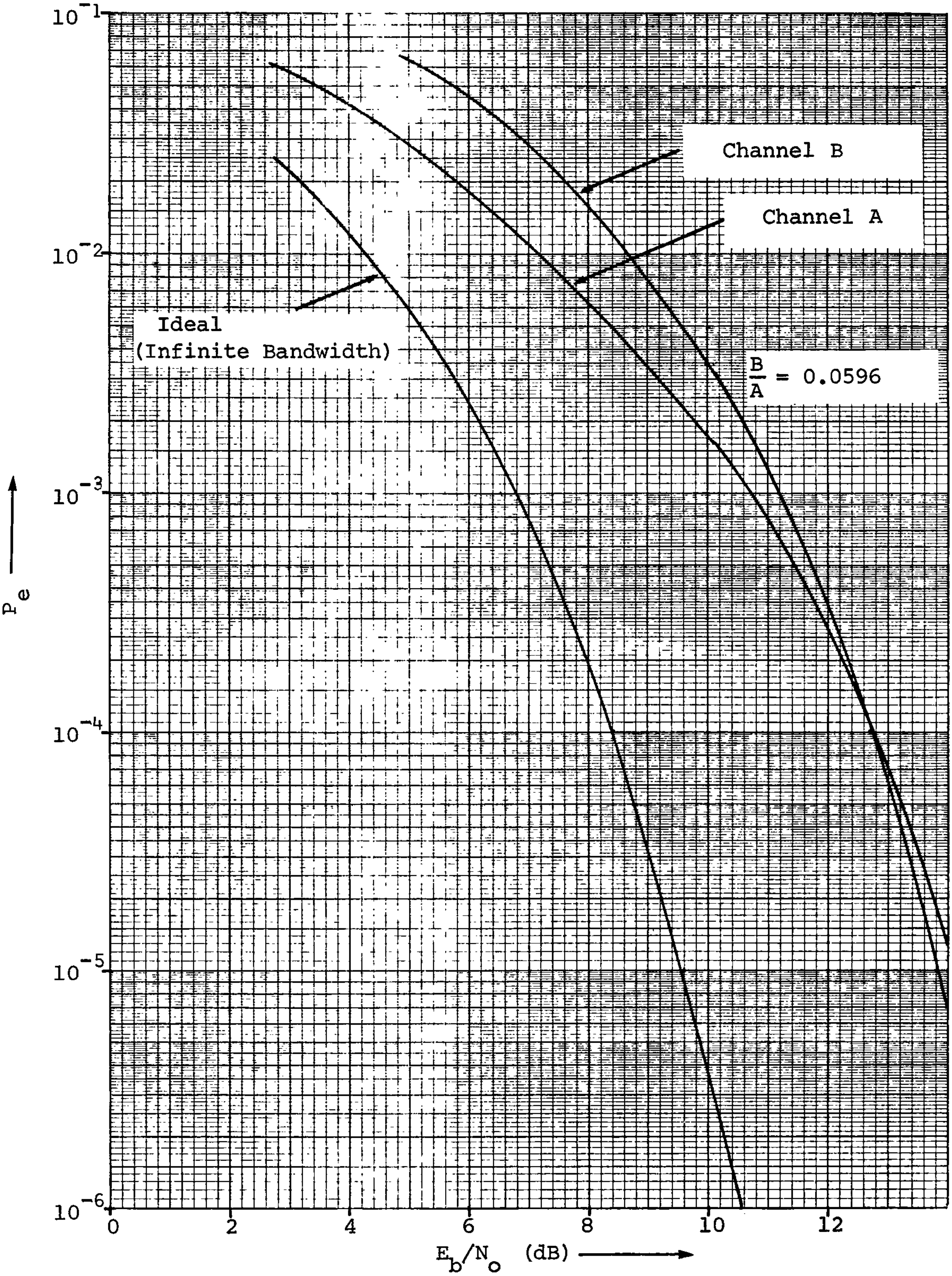

Fig. 4.13. - Iterated error probability results for dual-channel QPSK transmission with ideal rectangular filtering ($f_c T_A = 1$, $T_A/T_B = 0.01$, $B_{IF} T_A = 1$)

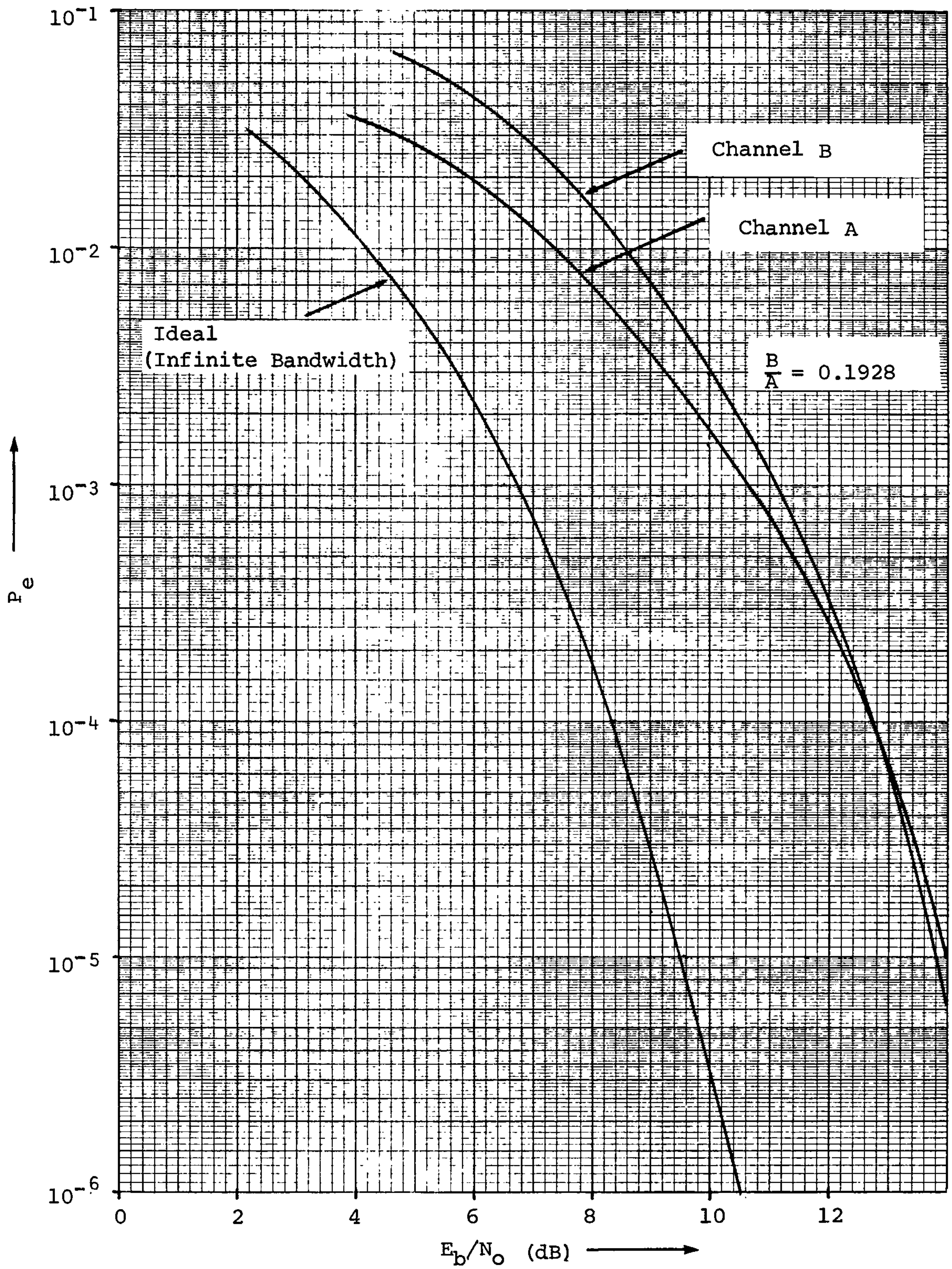

Fig. 4.14. - Iterated error probability results for dual-channel QPSK transmission with ideal rectangular filtering ($f_cT_A = 1$, $T_A/T_B = 0.1$, $B_{IF}T_A = 1$)

PRACTICAL FILTERING

In the previous section, the ideal rectangular filter was assumed to be the device which limited the bandwidth of the QPSK signal. Such a filter is nonrealizable, however, and can only be approximated in practice. It is of interest to determine the effects on bit error probability of bandlimiting a QPSK signal with a realizable filter. For this analysis, the simple first-order Butterworth (single-pole) filter will be assumed. The intent here is to illustrate an approach that can be used to analytically determine QPSK error rates for systems employing *any* particular filter type.

The frequency response for the lowpass equivalent of the single-pole bandpass filter is [14]

$$H_\ell(f) = \frac{A_0}{1 + j\left(\frac{2\pi f}{2\pi B_\ell}\right)} \tag{4-38}$$

where B_ℓ is the 3-dB cutoff frequency. As shown in [15], the frequency characteristic for the bandpass filter is

$$\begin{aligned} H(f) &= \begin{cases} H_\ell(f+f_c) & \text{for} \quad f<0 \\ H_\ell(f-f_c) & \text{for} \quad f>0 \end{cases} \\ &= \begin{cases} \dfrac{A_0}{1+j\left[\frac{2\pi(f+f_c)}{2\pi B_\ell}\right]} & \text{for} \quad f<0 \\ \dfrac{A_0}{1+j\left[\frac{2\pi(f-f_c)}{2\pi B_\ell}\right]} & \text{for} \quad f>0 \end{cases} \end{aligned} \tag{4-39}$$

Fig. 4.15 illustrates the frequency characteristics for the lowpass and bandpass versions of the single-pole RC filter. Since the 3-dB bandwidth of the bandpass filter is

$$B_{IF} = 2B_\ell \tag{4-40}$$

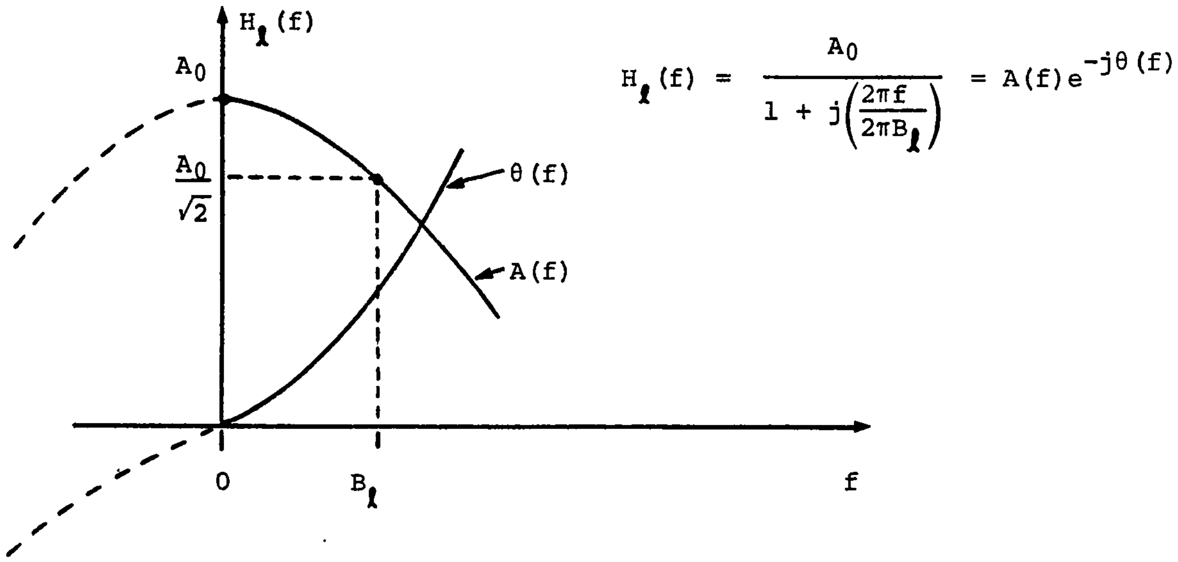

(a) Lowpass

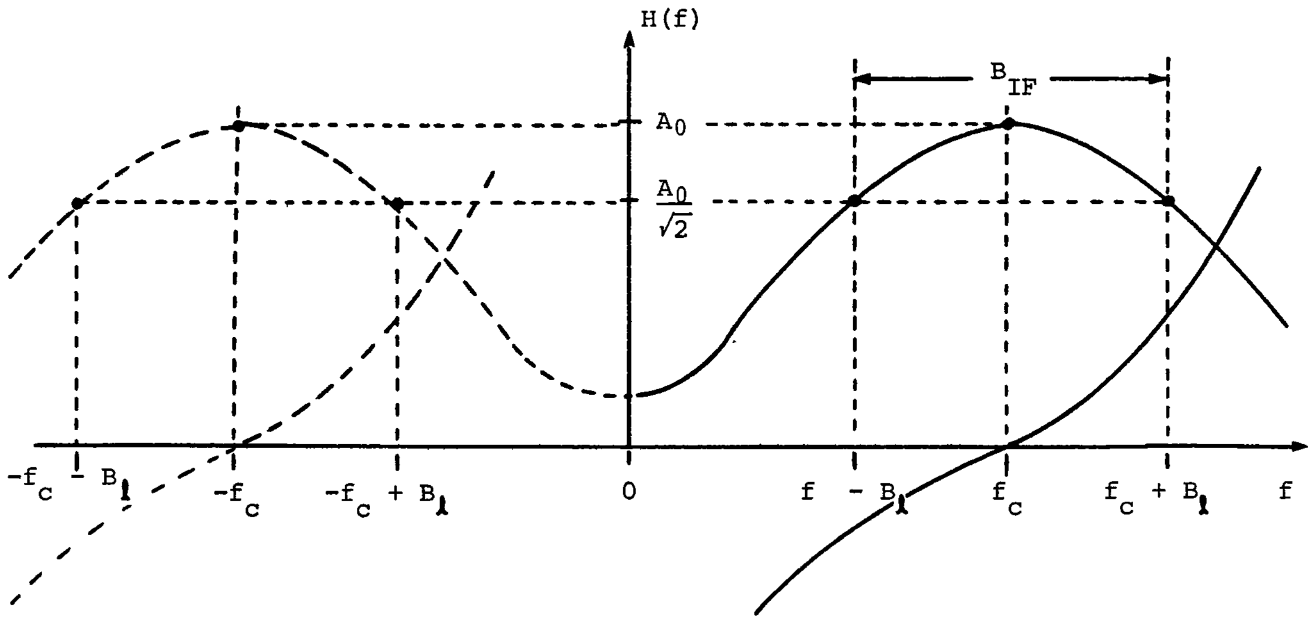

(b) Bandpass

Fig. 4.15. - Frequency characteristics of single-pole filter equivalents

then (4-39) can be written as

$$H(f) = \begin{cases} \dfrac{A_o}{1+j\left[\dfrac{2(f+f_c)}{B_{IF}}\right]} & \text{for} \quad f<0 \\ \dfrac{A_o}{1+j\left[\dfrac{2(f-f_c)}{B_{IF}}\right]} & \text{for} \quad f>0 \end{cases} \tag{4-41}$$

Normalizing (by letting $A_o = 1$) and rationalizing denominators, (4-41) becomes

$$H(f) = \begin{cases} \dfrac{1}{1+\left[\dfrac{2(f+f_c)}{B_{IF}}\right]^2} - j\,\dfrac{2\left(\dfrac{f+f_c}{B_{IF}}\right)}{1+\left[\dfrac{2(f+f_c)}{B_{IF}}\right]^2} & \text{for} \quad f<0 \\ \dfrac{1}{1+\left[\dfrac{2(f-f_c)}{B_{IF}}\right]^2} - j\,\dfrac{2\left(\dfrac{f-f_c}{B_{IF}}\right)}{1+\left[\dfrac{2(f-f_c)}{B_{IF}}\right]^2} & \text{for} \quad f>0 \end{cases} \tag{4-42}$$

The output of the bandpass filter corresponding to the m^{th} bit of Channel A of the QPSK signal can be expressed in the frequency domain as

$$S_{1A}(f) = A_m(f)\,H(f) \tag{4-43}$$

where $A_m(f)$ is the Fourier transform of the m^{th} bit of Channel A and is given by (4-5).

The time domain response of the bandpass filter to the m^{th} bit of Channel A is

$$\begin{aligned} s_{1A}(t) &= \mathcal{F}^{-1}\left[S_{1A}(f)\right] \\ &= \int_{-\infty}^{\infty} A_m(f)\,H(f)\,e^{+j2\pi ft}\,df \end{aligned} \tag{4-44}$$

Substituting (4-5) and (4-42) into (4-44),

$$S_{1A}(t) = \int_{-\infty}^{0} \frac{A_m f \sin(\pi f T_A)}{\pi(f^2 - f_c^2)} e^{-j\pi f(1+2m)T_A} \left\{ \frac{1}{1+\left[\frac{2(f+f_c)}{B_{IF}}\right]^2} - j \frac{2\left(\frac{f+f_c}{B_{IF}}\right)}{1+\left[\frac{2(f+f_c)}{B_{IF}}\right]^2} \right\} e^{+j2\pi f t} df$$

$$+ \int_{0}^{\infty} \frac{A_m f \sin(\pi f T_A)}{\pi(f^2 - f_c^2)} e^{-j\pi f(1+2m)T_A} \left\{ \frac{1}{1+\left[\frac{2(f-f_c)}{B_{IF}}\right]^2} - j \frac{2\left(\frac{f-f_c}{B_{IF}}\right)}{1+\left[\frac{2(f-f_c)}{B_{IF}}\right]^2} \right\} e^{+j2\pi f t} df$$

(4-45)

As shown in Appendix E, (4-45) can be reduced to

$$S_{1A}(t) = \frac{2A_m}{\pi} \int_{0}^{\infty} \frac{f \sin(\pi f T_A) \cos\left\{2\pi f\left[t - \left(\frac{1+2m}{2}\right)T_A\right]\right\}}{(f^2 - f_c^2)\left\{1 + \left[2\left(\frac{f-f_c}{B_{IF}}\right)\right]^2\right\}} df$$

$$+ \frac{4A_m}{\pi B_{IF}} \int_{0}^{\infty} \frac{f(f-f_c)\sin(\pi f T_A) \sin\left\{2\pi f\left[t - \left(\frac{1+2m}{2}\right)T_A\right]\right\}}{(f^2 - f_c^2)\left\{1 + \left[2\left(\frac{f-f_c}{B_{IF}}\right)\right]^2\right\}} df \qquad (4\text{-}46)$$

Likewise, the time domain output of the bandpass filter corresponding to the n^{th} bit of Channel B may be expressed as

$$S_{1B}(t) = \int_{-\infty}^{\infty} B_n(f) H(f) e^{+j2\pi f t} df \qquad (4\text{-}47)$$

Substituting (4-8) and (4-42) into (4-47) yields

$$S_{1B}(t) = \int_{-\infty}^{0} \frac{-j B_n f_c \sin(\pi f T_B)}{\pi(f^2 - f_c^2)} e^{-j\pi f(1+2n)T_B} \left\{ \frac{1}{1+\left[\frac{2(f+f_c)}{B_{IF}}\right]^2} - j \frac{2\left(\frac{f+f_c}{B_{IF}}\right)}{1+\left[\frac{2(f+f_c)}{B_{IF}}\right]^2} \right\} e^{+j2\pi f t} df$$

$$+ \int_{0}^{\infty} \frac{-j B_n f_c \sin(\pi f T_B)}{\pi(f^2 - f_c^2)} e^{-j\pi f(1+2n)T_B} \left\{ \frac{1}{1+\left[\frac{2(f-f_c)}{B_{IF}}\right]^2} - j \frac{2\left(\frac{f-f_c}{B_{IF}}\right)}{1+\left[\frac{2(f-f_c)}{B_{IF}}\right]^2} \right\} e^{+j2\pi f t} df$$

(4-48)

which, as shown in Appendix E, can be reduced to

$$S_{1B}(t) = \frac{2B_n f_c}{\pi}\int_0^{\infty}\frac{\sin(\pi f T_B)\sin\left\{2\pi f\left[t-\left(\frac{1+2n}{2}\right)T_B\right]\right\}}{(f^2-f_c^2)\left\{1+\left[2\left(\frac{f-f_c}{B_{IF}}\right)\right]^2\right\}}\,df$$

$$-\frac{4B_n f_c}{\pi B_{IF}}\int_0^{\infty}\frac{(f-f_c)\sin(\pi f T_B)\cos\left\{2\pi f\left[t-\left(\frac{1+2n}{2}\right)T_B\right]\right\}}{(f^2-f_c^2)\left\{1+\left[2\left(\frac{f-f_c}{B_{IF}}\right)\right]^2\right\}}\,df \tag{4-49}$$

The response of the bandpass filter to all m bits of Channel A and all n bits of Channel B is given by

$$S_1(t) = \sum_{m=-\infty}^{\infty} S_{1A}(t) + \sum_{n=-\infty}^{\infty} S_{1B}(t) \tag{4-50}$$

The time-domain output of the Channel A multiplier is

$$S_{2A}(t) = S_1(t)\cos(\omega_c t)$$

$$= \sum_{m=-\infty}^{\infty} S_{1A}(t)\cos(\omega_c t) + \sum_{n=-\infty}^{\infty} S_{1B}(t)\cos(\omega_c t) \tag{4-51}$$

The output of the Channel A integrate-and-dump circuit (at the sampling instant $K_1 + T_A$) is

$$S_{3A}(K_1+T_A) = \int_{K_1}^{K_1+T_A} S_{2A}(t)\,dt$$

$$= \int_{K_1}^{K_1+T_A}\left\{\sum_{m=-\infty}^{\infty}\frac{2A_m}{\pi}\int_0^{\infty}\frac{f\sin(\pi f T_A)\cos\left\{2\pi f\left[t-\left(\frac{1+2m}{2}\right)T_A\right]\right\}}{(f^2-f_c^2)\left\{1+\left[2\left(\frac{f-f_c}{B_{IF}}\right)\right]^2\right\}}\,df\right\}\cos(\omega_c t)\,dt$$

$$+\int_{K_1}^{K_1+T_A}\left\{\sum_{m=-\infty}^{\infty}\frac{4A_m}{\pi B_{IF}}\int_0^{\infty}\frac{f(f-f_c)\sin(\pi f T_A)\sin\left\{2\pi f\left[t-\left(\frac{1+2m}{2}\right)T_A\right]\right\}}{(f^2-f_c^2)\left\{1+\left[2\left(\frac{f-f_c}{B_{IF}}\right)\right]^2\right\}}\,df\right\}$$

$$\cdot\cos(\omega_c t)\,dt$$

$$+\int_{K_1}^{K_1+T_A}\left\{\sum_{n=-\infty}^{\infty}\frac{2B_n f_c}{\pi}\int_0^{\infty}\frac{\sin(\pi f T_B)\sin\{2\pi f[t-(\frac{1+2n}{2})T_B]\}}{(f^2-f_c^2)\{1+[2(\frac{f-f_c}{B_{IF}})]^2\}}df\right\}\cos(\omega_c t)dt$$

$$-\int_{K_1}^{K_1+T_A}\left\{\sum_{n=-\infty}^{\infty}\frac{4B_n f_c}{\pi B_{IF}}\int_0^{\infty}\frac{(f-f_c)\sin(\pi f T_B)\cos\{2\pi f[t-(\frac{1+2n}{2})T_B]\}}{(f^2-f_c^2)\{1+[2(\frac{f-f_c}{B_{IF}})]^2\}}df\right\}\cos(\omega_c t)dt \quad (4\text{-}52)$$

Interchanging the order of integrations in (4-52) and then performing the inner (time domain) integrations yields

$$S_{3A}(K_1+T_A) = \sum_{m=-\infty}^{\infty}\frac{2A_m}{\pi}\int_0^{\infty}\frac{f\sin^2(\pi f T_A)\{f\cos(X_1)\cos(X_2)+f_c\sin(X_1)\sin(X_2)\}}{\pi(f^2-f_c^2)^2\{1+[2(\frac{f-f_c}{B_{IF}})]^2\}}df$$

$$+\sum_{m=-\infty}^{\infty}\frac{4A_m}{\pi B_{IF}}\int_0^{\infty}\frac{f(f-f_c)\sin^2(\pi f T_A)\{f\sin(X_1)\cos(X_2)-f_c\cos(X_1)\sin(X_2)\}}{\pi(f^2-f_c^2)\{1+[2(\frac{f-f_c}{B_{IF}})]^2\}}df$$

$$+\sum_{n=-\infty}^{\infty}\frac{2B_n f_c}{\pi}\int_0^{\infty}\frac{\sin(\pi f T_B)\sin(\pi f T_A)\{f\sin(X_3)\cos(X_2)-f_c\cos(X_3)\sin(X_2)\}}{\pi(f^2-f_c^2)\{1+[2(\frac{f-f_c}{B_{IF}})]^2\}}df$$

$$-\sum_{n=-\infty}^{\infty}\frac{4B_n f_c}{\pi B_{IF}}\int_0^{\infty}\frac{(f-f_c)\sin(\pi f T_B)\sin(\pi f T_A)\{f\cos(X_3)\cos(X_2)+f_c\sin(X_3)\sin(X_2)\}}{\pi(f^2-f_c^2)\{1+[2(\frac{f-f_c}{B_{IF}})]^2\}}df \quad (4\text{-}53)$$

where

$$X_1 = 2\pi f T_A\left(\frac{K_1}{T_A}-m\right)$$

$$X_2 = 2\pi f_c K_1$$

and

$$X_3 = \pi f T_B\left[\frac{2K_1+T_A}{T_B}-(1+2n)\right]$$

Since the QPSK receiver is now *causal*, the output of the Channel A integrate-and-dump circuit is not affected by bits which occur *after* the sampling instant $K_1 + T_A$. Assuming that $K_1 < T_A$, the Channel A (high-rate channel) bits corresponding to $m \geq 2$ and the Channel B (low-rate channel) bits corresponding to $n \geq 2$ do not affect $S_{3_A}(K_1 + T_A)$. Modifying (4-53) accordingly, changing variables by letting $y = \pi f T_A$ in the first two integrals and $y = \pi f T_B$ in the last two integrals, and considering the effects of channel noise, the total Channel A output voltage becomes

$$e_{3A}(K_1+T_A) = \sum_{m=-\infty}^{+1} \frac{A_m T_A}{2}\left[\Psi_{B1}(m) - \Psi_{B2}(m)\right] + \sum_{n=-\infty}^{+\left(\frac{K_1}{T_A}\right)\left(\frac{R_B}{R_A}\right)} \frac{B_n T_B}{2}\left(\frac{1}{2\pi f_c T_B}\right)\left[\Psi_{B3}(n) - \Psi_{B4}(n)\right] + \underset{\sim}{n}_{out}(T_A) \tag{4-54}$$

The upper limit of the first infinite summation in (4-54) would be 0 if the integrate-and-dump circuit always integrated over a 0 to T_A interval. However, since integration was assumed to be from K_1 to $K_1 + T_A$, the effects of all bits *prior* $(-\infty \leq m \leq 0)$ to the bit under detection, plus the effect of the one bit $(m = +1)$ *following* the bit under detection must be considered.

Since the period of integration in the Channel A integrate-and-dump circuit was assumed to be K_1 to $K_1 + T_A$, the effects of crosstalk due to all bits in Channel B *prior* $(-\infty \leq n \leq 0)$ to the bit under detection, plus the bit in Channel B occupying the *same* time slot $(n = 0)$ as the same bit under detection must always be considered. Additionally, if the data rate in Channel B is equal to or higher than the data rate in Channel A, the effects of some additional number of bits in Channel B must be taken into account.

For data rates of R_A and R_B in Channels A and B, respectively, the effects of the bits from $n = +1$ to $n = +(R_B/R_A)(K_1/T_A)$ must be considered. Thus if $R_B = R_A$ and $\frac{K_1}{T_A} \leq 1$, then the upper limit of the second infinite summation in (4-54) is $+1$. On the other hand, assume that $R_B = 10R_A$ and that integration begins in the center of the Channel A bit period. For this example, the upper limit would have to be

$$\left(\frac{K_1}{T_A}\right)\left(\frac{R_B}{R_A}\right) = (0.5)(10) = 5 \tag{4-55}$$

The functions Ψ_{Bi} in (4-54) are defined by

$$\Psi_{B1}(m) = \frac{4}{\pi}\int_0^{\infty} \frac{y\sin^2(y)\left\{y\cos(\alpha)\cos(\beta) + \pi f_c T_A \sin(\alpha)\sin(\beta)\right\}}{\left[y^2 - (\pi f_c T_A)^2\right]^2 \left\{1 + \left[\frac{2(y - \pi f_c T_A)}{\pi B_{IF} T_A}\right]^2\right\}}\, dy \tag{4-56}$$

$$\Psi_{B2}(m) = -\left(\frac{2}{\pi B_{IF} T_A}\right)\left(\frac{4}{\pi}\right)\int_0^{\infty} \frac{y(y - \pi f_c T_A)\sin^2(y)\left\{y\sin(\alpha)\cos(\beta) - \pi f_c T_A \cos(\alpha)\sin(\beta)\right\}}{\left[y^2 - (\pi f_c T_A)^2\right]^2 \left\{1 + \left[\frac{2(y - \pi f_c T_A)}{\pi B_{IF} T_A}\right]^2\right\}}\, dy \tag{4-57}$$

$$\Psi_{B3}(n) = 8\pi (f_c T_B)^2 \int_0^{\infty} \frac{\sin(y)\sin\left[\left(\frac{T_A}{T_B}\right)y\right]\left\{y\sin(\gamma)\cos(\beta) - \pi f_c T_B \cos(\gamma)\sin(\beta)\right\}}{\left[y^2 - (\pi f_c T_B)^2\right]^2 \left\{1 + \left[\frac{2(y - \pi f_c T_B)}{\pi B_{IF} T_B}\right]^2\right\}}\, dy \tag{4-58}$$

$$\Psi_{B4}(n) = \frac{16 (f_c T_B)^2}{B_{IF} T_B}\int_0^{\infty} \frac{(y - \pi f_c T_B)\sin(y)\sin\left[\left(\frac{T_A}{T_B}\right)y\right]\left\{y\cos(\gamma)\cos(\beta) + \pi f_c T_B \sin(\gamma)\sin(\beta)\right\}}{\left[y^2 - (\pi f_c T_B)^2\right]^2 \left\{1 + \left[\frac{2(y - \pi f_c T_B)}{\pi B_{IF} T_B}\right]^2\right\}}\, dy \tag{4-59}$$

where

$$\alpha = 2y\left(\frac{K_1}{T_A} - m\right)$$

$$\beta = 2\pi f_c K_1$$

and

$$\gamma = y\left[\frac{2K_1 + T_A}{T_B} - (1 + 2n)\right]$$

Equation (4-54) is identical in form to equation (4-21), which was derived for ideal rectangular filtering. The $\left[\Psi_{B_1}(m) - \Psi_{B_2}(m)\right]$ terms represent signal, intersymbol interference, and aliasing, while the $\left[\Psi_{B_3}(n) - \Psi_{B_4}(n)\right]$ terms represent crosstalk from Channel B. All these terms are deterministic and can be evaluated directly for specific combinations of bits in Channels A and B. The noise voltage $\underset{\sim}{n}_{out}(K_1 + T_A)$ is a random variable, however, and its variance (which represents the noise power at the output of Channel A) is determined in Appendix F to be

$$\sigma_n^2 = \frac{N_o T_A}{4} \Psi_n \tag{4-60}$$

where Ψ_n is defined by

$$\Psi_n = \frac{4}{\pi} \int_0^\infty \frac{z^2 \sin^2(z)}{[z^2 - (\pi f_c T_A)^2]^2 \left\{1 + \left[\frac{2(z - \pi f_c T_A)}{\pi B_{IF} T_A}\right]^2\right\}} dz \tag{4-61}$$

and can be obtained from (4-56) by letting $m = 0$ and $K_1 = 0$.

Since (4-54) is exactly of the same form as (4-21), except for the summation limits, then the series expansion procedure detailed in Appendix D for computation of error probability for ideal rectangular filtering can be used for the practical filtering case now under consideration. The resultant expression for Channel A bit error probability is

$$P_e = \frac{1}{2}\left\{1 - \operatorname{erf}\sqrt{\frac{A^2 T_A}{2N_o} \frac{[\Psi_{B_1}(0) - \Psi_{B_2}(0)]^2}{\Psi_{B_1}(0)}}\right.$$

$$- \sum_{i=1}^{\infty} 2b_{2i}(-1)^i G_{2i-1} - \sum_{k=1}^{\infty} 2h_{2k}(-1)^k G_{2k-1}$$

$$- \sum_{i=1}^{\infty} \sum_{k=1}^{\infty} 2\, b_{2i}\, h_{2k} (-1)^{i+k} G_{2i+2k-1} \Bigg\} \qquad (4\text{-}62)$$

Note that (4-62) is the same as (4-23) for ideal rectangular filtering except that $\Psi_{I_1}(o)$ and $\Psi_{I_2}(o)$ have been replaced by $\Psi_{B1}(o)$ and $\Psi_{B2}(o)$, respectively. The b_{2i}, h_{2k}, and G_j in (4-62) are defined exactly as for ideal rectangular filtering in (D-27), (D-28), and (D-36), except that the $\Psi_{I1}(m)$, $\Psi_{I2}(m)$, $\Psi_{I3}(n)$, and $\Psi_{I4}(n)$ are replaced by $\Psi_{B1}(m)$, $\Psi_{B2}(m)$, $\Psi_{B3}(n)$, and $\Psi_{B4}(n)$, respectively, and that appropriate modifications are made to account for the differences in summation limits in (4-21) and (4-54). The b_{2i} in (4-62) are therefore defined by a modified form of (D-27).

$$\prod_{\substack{m=-\infty \\ m \neq 0}}^{+1} \cos\left\{\left[\Psi_{B1}(m) - \Psi_{B2}(m)\right]\omega\right\} = 1 + \sum_{i=1}^{\infty} b_{2i}\, \omega^{2i} \qquad (4\text{-}63)$$

Paralleling the procedure followed in (D-31) through (D-44) for evaluation of the b_{2i} for ideal rectangular filtering, it is readily seen that if

$$d_{2l-1} = \frac{(-1)^{l-1} 2^{2l} (2^{2l}-1)}{(2l)!} B_{2l} \sum_{\substack{m=-\infty \\ m \neq 0}}^{+1} \left[\Psi_{B1}(m) - \Psi_{B2}(m)\right]^{2l} \qquad (4\text{-}64)$$

then the recursive relationship given by (D-44) can be used to evaluate the b_{2i} for single-pole filtering.

The h_{2k} in (4-62) are likewise defined by a modified form of (D-28).

$$\prod_{n=-\infty}^{\left(\frac{K_1}{T_A}\right)\left(\frac{R_B}{R_A}\right)} \cos\left\{\left(\frac{B}{A}\right)\left(\frac{T_B}{T_A}\right)\left(\frac{1}{2\pi f_c T_B}\right)\left[\Psi_{B3}(n) - \Psi_{B4}(n)\right]\omega\right\} = 1 + \sum_{k=1}^{\infty} h_{2k}\, \omega^{2k}$$

(4-65)

Paralleling the procedure followed in (D-45) through (D-51) for evaluation of the h_{2k} for ideal rectangular filtering, it is seen that if

$$C_{2l-1} = \frac{(-1)^{l-1} 2^{2l} (2^{2l}-1)}{(2l)!} B_{2l} \sum_{n=-\infty}^{\left(\frac{K_1}{T_A}\right)\left(\frac{R_B}{R_A}\right)} \left\{ \left(\frac{B}{A}\right)\left(\frac{T_B}{T_A}\right)\left(\frac{1}{2\pi f_c T_B}\right) \left[\Psi_{B3}(n) - \Psi_{B4}(n) \right] \right\}^{2l} \tag{4-66}$$

then the recursive relationship given by (D-51) can be used to evaluate the h_{2k} for single-pole filtering.

The G_j in (4-62) can be evaluated using the recursive relationship given by (D-37), if $\left[\Psi_{I_1}(o) - \Psi_{I_2}(o)\right]$ is replaced by $\left[\Psi_{B_1}(o) - \Psi_{B_2}(o)\right]$.

The expression for the probability of error in Channel A given by (4-62) can be changed to the following form:

$$P_e = P_{e1} + P_{e2} + P_{e3} + P_{e4} \tag{4-67}$$

where

$$P_{e1} = \frac{1}{2}\left\{ 1 - \operatorname{erf} \sqrt{\frac{A^2 T_A}{2 N_o} \frac{\left[\Psi_{B1}(o) - \Psi_{B2}(o)\right]^2}{\Psi_{B1}(o)}} \right\}$$

$$P_{e2} = \sum_{i=1}^{\infty} 2\, b_{2i} (-1)^{i+1} G_{2i-1}$$

$$P_{e3} = \sum_{k=1}^{\infty} 2\, h_{2k} (-1)^{k+1} G_{2k-1}$$

$$P_{e4} = \sum_{i=1}^{\infty} \sum_{k=1}^{\infty} 2\, b_{2i} h_{2k} (-1)^{i+k+1} G_{2i+2k-1}$$

Equation (4-67) is exactly of the same form as (4-24) for ideal rectangular filtering and it might be expected that the individual P_{ei} terms would have the same significance for both cases. That this is actually true, becomes evident upon a detailed review of the derivations of the Ψ_{I_i} and the Ψ_{B_i}, and upon a review of Appendix D. The term P_{e1} again represents the contribution to the total probability of error due to the bit being detected, P_{e_2} represents the contribution due to intersymbol interference and aliasing, P_{e_3} represents the contribution due to crosstalk from Channel B, and P_{e_4} again results from a cross-product of the characteristic functions of the intersymbol interference and crosstalk terms.

In order to obtain numerical results using (4-67), it is once again necessary to assume that the effects of intersymbol interference and crosstalk are confined to a finite number of bits preceding and following the bit under detection. The numerical values for $\left[\Psi_{B_1}(m) - \Psi_{B_2}(m)\right]$ and $\left[\Psi_{B_3}(n) - \Psi_{B_4}(n)\right]$ contained in Tables 4.8 and 4.9 indicate that these quantities are negligibly small for values of m and n less than about -3 or -4.

Assuming that the effects of intersymbol interference were limited to the 5 bits prior to the bit under detection and to the single bit following the bit under detection, values of P_e were computed for several cases of interest. Since it was necessary to use time-consuming numerical integration techniques to evaluate the Ψ_{B_i} functions, and since many such integrations were required for each value of P_e computed, the cases considered were limited to single-channel operation ($T_A/T_B = 1$). However, the results obtained are quite sufficient to provide an indication of the relative performance of a QPSK transmission system employing single-pole IF filtering.

It was determined that, for most of the cases considered, P_e was a fairly sensitive function of the normalized starting time (K_1/T_A) of the integrate-and-dump circuits. Consequently, for each case, K_1/T_A was varied over a wide range and the value which minimized P_e was finally

Table 4.8. - Some values of $\left[\Psi_{B_1}(m) - \Psi_{B_2}(m)\right]$

$(K_1 = 0)$

$f_c T_A$	$B_{IF} T_A$	$\Psi_{B_1}(0) - \Psi_{B_2}(0)$	$\Psi_{B_1}(-1) - \Psi_{B_2}(-1)$	$\Psi_{B_1}(-2) - \Psi_{B_2}(-2)$	$\Psi_{B_1}(-3) - \Psi_{B_2}(-3)$	$\Psi_{B_1}(-4) - \Psi_{B_2}(-4)$
1	1	0.6833	0.2966	0.0132	0.0006	0.0000
	2	0.8237	0.1678	0.0001	-0.0000	....
	3	0.8753	0.1160	-0.0003	-0.0000	....
	5	0.9186	0.0730	-0.0002	-0.0000	....
	10	0.9542	0.0390	-0.0001	-0.0000	....
2	1	0.6917	0.2930	0.0128	0.0006	0.0000
	2	0.8347	0.1618	0.0003	-0.0000	....
	3	0.8860	0.1101	-0.0000	....	....
	5	0.9273	0.0682	-0.0000	....	....
	10	0.9593	0.0363	-0.0000	....	....
6	1	0.6950	0.2916	0.0126	0.0005	0.0000
	2	0.8402	0.1590	0.0003	0.0000	....
	3	0.8926	0.1068	0.0000	....	....
	5	0.9344	0.0646	-0.0000	....	....
	10	0.9654	0.0332	-0.0000	....	....
10	1	0.6954	0.2914	0.0126	0.0005	0.0000
	2	0.8410	0.1586	0.0003	0.0000	....
	3	0.8938	0.1062	0.0000	....	....
	5	0.9361	0.0638	0.0000	....	....
	10	0.9678	0.0320	0.0000	....	....

Table 4.9. - Some values of $\left[\Psi_{B_3}(n) - \Psi_{B_4}(n)\right]$ ($K_1 = 0$, $T_A/T_B = 1$)

f_cT_B	$B_{IF}T_B$	$\Psi_{B_3}(0) - \Psi_{B_4}(0)$	$\Psi_{B_3}(-1) - \Psi_{B_4}(-1)$	$\Psi_{B_3}(-2) - \Psi_{B_4}(-2)$	$\Psi_{B_3}(-3) - \Psi_{B_4}(-3)$	$\Psi_{B_3}(-4) - \Psi_{B_4}(-4)$	$\Psi_{B_3}(-5) - \Psi_{B_4}(-5)$
1	1	-0.0945	0.0455	0.0012	0.0005	0.0001	0.0001
	2	-0.1175	0.0512	0.0048	0.0008	0.0002	0.0001
	3	-0.1194	0.0523	0.0047	0.0007	0.0002	0.0001
	5	-0.1073	0.0487	0.0033	0.0005	0.0002	0.0001
	10	-0.0767	0.0361	0.0016	0.0003	0.0001	0.0000
2	1	-0.0631	0.0318	-0.0000	....	....	....
	2	-0.0993	0.0484	0.0009	0.0001	0.0000	....
	3	-0.1184	0.0574	0.0013	0.0002	0.0001	0.0000
	5	-0.1293	0.0628	0.0013	0.0002	0.0001	0.0000
	10	-0.1140	0.0558	0.0009	0.0001	0.0000	....
6	1	-0.0236	0.0122	-0.0001	-0.0000	....	....
	2	-0.0453	0.0229	0.0000	....	....	....
	3	-0.0636	0.0318	0.0001	-0.0000	....	....
	5	-0.0915	0.0457	0.0001	0.0000	....	....
	10	-0.1253	0.0624	0.0001	0.0000	....	....
10	1	-0.0072	0.0037	-0.0000	....	....	....
	2	-0.0141	0.0073	-0.0000	....	....	....
	3	-0.0206	0.0107	-0.0000	....	....	....
	5	-0.0334	0.0171	-0.0000	....	....	....
	10	-0.0628	0.0317	-0.0000	....	....	....

chosen. Fig. 4.16 illustrates the sensitivity of P_e to variations in K_1/T_A.

Tables 4.10 and 4.11 show values of P_{e_1}, P_{e_2}, P_{e_3}, P_{e_4}, and P_e for the optimum values of K_1/T_A, for two different values of f_cT_A (10 and 1) for three values of $B_{IF}T_A$ (1, 3, and 5), and for various signal-to-noise ratios (E_{bA}/N_o). From Table 4.10 it can be seen that when f_cT_A is high and $B_{IF}T_A$ is low, P_{e_1} dominates at low signal-to-noise ratios and P_{e_2} dominates at high signal-to-noise ratios. This same observation was made earlier for the case of ideal rectangular filtering. Table 4.11 indicates that when f_cT_A is low, the QPSK transmission system employing practical (single-pole) filtering becomes crosstalk-limited (P_{e_4} dominates).

Some of the results presented in Tables 4.10 and 4.11 are plotted in Figs. 4.17 and 4.18, along with the corresponding results previously obtained for the ideal rectangular filtering case. A comparison of these results reveals that better performance is generally provided by the ideal rectangular filter at the lower signal-to-noise ratios, while the single-pole filter appears superior at the higher signal-to-noise ratios. Such an outcome is not unreasonable, as the finite area under the ideal filter characteristic could be expected to pass less noise and thus provide superior performance in the noise-limited region. On the other hand, in the region where intersymbol interference is significant, the practical filter could be expected to offer some potential improvement. This is because, heuristically, the output of the ideal filter is sharply limited in frequency and hence must be "smeared" in time, while the output of the practical filter is not sharply limited in frequency and thus should not experience the same degree of time-spreading.

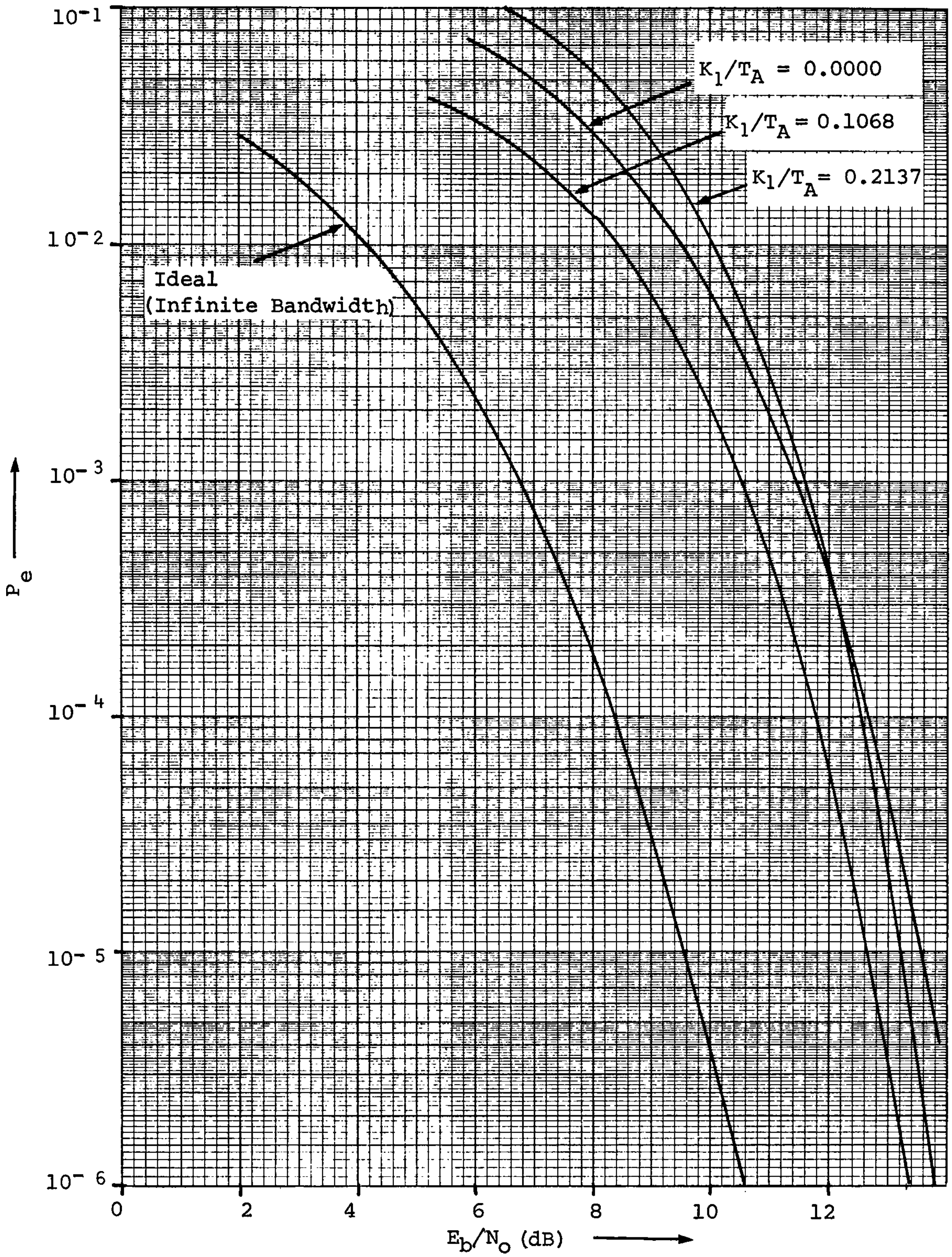

Fig. 4.16. - Error probability results for single-channel QPSK transmission with practical filtering (K_1/T_A varying, $f_c T_A = 1$, $B_{IF} T_A = 1$, $T_A/T_B = 1$)

Fig. 4.10. - Error probability results for single-channel QPSK transmission with practical filtering ($f_c T_A$ = 10)

$B_{IF}T_A$	$\frac{K_1}{T_A}$	$\frac{E_{bA}}{N_o}$ (dB)	P_{e1}	P_{e2}	P_{e3}	P_{e4}	P_e
1.0	0.0250	0	1.119×10^{-1}	2.358×10^{-2}	1.808×10^{-6}	-2.793×10^{-7}	1.355×10^{-1}
		2	6.281×10^{-2}	3.075×10^{-2}	2.340×10^{-6}	-2.812×10^{-7}	9.355×10^{-2}
		4	2.691×10^{-2}	3.229×10^{-2}	2.351×10^{-6}	2.375×10^{-7}	5.921×10^{-2}
		6	7.602×10^{-3}	2.508×10^{-2}	1.582×10^{-6}	1.476×10^{-6}	3.268×10^{-2}
		8	1.122×10^{-3}	1.305×10^{-2}	5.633×10^{-7}	2.482×10^{-6}	1.418×10^{-2}
		10	5.972×10^{-5}	9.804×10^{-4}	7.323×10^{-8}	9.035×10^{-7}	1.041×10^{-3}
		12	6.380×10^{-7}	2.579×10^{-5}	1.927×10^{-9}	6.531×10^{-8}	2.650×10^{-5}
3.0	0.0735	0	8.293×10^{-2}	7.790×10^{-4}	2.331×10^{-4}	-9.283×10^{-7}	8.394×10^{-2}
		2	4.054×10^{-2}	8.874×10^{-4}	2.654×10^{-4}	4.814×10^{-8}	4.169×10^{-2}
		4	1.404×10^{-2}	7.300×10^{-4}	2.178×10^{-4}	3.606×10^{-6}	1.499×10^{-2}
		6	2.848×10^{-3}	3.597×10^{-4}	1.066×10^{-4}	7.187×10^{-6}	3.322×10^{-3}
		8	2.501×10^{-4}	7.938×10^{-5}	2.307×10^{-5}	4.951×10^{-6}	3.575×10^{-4}
		10	5.884×10^{-6}	5.006×10^{-6}	1.383×10^{-6}	8.965×10^{-7}	1.317×10^{-5}
		12	1.730×10^{-8}	4.556×10^{-8}	1.107×10^{-8}	2.336×10^{-8}	9.728×10^{-8}
5.0	0.0250	0	8.196×10^{-2}	4.240×10^{-4}	5.951×10^{-5}	-1.273×10^{-7}	8.245×10^{-2}
		2	3.985×10^{-2}	4.802×10^{-4}	6.738×10^{-5}	1.430×10^{-8}	4.040×10^{-2}
		4	1.369×10^{-2}	3.909×10^{-4}	5.478×10^{-5}	5.137×10^{-7}	1.413×10^{-2}
		6	2.740×10^{-3}	1.888×10^{-4}	2.637×10^{-5}	9.930×10^{-7}	2.956×10^{-3}
		8	2.357×10^{-4}	4.002×10^{-5}	5.533×10^{-6}	6.528×10^{-7}	2.819×10^{-4}
		10	5.366×10^{-6}	2.319×10^{-6}	3.122×10^{-7}	1.068×10^{-7}	8.105×10^{-6}
		12	1.499×10^{-8}	1.758×10^{-8}	2.211×10^{-9}	2.204×10^{-9}	3.698×10^{-8}

Table 4.11 - Error probability results for single-channel QPSK transmiss with practical filtering ($f_c T_A = 1$)

$B_{IF}T_A$	$\frac{K_1}{T_A}$	$\frac{E_{bA}}{N_o}$ (dB)	P_{e_1}	P_{e_2}	P_{e_3}	P_{e_4}	P_e
1.0	0.1068	0	9.242×10^{-2}	9.719×10^{-3}	1.663×10^{-2}	-9.338×10^{-4}	1.178×10^{-1}
		2	4.752×10^{-2}	1.169×10^{-2}	2.025×10^{-2}	-3.104×10^{-4}	7.916×10^{-2}
		4	1.779×10^{-2}	1.070×10^{-2}	1.947×10^{-2}	1.400×10^{-3}	4.936×10^{-2}
		6	4.075×10^{-3}	6.533×10^{-3}	1.371×10^{-2}	5.019×10^{-3}	2.934×10^{-2}
		8	4.329×10^{-4}	2.247×10^{-3}	2.558×10^{-3}	6.887×10^{-3}	1.213×10^{-2}
		10	1.375×10^{-5}	1.139×10^{-4}	1.990×10^{-4}	1.300×10^{-2}	1.627×10^{-2}
		12	6.494×10^{-8}	1.328×10^{-6}	2.321×10^{-6}	4.097×10^{-5}	4.468×10^{-5}
3.0	0.0368	0	8.424×10^{-2}	1.102×10^{-3}	1.219×10^{-2}	-7.140×10^{-5}	9.745×10^{-2}
		2	4.149×10^{-2}	1.265×10^{-3}	1.427×10^{-2}	6.692×10^{-7}	4.702×10^{-2}
		4	1.453×10^{-2}	1.054×10^{-3}	1.269×10^{-2}	1.983×10^{-4}	2.848×10^{-2}
		6	3.001×10^{-3}	5.315×10^{-4}	7.805×10^{-3}	4.908×10^{-4}	1.183×10^{-2}
		8	2.709×10^{-4}	1.225×10^{-4}	1.284×10^{-3}	5.277×10^{-4}	2.205×10^{-3}
		10	6.658×10^{-6}	8.422×10^{-6}	7.741×10^{-5}	6.408×10^{-5}	1.566×10^{-4}
		12	2.098×10^{-8}	9.105×10^{-8}	6.028×10^{-7}	1.340×10^{-6}	2.055×10^{-6}
5.0	0.0441	0	8.302×10^{-2}	4.846×10^{-4}	1.066×10^{-2}	-2.703×10^{-5}	9.414×10^{-2}
		2	4.061×10^{-2}	5.522×10^{-4}	1.237×10^{-2}	1.811×10^{-6}	5.354×10^{-2}
		4	1.408×10^{-2}	4.541×10^{-4}	1.237×10^{-2}	1.811×10^{-6}	2.545×10^{-2}
		6	2.859×10^{-3}	2.232×10^{-4}	6.436×10^{-3}	1.923×10^{-4}	9.710×10^{-3}
		8	2.516×10^{-4}	4.887×10^{-5}	2.283×10^{-3}	1.927×10^{-4}	2.776×10^{-3}
		10	5.937×10^{-6}	3.012×10^{-6}	6.118×10^{-5}	2.268×10^{-5}	9.281×10^{-5}
		12	1.754×10^{-8}	2.580×10^{-8}	4.469×10^{-7}	4.445×10^{-7}	9.347×10^{-7}

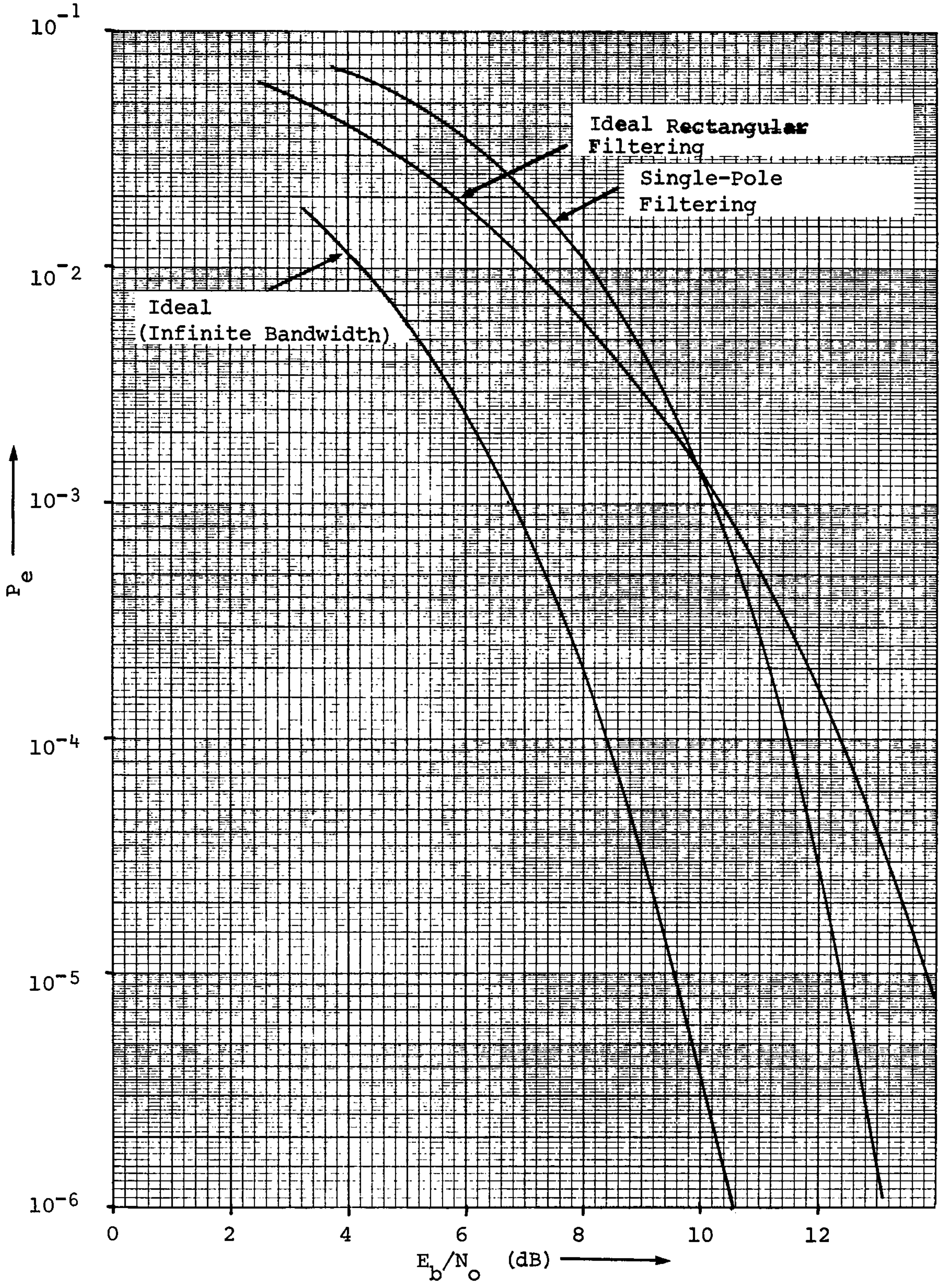

Fig. 4.17. - Comparison of Error probability results for single-channel QPSK transmission ($f_c T_A = 10$, $T_A/T_B = 1$, $B_{IF} T_A = 1$)

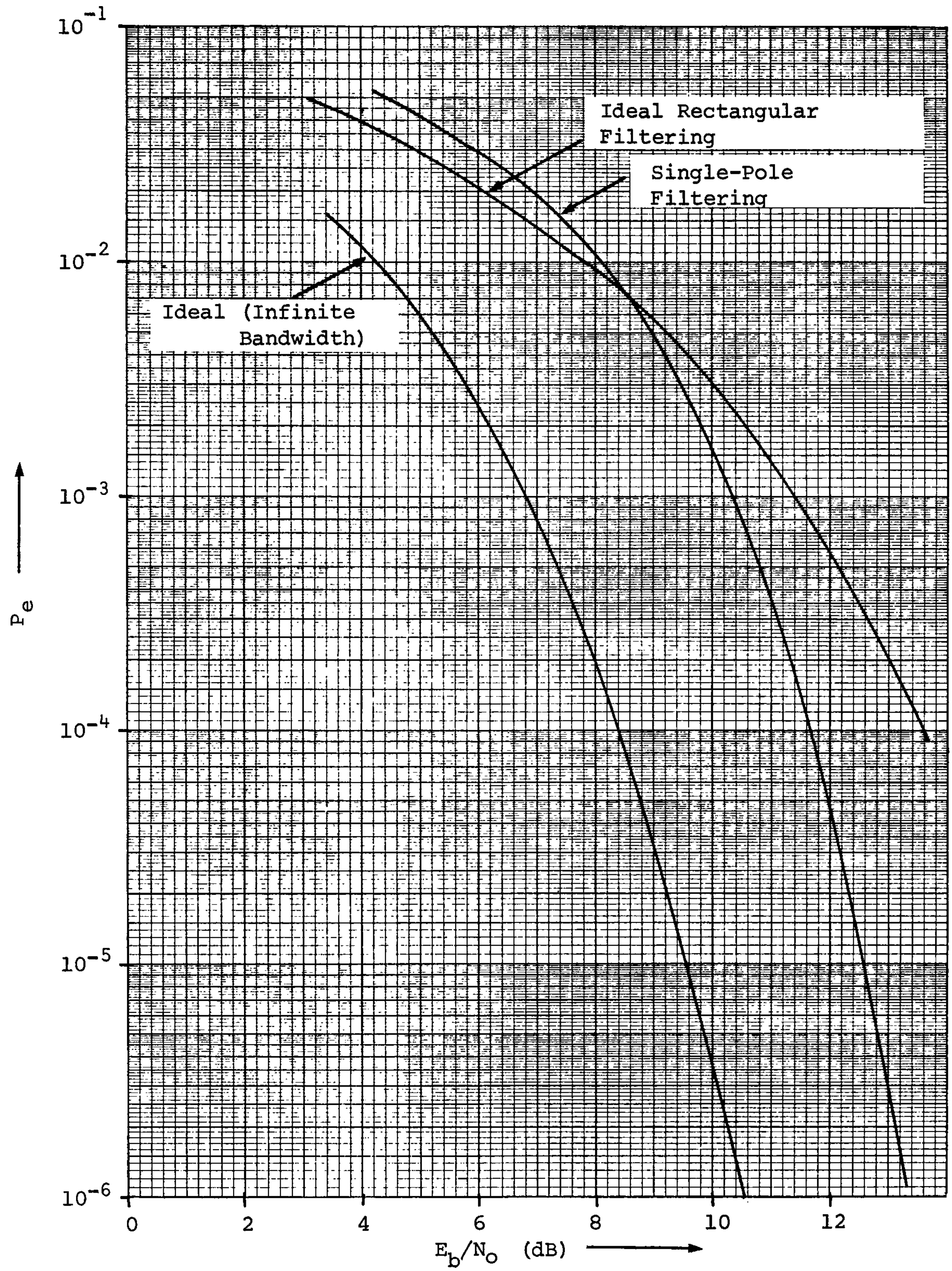

Fig. 4.18. - Comparison of error probability results for single-channel QPSK transmission ($f_c T_A = 1$, $T_A/T_B = 1$, $B_{IF} T_A = 1$)

CHAPTER V

CONCLUSIONS AND RECOMMENDATIONS

The effects of bandlimiting on the error rate performance of QPSK transmission systems utilizing integrate-and-dump detectors have been investigated. Two different IF filter types were considered, and computations of error probability were made for several combinations of system parameters for each filter type.

It was observed that, for a given ratio of filter bandwidth to total transmission rate, the QPSK system provided better performance (lower probability of error) than did a PSK system transmitting the same bit rate. The reason for this result is obvious, since each parallel channel of the QPSK system operates at only half the total transmission rate and hence is not as severely bandlimited as the single channel for PSK.

A comparison of the results obtained for the case of ideal rectangular filtering and for the case of practical (single-pole) filtering indicated that the ideal filter provided superior performance in the noise-limited (low signal-to-noise ratio) region of operation. However, better performance was provided by the practical filter in the region of high signal-to-noise ratio where intersymbol interference and crosstalk became significant.

The results obtained herein were critically dependent on the assumptions stated at the beginning of Chapter IV, namely that (1) the demodulator reference signals were noise-free, (2) timing for the integrate-and-dump detectors was perfect, and (3) the channel noise was additive, white, Gaussian, and zero-mean. For any real system encountered in practice, it is anticipated that at least one of these assumptions would prove to be false. Several topics for future study are suggested by considering this possibility.

Another assumption which was made to simplify the analysis was that the carrier frequency was integrally related to the bit rates in each channel of the QPSK system, or that $f_c T_A$ and $f_c T_B$ were integers. It is not believed that this assumption caused optimistic results to be obtained, but the assumption is by no means always valid in practical systems. Hence it could be of interest to devote some study to cases in which $f_c T_A$ and $f_c T_B$ assume non-integral values.

It was necessary to make still another very important assumption in order to apply the series expansion method of Shimbo and Celebiler to obtain error probability expressions for the cases involving ideal and practical filtering. This was that all of the symbols in the Channel A and Channel B data streams were mutually independent. However, as pointed out by Glave [16], *correlated* data streams are characteristic of many practical PCM systems. In addition to the study by Glave, in which an upper bound was derived for the probability of error due to intersymbol interference in a baseband system for both correlated and uncorrelated signals, an approximation technique for computing the error probability for certain kinds of correlated signals was developed by Hill [17]. It is suggested that these works could be extended to carrier systems such as PSK, DPSK, and QPSK.

A final area suggested for future investigation is associated with the use of detectors other than the integrate-and-dump detector for bandlimited systems. The integrate and dump detector is optimum only for systems having infinite bandwidth. Under conditions of severe bandlimiting, it is possible that (1) a better detector could be implemented for PSK and QPSK or (2) a suboptimum signaling scheme with a nonlinear detector (such as ASK with envelope detection or FSK with discriminator detection) could provide better performance.

REFERENCES

1. J. M. Wozencraft and I. Jacobs, *Principles of Communication Engineering*. New York: McGraw-Hill, 1965.

2. A. J. Viterbi, *Principles of Coherent Communication*. New York: McGraw-Hill, 1966.

3. M. Schwartz, W. R. Bennett, and S. Stein, *Communication Systems and Techniques*. New York: McGraw-Hill, 1966.

4. S. Stein and J. J. Jones, *Modern Communication Principles*. New York: McGraw-Hill, 1967.

5. J. H. Park, "Effects of Band Limiting on the Detection of Binary Signals," *IEEE Trans. on Aerospace and Electronic Systems*, vol. AES-5, pp. 867-870, September 1969.

6. N. M. Shehadeh and K. Tu, "Comments on 'Effects of Band Limiting on the Detection of Binary Signals,'" *IEEE Trans. on Aerospace and Electronic Systems*, vol. AES-8, pp. 719-722, July 1971.

7. B. R. Saltzberg, "Intersymbol Interference Error Bounds with Application to Ideal Bandlimited Signaling," *IEEE Trans. on Information Theory*, vol. IT-14, pp. 563-568, July 1968.

8. H. F. Martinides and G. L. Reijns, "Influence of Bandwidth Restriction on the Signal-to-Noise Performance of a PCM/NRZ Signal," *IEEE Trans. on Aerospace and Electronic Systems*, vol. AES-4, pp. 35-40, January 1968.

9. K. Tu, *The Effects of Bandlimiting on the Performance of Digital Communication Systems*. Ph.D. Dissertation, University of Houston, 1971.

10. R. W. Lucky, J. Salz, and E. J. Weldon, Jr., *Principles of Data Communication*. New York: McGraw-Hill, 1968.

11. H. R. Hartmann, "Degradation of Signal-to-Noise Ratio Due to IF Filtering," *IEEE Trans. on Aerospace and Electronic Systems*, vol. AES-5, pp. 22-32, January 1969.

12. R. Lugannani, "Intersymbol Interference and Probability of Error in Digital Systems," *IEEE Trans. on Information Theory*, vol. IT-15, pp. 682-688, November 1969.

13. O. Shimbo and M. I. Celebiler, "The Probability of Error Due to Intersymbol Interference and Gaussian Noise in Digital Communication Systems," *IEEE Trans. on Communication Technology*, vol. COM-19, pp. 113-119, April 1971.

14. H. Taub and D. L. Schilling, *Principles of Communication Systems*. New York: McGraw-Hill, 1971.

15. A. Papoulis, *The Fourier Integral and Its Applications*. New York: McGraw-Hill, 1965.

16. F. E. Glave, "An Upper Bound on the Probability of Error Due to Intersymbol Interference for Correlated Digital Signals," *IEEE Trans. on Information Theory*, vol. IT-18, pp. 356-363, May 1972.

17. F. S. Hill, Jr., "The Computation of Error Probability for Digital Transmission," *Bell System Technical Journal*, vol. 50, pp. 2055-2077, July-August 1971.

18. B. P. Lathi, *Signals, Systems, and Communication*. New York: Wiley, 1965.

19. A. Papoulis, *Probability, Random Variables, and Stochastic Processes*. New York: McGraw-Hill, 1965.

20. W. B. Davenport and W. L. Root, *Random Signals and Noise*. New York: McGraw-Hill, 1958.

21. M. Abramowitz and I. Stegun, *Handbook of Mathematical Functions*. National Bureau of Standards, 1964.

APPENDIX A

EVALUATION OF IDEAL RECTANGULAR BANDPASS FILTER RESPONSE TO QPSK SIGNAL

Chapter IV shows that if the QPSK signal

$$s(t) = \sum_{m=-\infty}^{\infty} a_m(t)\cos(\omega_c t) + \sum_{n=-\infty}^{\infty} b_n(t)\sin(\omega_c t) \tag{A-1}$$

is applied to the input of the ideal rectangular filter (with no delay), and if an integral number of cycles of the carrier frequency f_c occurs in each bit period T_A of Channel A, the time domain response of the filter to the m^{th} bit of Channel A is

$$S_{1A}(t) = \int_{-f_c-\frac{B_{IF}}{2}}^{-f_c+\frac{B_{IF}}{2}} \frac{A_m f \sin(\pi f T_A)}{\pi(f^2-f_c^2)} e^{-j\pi f(1+2m)T_A} e^{+j2\pi f t}\, df + \int_{f_c-\frac{B_{IF}}{2}}^{f_c+\frac{B_{IF}}{2}} \frac{A_m f \sin(\pi f T_A)}{\pi(f^2-f_c^2)} e^{-j\pi f(1+2m)T_A} e^{+j2\pi f t}\, df \tag{A-2}$$

The first term of (A-2) can be simplified by a change of variable. Letting $x = f + f_c$, this term becomes

$$T_1 = \frac{A_m}{\pi}\int_{-\frac{B_{IF}}{2}}^{+\frac{B_{IF}}{2}} \frac{(x-f_c)\sin[\pi(x-f_c)T_A]}{(x-f_c)^2 - f_c^2} e^{+j2\pi(x-f_c)\left[t-\left(\frac{1+2m}{2}\right)T_A\right]}\, dx \tag{A-3}$$

Using the previous assumption that f_cT_A is an integer, T_1 can be further reduced to

$$T_1 = \frac{A_m}{\pi} e^{-j2\pi f_c t}\int_{-\frac{B_{IF}}{2}}^{+\frac{B_{IF}}{2}} \frac{(x-f_c)\sin(\pi x T_A)\, e^{j2\pi x\left[t-\left(\frac{1+2m}{2}\right)T_A\right]}}{x(x-2f_c)}\, dx \tag{A-4}$$

Again changing variables by letting $y = \pi x T_A$,

$$T_1 = \frac{A_m e^{-j2\pi f_c t}}{\pi} \int_{-\frac{\pi B_{IF} T_A}{2}}^{+\frac{\pi B_{IF} T_A}{2}} \frac{(y - \pi f_c T_A)\sin(y)\, e^{j\left[2\left(\frac{t}{T_A}\right) - (1+2m)\right] y}}{y(y - 2\pi f_c T_A)}\, dy$$

$$= \frac{A_m}{\pi}\left[\cos(2\pi f_c t) - j\sin(2\pi f_c t)\right] \int_{-\frac{\pi B_{IF} T_A}{2}}^{+\frac{\pi B_{IF} T_A}{2}} \frac{(y - \pi f_c T_A)\sin(y)\, e^{j\left[2\left(\frac{t}{T_A}\right) - (1+2m)\right] y}}{y(y - 2\pi f_c T_A)}\, dy \qquad \text{(A-5)}$$

By substituting $x = f - f_c$, the second term of (A-2) becomes

$$T_2 = \frac{A_m}{\pi} \int_{-\frac{B_{IF}}{2}}^{+\frac{B_{IF}}{2}} \frac{(x+f_c)\sin[\pi(x+f_c)T_A]}{(x+f_c)^2 - f_c^2}\, e^{+j2\pi(x+f_c)\left[t - \left(\frac{1+2m}{2}\right)T_A\right]}\, dx \qquad \text{(A-6)}$$

which, if $f_c T_A$ is an integer, can be further simplified to

$$T_2 = \frac{A_m}{\pi} e^{+j2\pi f_c t} \int_{-\frac{B_{IF}}{2}}^{+\frac{B_{IF}}{2}} \frac{(x+f_c)\sin(\pi x T_A)\, e^{j2\pi x\left[t - \left(\frac{1+2m}{2}\right)T_A\right]}}{x(x+2f_c)}\, dx \qquad \text{(A-7)}$$

By substituting $y = \pi x T_A$, T_2 can be reduced to

$$T_2 = \frac{A_m e^{+j2\pi f_c t}}{\pi} \int_{-\frac{\pi B_{IF} T_A}{2}}^{+\frac{\pi B_{IF} T_A}{2}} \frac{(y + \pi f_c T_A)\sin(y)\, e^{j\left[2\left(\frac{t}{T_A}\right) - (1+2m)\right] y}}{y(y + 2\pi f_c T_A)}\, dy$$

$$= \frac{A_m}{\pi}\left[\cos(2\pi f_c t) + j\sin(2\pi f_c t)\right] \int_{-\frac{\pi B_{IF} T_A}{2}}^{+\frac{\pi B_{IF} T_A}{2}} \frac{(y + \pi f_c T_A)\sin(y)\, e^{j\left[2\left(\frac{t}{T_A}\right) - (1+2m)\right] y}}{y(y + 2\pi f_c T_A)}\, dy \qquad \text{(A-8)}$$

By substituting (A-5) and (A-8) into (A-2) and collecting like terms, the following expression is obtained for the time domain response of the filter to the m^{th} bit of Channel A.

$$S_{1A}(t) = \frac{A_m \cos(2\pi f_c t)}{\pi} \int_{-\frac{\pi B_{IF} T_A}{2}}^{+\frac{\pi B_{IF} T_A}{2}} \frac{\sin(y)\, e^{j\left[2\left(\frac{t}{T_A}\right) - (1+2m)\right] y}}{y} \left[\frac{y - \pi f_c T_A}{y - 2\pi f_c T_A} + \frac{y + \pi f_c T_A}{y + 2\pi f_c T_A}\right] dy$$

$$+ \frac{j A_m \sin(2\pi f_c t)}{\pi} \int_{-\frac{\pi B_{IF} T_A}{2}}^{+\frac{\pi B_{IF} T_A}{2}} \frac{\sin(y)\, e^{j\left[2\left(\frac{t}{T_A}\right) - (1+2m)\right] y}}{y} \left[-\frac{y - \pi f_c T_A}{y - 2\pi f_c T_A} + \frac{y + \pi f_c T_A}{y + 2\pi f_c T_A}\right] dy$$

$$= \frac{A_m \cos(2\pi f_c t)}{\pi} \int_{-\frac{\pi B_{IF} T_A}{2}}^{+\frac{\pi B_{IF} T_A}{2}} \frac{\sin(y)\left[2y^2 - (2\pi f_c T_A)^2\right]}{y\left[y^2 - (2\pi f_c T_A)^2\right]} e^{j\left[2\left(\frac{t}{T_A}\right) - (1+2m)\right] y} \, dy$$

$$- \frac{j A_m \sin(2\pi f_c t)}{\pi} \int_{-\frac{\pi B_{IF} T_A}{2}}^{+\frac{\pi B_{IF} T_A}{2}} \frac{2\pi f_c T_A \sin(y)}{y^2 - (2\pi f_c T_A)^2} e^{j\left[2\left(\frac{t}{T_A}\right) - (1+2m)\right] y} \, dy \tag{A-9}$$

Equation (A-9) can be simplified considerably by substituting

$$e^{j\left[2\left(\frac{t}{T_A}\right) - (1+2m)\right] y} = \cos\left\{\left[2\left(\frac{t}{T_A}\right) - (1+2m)\right] y\right\} + j \sin\left\{\left[2\left(\frac{t}{T_A}\right) - (1+2m)\right] y\right\} \tag{A-10}$$

and then observing (1) that the integral of an *even* function between the limits $-\alpha$ to $+\alpha$ is twice the integral of the function from 0 to $+\alpha$, and (2) that the integral of an *odd* function between the limits $-\alpha$ to $+\alpha$ is zero. The resultant expression is

$$s_{1A}(t) = \frac{2A_m}{\pi} \left\{ \int_0^{\frac{\pi B_{IF} T_A}{2}} \frac{\sin(y)\left[2y^2 - (2\pi f_c T_A)^2\right]}{y\left[y^2 - (2\pi f_c T_A)^2\right]} \cos\left\{\left[2\left(\frac{t}{T_A}\right) - (1+2m)\right] y\right\} dy \right\} \cos(2\pi f_c t)$$

$$+ \frac{2A_m}{\pi} \left\{ \int_0^{\frac{\pi B_{IF} T_A}{2}} \frac{2\pi f_c T_A \sin(y)}{y^2 - (2\pi f_c T_A)^2} \sin\left\{\left[2\left(\frac{t}{T_A}\right) - (1 \;\; 2m)\right] y\right\} dy \right\} \sin(2\pi f_c t) \tag{A-11}$$

The above procedure can be repeated to determine a simplified expression for the time domain response of the filter to the n^{th} bit of Channel B. Equation (4-9) shows that if $f_c T_B$ is an integer

$$s_{1B}(t) = \int_{-f_c-\frac{B_{IF}}{2}}^{-f_c+\frac{B_{IF}}{2}} \frac{-jB_n f_c \sin(\pi f T_B)}{\pi(f^2-f_c^2)} e^{-j\pi f(1+2n)T_B} e^{+j2\pi f t} df$$

$$+ \int_{f_c-\frac{B_{IF}}{2}}^{f_c+\frac{B_{IF}}{2}} \frac{-jB_n f_c \sin(\pi f T_B)}{\pi(f^2-f_c^2)} e^{-j\pi f(1+2n)T_B} e^{+j2\pi f t} df$$

$$= T_3 + T_4 \qquad \text{(A-12)}$$

By substituting $x = f + f_c$ into the expression for T_3 and $x = f - f_c$ into the expression for T_4, and by making the simplifications which apply when f_cT_B is an integer, (A-12) becomes

$$s_{1B}(t) = \frac{-jB_n f_c e^{-j2\pi f_c t}}{\pi} \int_{-\frac{B_{IF}}{2}}^{+\frac{B_{IF}}{2}} \frac{\sin(\pi x T_B)}{x(x-2f_c)} e^{j2\pi x[t-(\frac{1+2n}{2})T_B]} dx$$

$$- \frac{jB_n f_c e^{+j2\pi f_c t}}{\pi} \int_{-\frac{B_{IF}}{2}}^{+\frac{B_{IF}}{2}} \frac{\sin(\pi x T_B)}{x(x+2f_c)} e^{j2\pi x[t-(\frac{1+2n}{2})T_B]} dx \qquad \text{(A-13)}$$

Equation (A-13) can be further simplified by substituting $y = \pi X T_B$ and collecting like terms. The result is

$$s_{1B}(t) = -jB_n f_c T_B \cos(2\pi f_c t) \int_{-\frac{\pi B_{IF} T_B}{2}}^{+\frac{\pi B_{IF} T_B}{2}} \frac{2\sin(y)}{y^2-(2\pi f_c T_B)^2} e^{j[2(\frac{t}{T_B})-(1+2n)]y} dy$$

$$+ B_n f_c T_B \sin(2\pi f_c t) \int_{-\frac{\pi B_{IF} T_B}{2}}^{+\frac{\pi B_{IF} T_B}{2}} \frac{-4\pi f_c T_B \sin(y)}{y[y^2-(2\pi f_c T_B)^2]} e^{j[2(\frac{t}{T_B})-(1+2n)]y} dy$$

$$= 2B_n f_c T_B \left\{ \int_0^{\frac{\pi B_{IF} T_B}{2}} \frac{2\sin(y)}{y^2 - (2\pi f_c T_B)^2} \sin\left\{\left[2\left(\frac{t}{T_B}\right) - (1+2n)\right] y\right\} dy \right\} \cos(2\pi f_c t)$$

$$-2B_n f_c T_B \left\{ \int_0^{\frac{\pi B_{IF} T_B}{2}} \frac{4\pi f_c T_B \sin(y)}{y\left[y^2 - (2\pi f_c T_B)^2\right]} \cos\left\{\left[2\left(\frac{t}{T_B}\right) - (1+2n)\right] y\right\} dy \right\} \sin(2\pi f_c t) \qquad \text{(A-14)}$$

APPENDIX B

EVALUATION OF CHANNEL A SIGNAL AND CROSSTALK VOLTAGES FOR IDEAL RECTANGULAR FILTERING

SIGNAL TERM

Chapter IV shows that for ideal rectangular filtering the output signal voltage for Channel A, at the sampling instant T_A, is given by

$$S_{4A,\,signal}(T_A) = \sum_{m=-\infty}^{\infty} \frac{A_m T_A}{\pi} \int_0^{\frac{\pi B_{IF} T_A}{2}} \frac{[2y^2 - (2\pi f_c T_A)^2]\,\sin^2(y)\cos(2my)}{y^2[y^2 - (2\pi f_c T_A)^2]}\,dy \tag{B-1}$$

The above integral can be expressed as the sum of two integrals, resulting in the following expression:

$$S_{4A,\,signal}(T_A) = \sum_{m=-\infty}^{\infty} \frac{A_m T_A}{\pi} \left\{ \int_0^{\frac{\pi B_{IF} T_A}{2}} \frac{2\sin^2(y)\cos(2my)}{y^2 - (2\pi f_c T_A)^2}\,dy - \int_0^{\frac{\pi B_{IF} T_A}{2}} \frac{(2\pi f_c T_A)^2 \sin^2(y)\cos(2my)}{y^2[y^2 - (2\pi f_c T_A)^2]}\,dy \right\}$$

$$= \sum_{m=-\infty}^{\infty} \frac{A_m T_A}{\pi} \left\{ \int_0^{\frac{\pi B_{IF} T_A}{2}} \frac{2\sin^2(y)\cos(2my)}{y^2 - (2\pi f_c T_A)^2}\,dy - \int_0^{\frac{\pi B_{IF} T_A}{2}} \left[\frac{\sin^2(y)\cos(2my)}{y^2 - (2\pi f_c T_A)^2} - \frac{\sin^2(y)\cos(2my)}{y^2} \right] dy \right\}$$

$$= \sum_{m=-\infty}^{\infty} \frac{A_m T_A}{2} \left[\frac{2}{\pi} \int_0^{\frac{\pi B_{IF} T_A}{2}} \frac{\sin^2(y)\cos(2my)}{y^2} dy - \frac{2}{\pi} \int_0^{\frac{\pi B_{IF} T_A}{2}} \frac{\sin^2(y)\cos(2my)}{(2\pi f_c T_A)^2 - y^2} dy \right]$$

$$= \sum_{m=-\infty}^{\infty} \frac{A_m T_A}{2} \left[\Psi_{I1}(m) - \Psi_{I2}(m) \right] \tag{B-2}$$

Reduction of $\Psi_{I_1}(m)$

The function

$$\Psi_{I1}(m) = \frac{2}{\pi} \int_0^{\frac{\pi B_{IF} T_A}{2}} \frac{\sin^2(y)\cos(2my)}{y^2} dy \tag{B-3}$$

can be simplified in terms of elementary functions and the tabulated sine integral. It is first noted that for $m = 0$,

$$\Psi_{I1}(0) = \frac{2}{\pi} \int_0^{\frac{\pi B_{IF} T_A}{2}} \frac{\sin^2(y)}{y^2} dy$$

$$= \frac{2}{\pi} \left[\int_0^{\frac{\pi B_{IF} T_A}{2}} \frac{dy}{2y^2} - \int_0^{\frac{\pi B_{IF} T_A}{2}} \frac{\cos(2y)}{2y^2} dy \right] \tag{B-4}$$

By substituting $z = 2y$, (B-4) becomes

$$\Psi_{I1}(0) = \frac{2}{\pi} \left[\int_0^{\pi B_{IF} T_A} \frac{dz}{z^2} - \int_0^{\pi B_{IF} T_A} \frac{\cos(z)}{z^2} dz \right]$$

$$= \frac{2}{\pi} \left[-\frac{1}{z} \right]_0^{\pi B_{IF} T_A} + \frac{2}{\pi} \left[\frac{\cos(z)}{z} \right]_0^{\pi B_{IF} T_A} + \frac{2}{\pi} \int_0^{\pi B_{IF} T_A} \frac{\sin(z)}{z} dz$$

$$= \frac{2}{\pi} Si\left(\pi B_{IF} T_A\right) - \frac{2}{\pi}\left[\frac{\sin^2\left(\frac{\pi B_{IF} T_A}{2}\right)}{\left(\frac{\pi B_{IF} T_A}{2}\right)}\right] \quad \text{(B-5)}$$

where

$$Si\left(\pi B_{IF} T_A\right) = \int_0^{\pi B_{IF} T_A} \frac{\sin(z)}{z}\, dz$$

For $m \neq 0$,

$$\Psi_{I1}(m) = \frac{2}{\pi}\int_0^{\frac{\pi B_{IF} T_A}{2}} \frac{[1-\cos(2y)]\cos(2my)}{2y^2}\, dy$$

$$= \frac{1}{\pi}\int_0^{\frac{\pi B_{IF} T_A}{2}} \frac{\cos(2my)}{y^2}\, dy - \frac{1}{2\pi}\int_0^{\frac{\pi B_{IF} T_A}{2}} \frac{\cos[(m+1)2y]}{y^2}\, dy$$

$$- \frac{1}{2\pi}\int_0^{\frac{\pi B_{IF} T_A}{2}} \frac{\cos[(m-1)2y]}{y^2}\, dy \quad \text{(B-6)}$$

Substituting $z = 2my$ into the first term of the preceding equation, $z = (m+1)2y$ into the second term, $z = (m-1)2y$ into the third term, and simplifying all three terms yields

$$\Psi_{I1}(m) = \frac{2m}{\pi}\int_0^{m\pi B_{IF} T_A} \frac{\cos(z)}{z^2}\, dz - \frac{m+1}{\pi}\int_0^{(m+1)\pi B_{IF} T_A} \frac{\cos(z)}{z^2}\, dz$$

$$- \frac{m-1}{\pi}\int_0^{(m-1)\pi B_{IF} T_A} \frac{\cos(z)}{z^2}\, dz$$

$$= -\frac{2m}{\pi}\left[\frac{\cos(m\pi B_{IF}T_A)}{m\pi B_{IF}T_A}\right] - \frac{2m}{\pi}\,Si\,(m\pi B_{IF}T_A)$$

$$+ \frac{m+1}{\pi}\left\{\frac{\cos[(m+1)\pi B_{IF}T_A]}{(m+1)\pi B_{IF}T_A}\right\} + \frac{m+1}{\pi}\,Si\,[(m+1)\pi B_{IF}T_A]$$

$$+ \frac{m-1}{\pi}\left\{\frac{\cos[(m-1)\pi B_{IF}T_A]}{(m-1)\pi B_{IF}T_A}\right\} + \frac{m-1}{\pi}\,Si\,[(m-1)\pi B_{IF}T_A]$$

$$= -m\left\{\frac{2}{\pi}Si\,(m\pi B_{IF}T_A) - \frac{2}{\pi}\left[\frac{\sin^2\left(\frac{m\pi B_{IF}T_A}{2}\right)}{\frac{m\pi B_{IF}T_A}{2}}\right]\right\}$$

$$+ \frac{m+1}{2}\left\{\frac{2}{\pi}Si\,[(m+1)\pi B_{IF}T_A] - \frac{2}{\pi}\left[\frac{\sin^2\frac{(m+1)\pi B_{IF}T_A}{2}}{\frac{(m+1)\pi B_{IF}T_A}{2}}\right]\right\}$$

$$+ \frac{m-1}{2}\left\{\frac{2}{\pi}Si\,[(m-1)\pi B_{IF}T_A] - \frac{2}{\pi}\left[\frac{\sin^2\frac{(m-1)\pi B_{IF}T_A}{2}}{\frac{(m-1)\pi B_{IF}T_A}{2}}\right]\right\}$$

$$= -m\Psi_{I1}(0)\Big|_{B_{IF}T_A \to mB_{IF}T_A} + \left(\frac{m+1}{2}\right)\Psi_{I1}(0)\Big|_{B_{IF}T_A \to (m+1)B_{IF}T_A}$$

$$+ \left(\frac{m-1}{2}\right)\Psi_{I1}(0)\Big|_{B_{IF}T_A \to (m-1)B_{IF}T_A}$$

(B-7)

Reduction of $\Psi_{I_2}(m)$

The function

$$\Psi_{I2}(m) = \frac{2}{\pi}\int_0^{\frac{\pi B_{IF}T_A}{2}} \frac{\sin^2(y)\cos(2my)}{(2\pi f_c T_A)^2 - y^2}\,dy \tag{B-8}$$

can be evaluated in terms of elementary functions and the tabulated cosine integral. It will be convenient to define the function first for $m = 0$ and then to express the function in terms of this value. Thus,

$$\Psi_{I2}(0) = \frac{2}{\pi}\int_0^{\frac{\pi B_{IF}T_A}{2}} \frac{\sin^2(y)}{(2\pi f_c T_A)^2 - y^2}\,dy \tag{B-9}$$

For $m \neq 0$

$$\Psi_{I2}(m) = \frac{2}{\pi}\int_0^{\frac{\pi B_{IF}T_A}{2}} \frac{\frac{1}{2}[1-\cos(2y)]\cos(2my)}{(2\pi f_c T_A)^2 - y^2}\,dy$$

$$= \frac{1}{\pi}\int_0^{\frac{\pi B_{IF}T_A}{2}} \frac{\cos(2my)}{(2\pi f_c T_A)^2 - y^2}\,dy - \frac{1}{2\pi}\int_0^{\frac{\pi B_{IF}T_A}{2}} \frac{\cos[(m+1)2y]}{(2\pi f_c T_A)^2 - y^2}\,dy$$

$$- \frac{1}{2\pi}\int_0^{\frac{\pi B_{IF}T_A}{2}} \frac{\cos[(m-1)2y]}{(2\pi f_c T_A)^2 - y^2}\,dy$$

$$= -\frac{2}{\pi}\int_0^{\frac{\pi B_{IF}T_A}{2}} \frac{\sin^2(my)}{(2\pi f_c T_A)^2 - y^2}\,dy + \frac{1}{\pi}\int_0^{\frac{\pi B_{IF}T_A}{2}} \frac{\sin^2[(m+1)y]}{(2\pi f_c T_A)^2 - y^2}\,dy$$

$$+ \frac{1}{\pi}\int_0^{\frac{\pi B_{IF}T_A}{2}} \frac{\sin^2[(m-1)y]}{(2\pi f_c T_A)^2 - y^2}\,dy \tag{B-10}$$

Substituting $z = my$ into the first term of (B-10), $z = (m + 1)y$ into the second term, and $z = (m - 1)y$ into the third term results in the following expression:

$$\Psi_{I2}(m) = -m \frac{2}{\pi}\int_0^{\frac{m\pi B_{IF}T_A}{2}} \frac{\sin^2(z)}{(2m\pi f_c T_A)^2 - z^2}\, dz$$

$$+ \frac{m+1}{2} \frac{2}{\pi}\int_0^{\frac{(m+1)\pi B_{IF}T_A}{2}} \frac{\sin^2(z)}{[2(m+1)\pi f_c T_A]^2 - z^2}\, dz$$

$$+ \frac{m-1}{2} \frac{2}{\pi}\int_0^{\frac{(m-1)\pi B_{IF}T_A}{2}} \frac{\sin^2(z)}{[2(m-1)\pi f_c T_A]^2 - z^2}\, dz$$

$$= -m\Psi_{I2}(0)\Big|_{\substack{B_{IF}T_A \to mB_{IF}T_A \\ f_cT_A \to mf_cT_A}} + \left(\frac{m+1}{2}\right)\Psi_{I2}(0)\Big|_{\substack{B_{IF}T_A \to (m+1)B_{IF}T_A \\ f_cT_A \to (m+1)f_cT_A}}$$

$$+ \left(\frac{m-1}{2}\right)\Psi_{I2}(0)\Big|_{\substack{B_{IF}T_A \to (m-1)B_{IF}T_A \\ f_cT_A \to (m-1)f_cT_A}}$$

(B-11)

It is now necessary to evaluate

$$\Psi_{I2}(0)\Big|_{\substack{B_{IF}T_A \to mB_{IF}T_A \\ f_cT_A \to mf_cT_A}} = \frac{2}{\pi}\int_0^{\frac{m\pi B_{IF}T_A}{2}} \frac{\sin^2(z)}{(2m\pi f_c T_A)^2 - z^2}\, dz$$

$$= \left(\frac{2}{\pi}\right)\left(\frac{1}{4m\pi f_c T_A}\right)\left[\int_0^{\frac{m\pi B_{IF}T_A}{2}} \frac{\sin^2(z)}{2m\pi f_c T_A + z}\, dz + \int_0^{\frac{m\pi B_{IF}T_A}{2}} \frac{\sin^2(z)}{2m\pi f_c T_A - z}\, dz\right]$$

(B-12)

Substituting $x = z + 2m\pi f_c T_A$ into the first term of the preceding equation and $x = -z + 2m\pi f_c T_A$ into the second term yields

$$\Psi_{I2}(0)\Bigg|_{\substack{B_{IF}T_A \to mB_{IF}T_A \\ f_cT_A \to mf_cT_A}} = \frac{1}{2m\pi^2 f_c T_A}\left[\int_{2m\pi f_c T_A}^{2m\pi f_c T_A + \frac{m\pi B_{IF}T_A}{2}} \frac{\sin^2(x - 2m\pi f_c T_A)}{x}\,dx + \int_{2m\pi f_c T_A - \frac{m\pi B_{IF}T_A}{2}}^{2m\pi f_c T_A} \frac{\sin^2(x - 2m\pi f_c T_A)}{x}\,dx\right] \qquad \text{(B-13)}$$

If $f_c T_A$ is an integer, then (B-13) reduces to

$$\Psi_{I2}(0)\Bigg|_{\substack{B_{IF}T_A \to mB_{IF}T_A \\ f_cT_A \to mf_cT_A}} = \frac{1}{2m\pi^2 f_c T_A}\left[\int_{2m\pi f_c T_A}^{2m\pi f_c T_A + \frac{m\pi B_{IF}T_A}{2}} \frac{\sin^2(x)}{x}\,dx + \int_{2m\pi f_c T_A - \frac{m\pi B_{IF}T_A}{2}}^{2m\pi f_c T_A} \frac{\sin^2(x)}{x}\,dx\right]$$

$$= \frac{1}{2m\pi^2 f_c T_A}\int_{2m\pi f_c T_A - \frac{m\pi B_{IF}T_A}{2}}^{2m\pi f_c T_A + \frac{m\pi B_{IF}T_A}{2}} \frac{\sin^2(x)}{x}\,dx$$

$$= \frac{1}{2m\pi^2 f_c T_A}\left[\cancelto{0}{\int_{2m\pi f_c T_A - \frac{m\pi B_{IF}T_A}{2}}^{\left|2m\pi f_c T_A - \frac{m\pi B_{IF}T_A}{2}\right|} \frac{\sin^2(x)}{x}\,dx} + \int_{\left|2m\pi f_c T_A - \frac{m\pi B_{IF}T_A}{2}\right|}^{2m\pi f_c T_A + \frac{m\pi B_{IF}T_A}{2}} \frac{\sin^2(x)}{x}\,dx\right]$$

$$= \frac{1}{4m\pi^2 f_c T_A}\left[\int_{\left|2m\pi f_c T_A - \frac{m\pi B_{IF}T_A}{2}\right|}^{2m\pi f_c T_A + \frac{m\pi B_{IF}T_A}{2}} \frac{dx}{x} - \int_{\left|2m\pi f_c T_A - \frac{m\pi B_{IF}T_A}{2}\right|}^{2m\pi f_c T_A + \frac{m\pi B_{IF}T_A}{2}} \frac{\cos(2z)}{z}\,dz\right]$$

$$= \frac{1}{4m\pi^2 f_c T_A}\left[\ln\frac{2\pi m f_c T_A + \frac{\pi m B_{IF}T_A}{2}}{\left|2\pi m f_c T_A - \frac{\pi m B_{IF}T_A}{2}\right|} - Ci\left(4\pi m f_c T_A + \pi m B_{IF}T_A\right) + Ci\left(\left|4\pi m f_c T_A - \pi m B_{IF}T_A\right|\right)\right] \qquad \text{(B-14)}$$

where $Ci(\alpha) = \int_{\infty}^{\alpha} \frac{\cos(y)}{y}\,dy$

CROSSTALK TERM

Chapter IV shows that for ideal rectangular filtering the crosstalk voltage for Channel A at the sampling instant T_A is given by

$$S_{4A,\,crosstalk}(T_A) = -\sum_{n=-\infty}^{\infty} 2B_n f_c T_B^2 \int_0^{\frac{\pi B_{IF} T_B}{2}} \frac{\sin(y)\sin\left[\left(\frac{T_A}{T_B}\right)y\right]\sin\left[\left(1-\frac{T_A}{T_B}+2n\right)y\right]}{y\left[y^2-(2\pi f_c T_B)^2\right]}\,dy \tag{B-15}$$

The single integral in this expression can be first expressed as the sum of two integrals, giving

$$S_{4A,\,crosstalk}(T_A) = \sum_{n=-\infty}^{\infty} \frac{B_n}{2\pi^2 f_c} \int_0^{\frac{\pi B_{IF} T_B}{2}} \frac{\sin(y)\sin\left[\left(\frac{T_A}{T_B}\right)y\right]\sin\left[\left(1-\frac{T_A}{T_B}+2n\right)y\right]}{y}\,dy - \int_0^{\frac{\pi B_{IF} T_B}{2}} \frac{y\sin(y)\sin\left[\left(\frac{T_A}{T_B}\right)y\right]\sin\left[\left(1-\frac{T_A}{T_B}+2n\right)y\right]}{y^2-(2\pi f_c T_B)^2}\,dy$$

$$= \sum_{n=-\infty}^{\infty} \left(\frac{B_n T_B}{2}\right)\left(\frac{1}{2\pi f_c T_B}\right)\left[\frac{2}{\pi}\int_0^{\frac{\pi B_{IF} T_B}{2}} \frac{\sin(y)\sin\left[\left(\frac{T_A}{T_B}\right)y\right]\sin\left[\left(1-\frac{T_A}{T_B}+2n\right)y\right]}{y}\,dy - \frac{2}{\pi}\int_0^{\frac{\pi B_{IF} T_B}{2}} \frac{y\sin(y)\sin\left[\left(\frac{T_A}{T_B}\right)y\right]\sin\left[\left(1-\frac{T_A}{T_B}+2n\right)y\right]}{y^2-(2\pi f_c T_B)^2}\,dy\right]$$

$$= \sum_{n=-\infty}^{\infty} \left(\frac{B_n T_B}{2}\right)\left(\frac{1}{2\pi f_c T_B}\right)\left[\Psi_{I3}(n) - \Psi_{I4}(n)\right] \tag{B-16}$$

Reduction of $\Psi_{I_3}(n)$

The function

$$\Psi_{I3}(n) = \frac{2}{\pi}\int_0^{\frac{\pi B_{IF}T_B}{2}} \frac{\sin(y)\sin\left[\left(\frac{T_A}{T_B}\right)y\right]\sin\left[\left(1-\frac{T_A}{T_B}+2n\right)y\right]}{y}\,dy \tag{B-17}$$

can be simplified in terms of the tabulated sine integral. Application of trigonometric product formulas yields

$$\begin{aligned}\Psi_{I3}(n) = {} & \frac{1}{2\pi}\int_0^{\frac{\pi B_{IF}T_B}{2}} \frac{\sin\left[2\left(1-\frac{T_A}{T_B}+n\right)y\right]}{y}\,dy \\ & + \frac{1}{2\pi}\int_0^{\frac{\pi B_{IF}T_B}{2}} \frac{\sin(2ny)}{y}\,dy \\ & - \frac{1}{2\pi}\int_0^{\frac{\pi B_{IF}T_B}{2}} \frac{\sin\left[2(1+n)y\right]}{y}\,dy \\ & - \frac{1}{2\pi}\int_0^{\frac{\pi B_{IF}T_B}{2}} \frac{\sin\left[2\left(n-\frac{T_A}{T_B}\right)y\right]}{y}\,dy\end{aligned} \tag{B-18}$$

Making simple variable substitutions in each of the four integrals in the preceding equations provides the following result.

$$\begin{aligned}\Psi_{I3}(n) = \frac{1}{2\pi}\Big\{ & Si\left[\left(n+1-\frac{T_A}{T_B}\right)\pi B_{IF}T_B\right] + Si\left(n\pi B_{IF}T_B\right) \\ & - Si\left[(n+1)\pi B_{IF}T_B\right] - Si\left[\left(n-\frac{T_A}{T_B}\right)\pi B_{IF}T_B\right]\Big\}\end{aligned} \tag{B-19}$$

Reduction of $\Psi_{I_4}(n)$

Application of trigonometric product formulas and expansion by partial fractions allow the function

$$\Psi_{I4}(n) = \frac{2}{\pi}\int_0^{\frac{\pi B_{IF}T_B}{2}} \frac{y\sin(y)\sin\left[\left(\frac{T_A}{T_B}\right)y\right]\sin\left[\left(1-\frac{T_A}{T_B}+2n\right)y\right]}{y^2-(2\pi f_c T_B)^2}\,dy \tag{B-20}$$

to be expressed as the sum of eight simpler integrals

$$\begin{aligned}\Psi_{I4}(n) = \frac{1}{4\pi}\Bigg\{ & \int_0^{\frac{\pi B_{IF}T_B}{2}} \frac{\sin\left[2\left(1-\frac{T_A}{T_B}+n\right)y\right]}{y+2\pi f_c T_B}\,dy + \int_0^{\frac{\pi B_{IF}T_B}{2}} \frac{\sin(2ny)}{y+2\pi f_c T_B}\,dy \\ & - \int_0^{\frac{\pi B_{IF}T_B}{2}} \frac{\sin[2(1+n)y]}{y+2\pi f_c T_B}\,dy + \int_0^{\frac{\pi B_{IF}T_B}{2}} \frac{\sin\left[2\left(\frac{T_A}{T_B}-n\right)y\right]}{y+2\pi f_c T_B}\,dy \\ & + \int_0^{\frac{\pi B_{IF}T_B}{2}} \frac{\sin\left[2\left(1-\frac{T_A}{T_B}+n\right)y\right]}{y-2\pi f_c T_B}\,dy + \int_0^{\frac{\pi B_{IF}T_B}{2}} \frac{\sin(2ny)}{y-2\pi f_c T_B}\,dy \\ & - \int_0^{\frac{\pi B_{IF}T_B}{2}} \frac{\sin[2(1+n)y]}{y-2\pi f_c T_B}\,dy + \int_0^{\frac{\pi B_{IF}T_B}{2}} \frac{\sin\left[2\left(\frac{T_A}{T_B}-n\right)y\right]}{y-2\pi f_c T_B}\,dy \Bigg\}\end{aligned} \tag{B-21}$$

By making simple variable substitutions in each of these eight integrals and by making the simplifications that are possible for integral values of $f_c T_B$, the following result is obtained.

$$
\begin{aligned}
\Psi_{I4}(n) = \frac{1}{4\pi} \Big\{ & Si\left[\left(1-\frac{T_A}{T_B}+n\right)\pi T_B\left(4f_c+B_{IF}\right)\right] \\
& - Si\left[\left(1-\frac{T_A}{T_B}+n\right)\pi T_B\left(4f_c-B_{IF}\right)\right] \\
& + Si\left[n\pi T_B\left(4f_c+B_{IF}\right)\right] - Si\left[n\pi T_B\left(4f_c-B_{IF}\right)\right] \\
& - Si\left[(1+n)\pi T_B\left(4f_c+B_{IF}\right)\right] + Si\left[(1+n)\pi T_B\left(4f_c-B_{IF}\right)\right] \\
& + Si\left[\left(\frac{T_A}{T_B}-n\right)\pi T_B\left(4f_c+B_{IF}\right)\right] \\
& - Si\left[\left(\frac{T_A}{T_B}-n\right)\pi T_B\left(4f_c-B_{IF}\right)\right] \Big\} \qquad \text{(B-22)}
\end{aligned}
$$

APPENDIX C

EVALUATION OF CHANNEL A NOISE POWER FOR IDEAL RECTANGULAR FILTERING

As stated in the beginning of Chapter IV, the channel noise is assumed to be additive, white, Gaussian, zero-mean, and to have single-sided noise spectral density N_o watts/Hz. The channel noise is summed with the QPSK signal and applied to the input of the ideal rectangular bandpass filter. In order to be able to compute error probabilities at the outputs of the two quadrature channels of the QPSK detector, it is necessary that the variance of the noise at the output of each of the integrate-and-dump circuits be determined. For zero-mean processes, variance is equivalent to power, so it is actually the output noise power which will be determined.

The variance of the output noise for Channel A can be determined most readily by first combining the bandpass filter with the components of the Channel A detector and obtaining a composite frequency characteristic. The notation used for this step is summarized in Fig. C.1. It can first be observed that the bandpass filter output can be expressed in the frequency domain as

$$X_2(f) = \begin{cases} X_1(f) & \text{for } -f_c - \frac{B_{IF}}{2} \le f \le -f_c + \frac{B_{IF}}{2} \\ X_1(f) & \text{for } f_c - \frac{B_{IF}}{2} \le f \le f_c + \frac{B_{IF}}{2} \\ 0 & \text{otherwise} \end{cases} \tag{C-1}$$

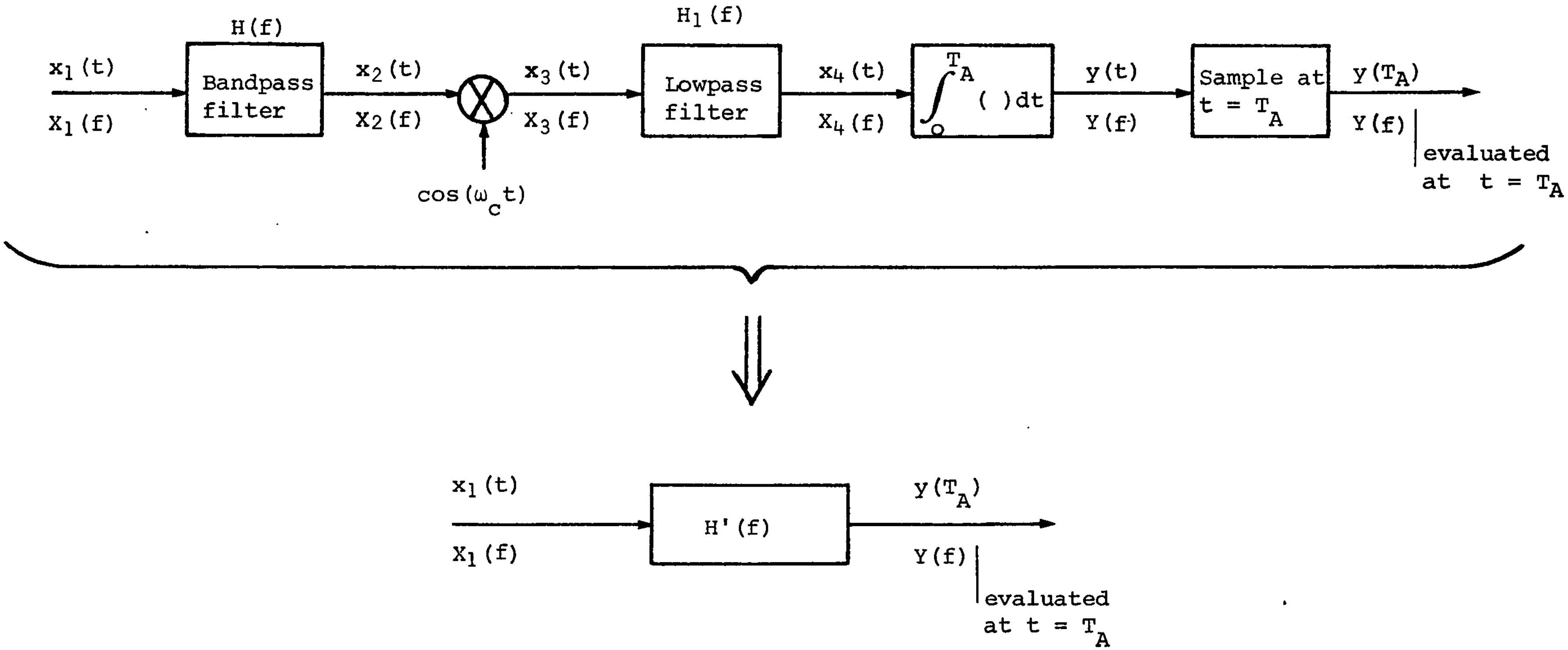

Fig. C.1. - Combination of bandpass filter with Channel A detector components

The time domain output of the bandpass filter is determined by taking the inverse Fourier transform of (C-1).

$$
\begin{aligned}
x_2(t) &= \mathcal{F}^{-1}\left[X_2(f)\right] \\
&= \int_{-\infty}^{\infty} X_2(f)\, e^{+j2\pi f t}\, df \\
&= \int_{-f_c-\frac{B_{IF}}{2}}^{-f_c+\frac{B_{IF}}{2}} X_1(f)\, e^{+j2\pi f t}\, df + \int_{f_c-\frac{B_{IF}}{2}}^{f_c+\frac{B_{IF}}{2}} X_1(f)\, e^{+j2\pi f t}\, df
\end{aligned}
\tag{C-2}
$$

The time domain output of the Channel A multiplier is given by

$$
\begin{aligned}
x_3(t) &= x_2(t)\cos(\omega_c t) \\
&= x_2(t)\left[\frac{e^{j2\pi f_c t} + e^{-j2\pi f_c t}}{2}\right] \\
&= \frac{1}{2}\int_{-f_c-\frac{B_{IF}}{2}}^{-f_c+\frac{B_{IF}}{2}} X_1(f)\left[e^{j2\pi(f+f_c)t} + e^{j2\pi(f-f_c)t}\right] df \\
&\quad + \frac{1}{2}\int_{f_c-\frac{B_{IF}}{2}}^{f_c+\frac{B_{IF}}{2}} X_1(f)\left[e^{j2\pi(f+f_c)t} + e^{j2\pi(f-f_c)t}\right] df
\end{aligned}
\tag{C-3}
$$

The frequency domain output of the Channel A multiplier is

$$
X_3(f) = \mathcal{F}\left[x_3(t)\right] = \mathcal{F}\left[x_2(t)\cos(\omega_c t)\right]
\tag{C-4}
$$

Applying the identity [18]

$$f(t)\cos(\omega_0 t) \longleftrightarrow \frac{1}{2}\left[F(\omega-\omega_0)+F(\omega+\omega_0)\right] \tag{C-5}$$

to (C-4) yields

$$X_3(f) = \frac{1}{2}\left[X_2(f-f_c)+X_2(f+f_c)\right] \tag{C-6}$$

Substitution of (C-1) into (C-6) gives

$$X_3(f) = \begin{cases} \frac{1}{2}\left[X_1(f-f_c)+X_1(f+f_c)\right] & \text{for } -\frac{B_{IF}}{2} \le f \le +\frac{B_{IF}}{2} \\ 0 & \text{otherwise} \end{cases} \tag{C-7}$$

The frequency domain output of the lowpass filter is given by

$$X_4(f) = \begin{cases} X_3(f) & \text{for } -\frac{B_{IF}}{2} \le f \le +\frac{B_{IF}}{2} \\ 0 & \text{otherwise} \end{cases}$$

$$= \begin{cases} \frac{1}{2}\left[X_1(f-f_c)+X_1(f+f_c)\right] & \text{for } -\frac{B_{IF}}{2} \le f \le +\frac{B_{IF}}{2} \\ 0 & \text{otherwise} \end{cases} \tag{C-8}$$

The time domain output of the lowpass filter is

$$x_4(t) = \mathcal{F}^{-1}\left[X_4(f)\right]$$

$$= \int_{-\frac{B_{IF}}{2}}^{+\frac{B_{IF}}{2}} \frac{1}{2}\left[X_1(f-f_c)+X_1(f+f_c)\right] e^{j2\pi ft}\, df \tag{C-9}$$

The time domain output of the integrate-and-dump circuit, at the sampling instant T_A, is

$$y(T_A) = \int_0^{T_A} X_4(t)\, dt$$

$$= \int_0^{T_A} \left\{ \int_{-\frac{B_{IF}}{2}}^{+\frac{B_{IF}}{2}} \frac{1}{2}\left[X_1(f-f_c) + X_1(f+f_c)\right] e^{j2\pi ft} df \right\} dt$$

$$= \int_{-\frac{B_{IF}}{2}}^{+\frac{B_{IF}}{2}} \left\{ \frac{1}{2}\left[X_1(f-f_c) + X_1(f+f_c)\right] \int_0^{T_A} e^{j2\pi ft} dt \right\} df$$

$$= \int_{-\frac{B_{IF}}{2}}^{+\frac{B_{IF}}{2}} \frac{1}{2}\left[X_1(f-f_c) + X_1(f+f_c)\right] T_A \frac{\sin(\pi f T_A)}{\pi f T_A} e^{+j\pi f T_A} df \tag{C-10}$$

Equation (C-10) can be simplified by expanding the single integral into two integrals and making simple variable substitutions. After making the simplifications which apply when $f_c T_A$ is an integer, the result is

$$y(T_A) = \int_{-f_c-\frac{B_{IF}}{2}}^{-f_c+\frac{B_{IF}}{2}} \frac{1}{2} X_1(f) \frac{T_A \sin(\pi f T_A)}{\pi(f+f_c)T_A} e^{j\pi f T_A} df$$

$$+ \int_{f_c-\frac{B_{IF}}{2}}^{f_c+\frac{B_{IF}}{2}} \frac{1}{2} X_1(f) \frac{T_A \sin(\pi f T_A)}{\pi(f-f_c)T_A} e^{j\pi f T_A} df \tag{C-11}$$

Expressing (C-11) as

$$y(T_A) = \int_{-\infty}^{\infty} X_1(f)\, H'(f)\, e^{+j2\pi f T_A} df \tag{C-12}$$

the desired composite frequency characteristic is readily determined to be

$$H'(f) = \begin{cases} \dfrac{T_A \sin(\pi f T_A)}{2\pi(f+f_c)T_A} e^{-j\pi f T_A} & -f_c - \frac{B_{IF}}{2} \le f \le -f_c + \frac{B_{IF}}{2} \\ \dfrac{T_A \sin(\pi f T_A)}{2\pi(f-f_c)T_A} e^{-j\pi f T_A} & f_c - \frac{B_{IF}}{2} \le f \le f_c + \frac{B_{IF}}{2} \\ 0 & \text{otherwise} \end{cases} \tag{C-13}$$

The power spectral density of the noise at the output of the integrate-and-dump circuit is given by

$$S_{n,out}(f) = \left| H'(f) \right|^2 S_{n,in}(f) \tag{C-14}$$

where $S_{n,in}(f)$ is the power spectral density of the input noise. Substituting (C-13) into (C-14) and using $N_o/2$ as the double-sided power spectral density of the input noise,

$$S_{n,out}(f) = \begin{cases} \dfrac{N_o T_A^2 \sin^2(\pi f T_A)}{8\pi^2 (f+f_c)^2 T_A^2} & -f_c - \frac{B_{IF}}{2} \le f \le -f_c + \frac{B_{IF}}{2} \\ \dfrac{N_o T_A^2 \sin^2(\pi f T_A)}{8\pi^2 (f-f_c)^2 T_A^2} & f_c - \frac{B_{IF}}{2} \le f \le f_c + \frac{B_{IF}}{2} \\ 0 & \text{otherwise} \end{cases} \tag{C-15}$$

The variance of the output noise is given by

$$\begin{aligned} \sigma_n^2 &= E\left\{ \underset{\sim}{n}_o^2(t) \right\} \\ &= \int_{-\infty}^{\infty} S_{n,out}(f)\, df \\ &= \frac{N_o}{8\pi^2} \left[\int_{-f_c - \frac{B_{IF}}{2}}^{-f_c + \frac{B_{IF}}{2}} \frac{\sin^2(\pi f T_A)}{(f+f_c)^2} df + \int_{f_c - \frac{B_{IF}}{2}}^{f_c + \frac{B_{IF}}{2}} \frac{\sin^2(\pi f T_A)}{(f-f_c)^2} df \right] \end{aligned} \tag{C-16}$$

Substituting $x = f + f_c$ into the first integral of the preceding equation and $x = f - f_c$ into the second integral, and then making the simplifications which apply when $f_c T_A$ is an integer, the output noise variance becomes

$$\sigma_n^2 = \frac{N_o}{8\pi^2}\left[\int_{-\frac{B_{IF}}{2}}^{+\frac{B_{IF}}{2}} \frac{\sin^2(\pi x T_A)}{x^2}\,dx + \int_{-\frac{B_{IF}}{2}}^{+\frac{B_{IF}}{2}} \frac{\sin^2(\pi x T_A)}{x^2}\,dx\right]$$

$$= \frac{N_o}{4\pi^2}\int_{-\frac{B_{IF}}{2}}^{+\frac{B_{IF}}{2}} \frac{\sin^2(\pi x T_A)}{x^2}\,dx$$

$$= \frac{N_o}{2\pi^2}\int_{0}^{+\frac{B_{IF}}{2}} \frac{\sin^2(\pi x T_A)}{x^2}\,dx \qquad \text{(C-17)}$$

Substituting $z = \pi x T_A$ allows still another simplification and provides the result in the more familiar form

$$\sigma_n^2 = \frac{N_o T_A}{4}\left[\frac{2}{\pi}\int_{0}^{\frac{\pi B_{IF} T_A}{2}} \frac{\sin^2(z)}{z^2}\,dz\right]$$

$$= \frac{N_o T_A}{4}\,\Psi_{I_1}(o) \qquad \text{(C-18)}$$

where $\Psi_{I_1}(o)$ is defined in Chapter IV for the signal at the output of Channel A.

APPENDIX D

DERIVATION OF ERROR PROBABILITY EXPRESSION FOR IDEAL RECTANGULAR FILTERING

As shown in Chapter IV, the total voltage (at the sampling instant T_A) at the output of Channel A of the bandlimited QPSK system is given by

$$e_{4A}(T_A) = \sum_{m=-\infty}^{\infty} \frac{A_m T_A}{2} \left[\Psi_{I1}(m) - \Psi_{I2}(m) \right] + \sum_{n=-\infty}^{\infty} \frac{B_n T_B}{2} \left(\frac{1}{2\pi f_c T_B} \right) \left[\Psi_{I3}(n) - \Psi_{I4}(n) \right] + \underset{\sim}{n}_{out}(T_A) \tag{D-1}$$

where $\frac{A_o T_A}{2} \Psi_{I_1}(o)$ is the voltage corresponding to the bit under detection (the o^{th} bit) and is reduced in amplitude (due to filtering) by the factor $\Psi_{I_1}(o)$. The $\Psi_{I_1}(m)$ terms for $m \neq 0$ represent intersymbol interference, the $\Psi_{I_2}(m)$ terms result from aliasing, and the $\left[\Psi_{I_3}(n) - \Psi_{I_4}(n)\right]$ terms represent crosstalk from Channel B. An expression for error probability at the output of Channel A will now be derived, using the series expansion method first described by Shimbo and Celebiler [13] and later applied by Tu [9] for bandlimited PSK systems.

Equation (D-1) is first modified slightly by separating the desired $(m = 0)$ signal term from the undesired $(m \neq 0)$ intersymbol interference terms and then normalizing by dividing by $AT_A/2$. The normalized Channel A output voltage is

$$X = \frac{e_{4A}(T_A)}{\frac{AT_A}{2}}$$

$$= z_o \left[\Psi_{I1}(0) - \Psi_{I2}(0)\right]$$

$$+ \sum_{\substack{m=-\infty \\ m \neq 0}}^{\infty} z_m \left[\Psi_{I1}(m) - \Psi_{I2}(m)\right]$$

$$+ \sum_{n=-\infty}^{\infty} z_n \left(\frac{B}{A}\right)\left(\frac{T_B}{T_A}\right)\left(\frac{1}{2\pi f_c T_B}\right)\left[\Psi_{I3}(n) - \Psi_{I4}(n)\right]$$

$$+ \frac{2\,\underset{\sim}{n}_{out}(T_A)}{AT_A} \tag{D-2}$$

where $z_m = \pm 1$ with the same sign as A_m, $z_n = \pm 1$ with the same sign as B_n, and A_m and B_n are as defined by (4-2).

Defining new symbols S_I, S_c, S_n to represent, respectively, the voltages due to intersymbol interference, crosstalk, and noise, (D-2) can be written as

$$X = z_o \left[\Psi_{I1}(0) - \Psi_{I2}(0)\right] + S_I + S_c + S_n \tag{D-3}$$

where

$$S_I = \sum_{\substack{m=-\infty \\ m \neq 0}}^{\infty} z_m \left[\Psi_{I1}(m) - \Psi_{I2}(m)\right] \quad \text{[intersymbol interference]}$$

$$S_c = \left(\frac{B}{A}\right)\left(\frac{T_B}{T_A}\right)\left(\frac{1}{2\pi f_c T_B}\right) \sum_{n=-\infty}^{\infty} z_n \left[\Psi_{I3}(n) - \Psi_{I4}(n)\right] \quad \text{[crosstalk]}$$

and

$$S_n = \frac{2\,\underset{\sim}{n}_{out}(T_A)}{AT_A} \quad \text{[noise]}$$

The normalized output voltage can be further expressed as

$$X = z_o \left[\Psi_{I1}(0) - \Psi_{I2}(0) \right] + S \tag{D-4}$$

where

$$S = S_I + S_c + S_n$$

A detection *error* in Channel A is said to occur if the normalized output voltage X is negative when the input signal is positive ($z_o = +1$) or if X is positive when the input signal is negative ($z_o = -1$). The probability of error is

$$P_e = P(X < 0 \mid z_o = +1)\, P(z_o = +1) + P(X > 0 \mid z_o = -1)\, P(z_o = -1) \tag{D-5}$$

For the binary symmetric channel,

$$P(z_o = +1) = P(z_o = -1) = \frac{1}{2} \tag{D-6}$$

and (D-5) becomes

$$P_e = \frac{1}{2} P(X < 0 \mid z_o = +1) + \frac{1}{2} P(X > 0 \mid z_o = -1) \tag{D-7}$$

From (D-4) it can be observed that $z_o = +1$ means that

$$X = \left[\Psi_{I1}(0) - \Psi_{I2}(0) \right] + S \tag{D-8}$$

and that $z_o = -1$ means that

$$X = -\left[\Psi_{I1}(0) - \Psi_{I2}(0) \right] + S \tag{D-9}$$

Then

$$\begin{aligned} P(X < 0 \mid z_o = +1) &= P\left\{ \left[\Psi_{I1}(0) - \Psi_{I2}(0) \right] + S < 0 \right\} \\ &= P\left\{ S < -\left[\Psi_{I1}(0) - \Psi_{I2}(0) \right] \right\} \end{aligned} \tag{D-10}$$

and

$$P(x>0\,|\,z_0=-1) = P\left\{-[\Psi_{I1}(0)-\Psi_{I2}(0)] + S > 0\right\}$$

$$= P\left\{S > [\Psi_{I1}(0)-\Psi_{I2}(0)]\right\} \qquad \text{(D-11)}$$

Substituting (D-10) and (D-11) into (D-7) yields

$$P_e = \frac{1}{2}\left\{P\left\{S < -[\Psi_{I1}(0)-\Psi_{I2}(0)]\right\} + P\left\{S > [\Psi_{I1}(0)-\Psi_{I2}(0)]\right\}\right\}$$

$$= \frac{1}{2}\left\{1 - P\left\{-[\Psi_{I1}(0)-\Psi_{I2}(0)] < S < [\Psi_{I1}(0)-\Psi_{I2}(0)]\right\}\right\}$$

$$= \frac{1}{2}[1-Q_e] \qquad \text{(D-12)}$$

where

$$Q_e = P\left\{-[\Psi_{I1}(0)-\Psi_{I2}(0)] < S < [\Psi_{I1}(0)-\Psi_{I2}(0)]\right\}$$

Q_e can be expressed in terms of the characteristic function of S using the relationship [19]

$$Q_e = \int_{-\infty}^{\infty} \frac{e^{j[\Psi_{I1}(0)-\Psi_{I2}(0)]\omega} - e^{-j[\Psi_{I1}(0)-\Psi_{I2}(0)]\omega}}{j2\pi\omega}\,\Phi_s(\omega)\,d\omega \qquad \text{(D-13)}$$

where $\Phi_s(\omega)$ is the characteristic function of S. If an expression for $\Phi_s(\omega)$ can be determined and if the above integration can be performed, then the desired result will be obtained. It is first recalled that S is the sum of the random variables S_I, S_c, and S_n. S_I, in turn, is the sum of the random variables

$$S_{Im} = z_m[\Psi_{I1}(m) - \Psi_{I2}(m)] \quad , \quad m \neq 0 \qquad \text{(D-14)}$$

and S_c is the sum of the random variables

$$S_{cn} = \left(\frac{B}{A}\right)\left(\frac{T_B}{T_A}\right)\left(\frac{1}{2\pi f_c T_B}\right) z_n \left[\Psi_{I3}(n) - \Psi_{I4}(n)\right] \qquad \text{(D-15)}$$

If it is assumed that the bit pattern (z_m's) in Channel A is completely random, then the S_{I_m} will all be statistically independent. Likewise, for a random bit pattern (z_n's) in Channel B, the S_{c_n} are statistically independent. Furthermore, the S_{I_m}, the S_{c_n}, and the S_n will be mutually independent.

Since S_{I_m} can assume only the values $\left[\Psi_{I_1}(m) - \Psi_{I_2}(m)\right]$ or $-\left[\Psi_{I_1}(m) - \Psi_{I_2}(m)\right]$ with equal probability, the probability density function of S_{I_m} is given by

$$p_{S_{Im}}(\alpha) = \frac{1}{2}\delta\left[\alpha + \Psi_{I_1}(m) - \Psi_{I_2}(m)\right] + \frac{1}{2}\delta\left[\alpha - \Psi_{I_1}(m) + \Psi_{I_2}(m)\right] \tag{D-16}$$

The characteristic function of S_{I_m} is given by [19]

$$\begin{aligned} \Phi_{S_{Im}}(\omega) &= \int_{-\infty}^{\infty} p_{S_{Im}}(\alpha)\, e^{j\omega\alpha}\, d\alpha \\ &= \frac{1}{2}\left\{e^{j\omega\left[\Psi_{I_1}(m) - \Psi_{I_2}(m)\right]} + e^{-j\omega\left[\Psi_{I_1}(m) - \Psi_{I_2}(m)\right]}\right\} \\ &= \cos\left\{\left[\Psi_{I_1}(m) - \Psi_{I_2}(m)\right]\omega\right\} \end{aligned} \tag{D-17}$$

The characteristic function of S_I (the sum of all S_{I_m} for $m \neq 0$) is given by the product of the individual characteristic functions of the S_{I_m}.

$$\Phi_{S_I}(\omega) = \prod_{\substack{m=-\infty \\ m \neq 0}}^{\infty} \cos\left\{\left[\Psi_{I_1}(m) - \Psi_{I_2}(m)\right]\omega\right\} \tag{D-18}$$

Likewise, the probability density function of the S_{c_n} is

$$p_{S_{cn}}(\alpha) = \frac{1}{2}\,\delta\left\{\alpha + \left(\frac{B}{A}\right)\left(\frac{T_B}{T_A}\right)\left(\frac{1}{2\pi f_c T_B}\right)\left[\Psi_{I3}(n) - \Psi_{I4}(n)\right]\right\}$$
$$+ \frac{1}{2}\left\{\delta\ \ \alpha - \left(\frac{B}{A}\right)\left(\frac{T_B}{T_A}\right)\left(\frac{1}{2\pi f_c T_B}\right)\left[\Psi_{I3}(n) - \Psi_{I4}(n)\right]\right\} \tag{D-19}$$

The characteristic function of S_{cn} is

$$\Phi_{S_{cn}}(\omega) = \int_{-\infty}^{\infty} p_{S_{cn}}(\alpha)\, e^{j\omega\alpha}\, d\alpha$$
$$= \cos\left\{\left(\frac{B}{A}\right)\left(\frac{T_B}{T_A}\right)\left(\frac{1}{2\pi f_c T_B}\right)\left[\Psi_{I3}(n) - \Psi_{I4}(n)\right]\right\} \tag{D-20}$$

and the characteristic function of S_c is

$$\Phi_{S_c}(\omega) = \prod_{n=-\infty}^{\infty} \cos\left\{\left(\frac{B}{A}\right)\left(\frac{T_B}{T_A}\right)\left(\frac{1}{2\pi f_c T_B}\right)\left[\Psi_{I3}(n) - \Psi_{I4}(n)\right]\right\} \tag{D-21}$$

The probability density of the Gaussian noise term S_n is

$$p_{S_n}(\alpha) = \frac{1}{\sqrt{2\pi}\,\sigma}\, e^{-\frac{\alpha^2}{2\sigma^2}} \tag{D-22}$$

where σ^2 is the variance of the normalized output noise. The variance for the (unnormalized) output noise $\underset{\sim}{n}_{out}(T_A)$ was shown in Appendix C to be

$$\sigma_n^2 = \frac{N_o T_A}{4}\,\Psi_{I1}(0) \tag{D-23}$$

Since the normalization factor is $2/AT_A$, the variance for the normalized output noise is

$$\sigma^2 = \left(\frac{2}{AT_A}\right)^2 \frac{N_o T_A}{4}\,\Psi_{I1}(0)$$
$$= \frac{N_o}{A^2 T_A}\,\Psi_{I1}(0) \tag{D-24}$$

The characteristic function of S_n is [20]

$$\Phi_{S_n}(\omega) = e^{-\frac{\omega^2\sigma^2}{2}} \tag{D-25}$$

The characteristic function of S can now be written as the product of the characteristic functions of S_I, S_C, and S_n.

$$\begin{aligned}\Phi_S(\omega) &= \Phi_{S_I}(\omega)\,\Phi_{S_C}(\omega)\,\Phi_{S_n}(\omega)\\ &= \left\{\prod_{\substack{m=-\infty\\ m\neq 0}}^{\infty} \Phi_{S_{Im}}(\omega)\right\}\left\{\prod_{n=-\infty}^{\infty} \Phi_{S_{Cn}}(\omega)\right\}\left\{\Phi_{S_n}(\omega)\right\}\\ &= \left\{\prod_{\substack{m=-\infty\\ m\neq 0}}^{\infty} \cos\left\{[\Psi_{I1}(m)-\Psi_{I2}(m)]\omega\right\}\right\}\left\{\prod_{n=-\infty}^{\infty} \cos\left\{\omega\left(\frac{B}{A}\right)\left(\frac{T_B}{T_A}\right)\left(\frac{1}{2\pi f_c T_B}\right)[\Psi_{I3}(n)-\Psi_{I4}(n)]\right\}\right\}\\ &\quad \cdot e^{-\frac{\omega^2\sigma^2}{2}}\end{aligned} \tag{D-26}$$

Equation (D-26) is not in an integrable form, so some modifications must be made in order to be able to evaluate the expression for Q_e given by (D-13). The first modification is to replace the expression for $\Phi_{S_I}(\omega)$ by a power series in ω.

$$\prod_{\substack{m=-\infty\\ m\neq 0}}^{\infty} \cos\left\{[\Psi_{I1}(m)-\Psi_{I2}(m)]\omega\right\} = 1 + \sum_{i=1}^{\infty} b_{2i}\,\omega^{2i} \tag{D-27}$$

The expression for $\Phi_{S_C}(\omega)$ can likewise be replaced by a power series in ω.

$$\prod_{n=-\infty}^{\infty} \cos\left\{\left(\frac{B}{A}\right)\left(\frac{T_B}{T_A}\right)\left(\frac{1}{2\pi f_c T_B}\right)[\Psi_{I3}(n)-\Psi_{I4}(n)]\omega\right\} = 1 + \sum_{k=1}^{\infty} h_{2k}\,\omega^{2k} \tag{D-28}$$

The characteristic function of S is now given by

$$\Phi_s(\omega) = \left(1 + \sum_{i=1}^{\infty} b_{2i}\omega^{2i}\right)\left(1 + \sum_{k=1}^{\infty} h_{2k}\omega^{2k}\right) e^{-\frac{\omega^2\sigma^2}{2}}$$

$$= e^{-\frac{\omega^2\sigma^2}{2}}\left(1 + \sum_{i=1}^{\infty} b_{2i}\omega^{2i} + \sum_{k=1}^{\infty} h_{2k}\omega^{2k} + \sum_{i=1}^{\infty} b_{2i}\omega^{2i} \sum_{k=1}^{\infty} h_{2k}\omega^{2k}\right) \quad \text{(D-29)}$$

Substitution of (D-29) into (D-13) yields

$$Q_e = \int_{-\infty}^{\infty} \frac{e^{j[\Psi_{I1}(0)-\Psi_{I2}(0)]\omega} - e^{-j[\Psi_{I1}(0)-\Psi_{I2}(0)]\omega}}{j2\pi\omega} e^{-\frac{\omega^2\sigma^2}{2}} d\omega$$

$$+ \int_{-\infty}^{\infty} \frac{e^{j[\Psi_{I1}(0)-\Psi_{I2}(0)]\omega} - e^{-j[\Psi_{I1}(0)-\Psi_{I2}(0)]\omega}}{j2\pi\omega} \cdot \left(\sum_{i=1}^{\infty} b_{2i}\omega^{2i}\right) e^{-\frac{\omega^2\sigma^2}{2}} d\omega$$

$$+ \int_{-\infty}^{\infty} \frac{e^{j[\Psi_{I1}(0)-\Psi_{I2}(0)]\omega} - e^{-j[\Psi_{I1}(0)-\Psi_{I2}(0)]\omega}}{j2\pi\omega} \cdot \left(\sum_{k=1}^{\infty} h_{2k}\omega^{2k}\right) e^{-\frac{\omega^2\sigma^2}{2}} d\omega$$

$$+ \int_{-\infty}^{\infty} \frac{e^{j[\Psi_{I1}(0)-\Psi_{I2}(0)]\omega} - e^{-j[\Psi_{I1}(0)-\Psi_{I2}(0)]\omega}}{j2\pi\omega} \cdot \left(\sum_{i=1}^{\infty} b_{2i}\omega^{2i} \sum_{k=1}^{\infty} h_{2k}\omega^{2k}\right) e^{-\frac{\omega^2\sigma^2}{2}} d\omega$$

$$= Q_{e1} + Q_{e2} + Q_{e3} + Q_{e4} \quad \text{(D-30)}$$

EVALUATION OF Q_{e_1}

Since $e^{\frac{-\omega^2\sigma^2}{2}}$ is the characteristic function of the normalized noise, the first term of (D-30) is the probability that the normalized output noise assumes a value between $+\left[\Psi_{I_1}(o) - \Psi_{I_2}(o)\right]$ and $-\left[\Psi_{I_1}(o) - \Psi_{I_2}(o)\right]$. This probability can alternately be expressed in terms of the probability density function of the normalized output noise [19].

$$Q_{e_1} = \int_{-\infty}^{\infty} \frac{e^{j[\Psi_{I_1}(o)-\Psi_{I_2}(o)]\omega} - e^{-j[\Psi_{I_1}(o)-\Psi_{I_2}(o)]\omega}}{j2\pi\omega} e^{-\frac{\omega^2\sigma^2}{2}} = \int_{-[\Psi_{I_1}(o)-\Psi_{I_2}(o)]}^{+[\Psi_{I_1}(o)-\Psi_{I_2}(o)]} \frac{1}{\sqrt{2\pi}\,\sigma} e^{-\frac{x^2}{2\sigma^2}} dx \qquad \text{(D-31)}$$

Substituting $t^2 = x^2/2\sigma^2$ and simplifying, the above expression becomes

$$Q_{e_1} = \frac{2}{\sqrt{\pi}} \int_0^{\frac{\Psi_{I_1}(o)-\Psi_{I_2}(o)}{\sqrt{2}\,\sigma}} e^{-t^2} dt$$

$$= \operatorname{erf}\left[\frac{\Psi_{I_1}(o) - \Psi_{I_2}(o)}{\sqrt{2}\,\sigma}\right]$$

$$= \operatorname{erf}\sqrt{\frac{[\Psi_{I_1}(o) - \Psi_{I_2}(o)]^2}{2\sigma^2}}$$

$$= \operatorname{erf}\sqrt{\left(\frac{\frac{A^2 T_A}{2}}{N_0}\right)\frac{[\Psi_{I_1}(o) - \Psi_{I_2}(o)]^2}{\Psi_{I_1}(o)}} \qquad \text{(D-32)}$$

EVALUATION OF Q_{e_2}

Interchanging the order of integration and summation allows the second term of (D-30) to be expressed as

$$Q_{e_2} = \sum_{i=1}^{\infty} b_{2i} \left\{ \int_{-\infty}^{\infty} \frac{e^{j[\Psi_{I1}(0)-\Psi_{I2}(0)]\omega}}{j2\pi\omega} \omega^{2i} e^{-\frac{\omega^2\sigma^2}{2}} d\omega - \int_{-\infty}^{\infty} \frac{e^{-j[\Psi_{I1}(0)-\Psi_{I2}(0)]\omega}}{j2\pi\omega} \omega^{2i} e^{-\frac{\omega^2\sigma^2}{2}} d\omega \right\} \tag{D-33}$$

Substituting $x = -\omega$ only in the first integral of (D-33), interchanging limits, and then substituting $\omega = x$ yields

$$Q_{e_2} = \sum_{i=1}^{\infty} b_{2i} \int_{-\infty}^{\infty} \frac{-2e^{-j[\Psi_{I1}(0)-\Psi_{I2}(0)]\omega}}{j2\pi\omega} \omega^{2i} e^{-\frac{\omega^2\sigma^2}{2}} d\omega$$

$$= \sum_{i=1}^{\infty} 2b_{2i}(-1)^{i} \frac{1}{2\pi}\int_{-\infty}^{\infty} e^{-\frac{\omega^2\sigma^2}{2}} (-j\omega)^{2i-1} e^{-j[\Psi_{I1}(0)-\Psi_{I2}(0)]\omega} d\omega \tag{D-34}$$

As shown in [20] the Gaussian probability density function results from the integration of the Gaussian characteristic, *i.e.*,

$$\frac{1}{2\pi}\int_{-\infty}^{\infty} e^{-\frac{\omega^2\sigma^2}{2}} e^{-j[\Psi_{I1}(0)-\Psi_{I2}(0)]\omega} d\omega = \frac{1}{\sqrt{2\pi}\,\sigma} e^{-\frac{[\Psi_{I1}(0)-\Psi_{I2}(0)]^2}{2\sigma^2}} \tag{D-35}$$

The integration indicated in (D-34) is similar to the above, but has the factor $(-j\omega)^{2i-1}$. Since multiplication of the characteristic function by $(-j\omega)$ results in differentation of the probability density function (D-34) can be written as

$$Q_{e_2} = \sum_{i=1}^{\infty} 2b_{2i}(-1)^{i} \left\{ \frac{d^{2i-1}}{d[\Psi_{I1}(0)-\Psi_{I2}(0)]^{2i-1}} \left[\frac{1}{\sqrt{2\pi}\,\sigma} e^{-\frac{[\Psi_{I1}(0)-\Psi_{I2}(0)]^2}{2\sigma^2}} \right] \right\}$$

$$= \sum_{i=1}^{\infty} 2 b_{2i} (-1)^{i} G_{2i-1} \tag{D-36}$$

The G_{2i-1} in this equation can be evaluated by means of a recursive relationship, as summarized below.

$$G_0 = \frac{1}{\sqrt{2\pi}\,\sigma} e^{-\frac{[\Psi_{I1}(0)-\Psi_{I2}(0)]^2}{2\sigma^2}}$$

$$G_1 = \frac{d}{d[\Psi_1(0)-\Psi_2(0)]}[G_0] = -\frac{[\Psi_{I1}(0)-\Psi_{I2}(0)]}{\sigma^2} G_0$$

$$G_2 = \frac{d}{d[\Psi_1(0)-\Psi_2(0)]}[G_1] = -\frac{[\Psi_{I1}(0)-\Psi_{I2}(0)]}{\sigma^2} G_1 - \frac{1}{\sigma^2} G_0$$

$$G_3 = \frac{d}{d[\Psi_{I1}(0)-\Psi_{I2}(0)]}[G_2] = -\frac{[\Psi_{I1}(0)-\Psi_{I2}(0)]}{\sigma^2} G_2 - \frac{2}{\sigma^2} G_1$$

$$\vdots$$

$$G_{2i-1} = -\frac{[\Psi_{I1}(0)-\Psi_{I2}(0)]}{\sigma^2} G_{2i-2} - \frac{2i-2}{\sigma^2} G_{2i-3} \tag{D-37}$$

Evaluation of the b_{2i} in (D-36) is somewhat more involved. First recall from (D-26) and (D-27) that

$$\Phi_{SI}(\omega) = \prod_{\substack{m=-\infty \\ m\neq 0}}^{\infty} \cos\left\{[\Psi_{I1}(0)-\Psi_{I2}(0)]\omega\right\} = 1 + \sum_{i=1}^{\infty} b_{2i}\,\omega^{2i} \tag{D-38}$$

Differentiating the infinite product of (D-38) with respect to ω yields

$$\begin{aligned} \Phi_{SI}'(\omega) &= \cdots + \cos\left\{\left\{[\Psi_{I1}(-1)-\Psi_{I2}(-1)]\omega\right\}\right\}' \frac{\Phi_{SI}(\omega)}{\cos\left\{[\Psi_{I1}(-1)-\Psi_{I2}(-1)]\omega\right\}} \\ &\quad + \cos\left\{\left\{[\Psi_{I1}(+1)-\Psi_{I2}(+1)]\omega\right\}\right\}' \frac{\Phi_{SI}(\omega)}{\cos\left\{[\Psi_{I1}(+1)-\Psi_{I2}(+1)]\omega\right\}} + \cdots \\ &= \cdots - [\Psi_{I1}(-1)-\Psi_{I2}(-1)] \tan\left\{[\Psi_{I1}(-1)-\Psi_{I2}(-1)]\omega\right\} \Phi_{SI}(\omega) \end{aligned}$$

$$- \left[\Psi_{I1}(+1) - \Psi_{I2}(+1)\right] \tan\left\{ \left[\Psi_{I1}(+1) - \Psi_{I2}(+1)\right]\omega \right\} \Phi_{S_I}(\omega) - \cdots$$

$$= - \Phi_{S_I}(\omega) \sum_{\substack{m=-\infty \\ m \neq 0}}^{\infty} \left[\Psi_{I1}(m) - \Psi_{I2}(m)\right] \tan\left[\Psi_{I1}(m) - \Psi_{I2}(m)\right]\omega \tag{D-39}$$

The power series expansion for tan z given by [21] will now be used. Thus

$$\tan z = z + \frac{z^3}{3} + \frac{2z^5}{15} + \cdots + \frac{(-1)^{\ell-1} 2^{2\ell}(2^{2\ell}-1) B_{2\ell}}{(2\ell)!} z^{2\ell-1} + \cdots \tag{D-40}$$

where

$$B_{2\ell} = \frac{(-1)^{\ell-1} 2 (2\ell)!}{(2\pi)^{2\ell}} \sum_{k=1}^{\infty} \frac{1}{k^{2\ell}}$$

Equation (D-39) becomes

$$\Phi_{S_I}'(\omega) = - \Phi_{S_I}(\omega) \sum_{\substack{m=-\infty \\ m \neq 0}}^{\infty} \left[\Psi_{I1}(m) - \Psi_{I2}(m)\right] \left\{ \sum_{\ell=1}^{\infty} \frac{(-1)^{\ell-1} 2^{2\ell}(2^{2\ell}-1)}{(2\ell)!} \cdot B_{2\ell} \left\{ \left[\Psi_{I1}(m) - \Psi_{I2}(m)\right]\omega \right\}^{2\ell-1} \right\}$$

$$= - \Phi_{S_I}(\omega) \sum_{\ell=1}^{\infty} \frac{(-1)^{\ell-1} 2^{2\ell}(2^{2\ell}-1)}{(2\ell)!} B_{2\ell}\, \omega^{2\ell-1} \sum_{\substack{m=-\infty \\ m \neq 0}}^{\infty} \left[\Psi_{I1}(m) - \Psi_{I2}(m)\right]^{2\ell}$$

$$= - \Phi_{S_I}(\omega) \sum_{\ell=1}^{\infty} d_{2\ell-1}\, \omega^{2\ell-1} \tag{D-41}$$

where

$$d_{2\ell-1} = \frac{(-1)^{\ell-1} 2^{2\ell}(2^{2\ell}-1)}{(2\ell)!} B_{2\ell} \sum_{\substack{m=-\infty \\ m \neq 0}}^{\infty} \left[\Psi_{I1}(m) - \Psi_{I2}(m)\right]^{2\ell}$$

An alternate expression for $\Phi_{S_I}'(\omega)$ can be obtained by differentiating the summation of (D-38).

$$\Phi_{SI}'(\omega) = \sum_{i=1}^{\infty} 2i\, b_{2i}\, \omega^{2i-1} \tag{D-42}$$

Setting (D-41) and (D-42) equal to each other now allows a solution for the b_{2i}.

$$\begin{aligned}
\sum_{i=1}^{\infty} 2i\, b_{2i}\, \omega^{2i-1} &= -\Phi_{SI}(\omega) \sum_{l=1}^{\infty} d_{2l-1}\, \omega^{2l-1} \\
&= -\left(1 + \sum_{i=1}^{\infty} b_{2i}\omega^{2i}\right) \sum_{l=1}^{\infty} d_{2l-1}\, \omega^{2l-1} \\
&= -\left[\sum_{l=1}^{\infty} d_{2l-1}\, \omega^{2l-1} + \left(\sum_{i=1}^{\infty} b_{2i}\omega^{2i}\right)\left(\sum_{l=1}^{\infty} d_{2l-1}\omega^{2l-1}\right)\right]
\end{aligned} \tag{D-43}$$

Equating coefficients of the powers of ω allows the following recursive relationship to be obtained.

$$\begin{aligned}
b_0 &= 1 \\
b_2 &= -\tfrac{1}{2} d_1 \\
b_4 &= -\tfrac{1}{4}(d_3 + b_2 d_1) \\
b_6 &= -\tfrac{1}{6}(d_5 + b_4 d_1 + b_2 d_3) \\
&\;\;\vdots \\
b_{2i} &= -\tfrac{1}{2i}\left[d_{2i-1} + \sum_{l=1}^{i-1} b_{2i-2l}\, d_{2l-1}\right]
\end{aligned} \tag{D-44}$$

EVALUATION OF Q_{e_3}

Referring back to (D-30), it can be observed that the term Q_{e_3} has exactly the same form as the term Q_{e_2}, with $\sum_{i=1}^{\infty} b_{2i}\omega^{2i}$ replaced by $\sum_{k=1}^{\infty} h_{2k}\omega^{2k}$. Evaluation of Q_{e_3} is therefore performed in the same manner as Q_{e_2}. The result is

$$Q_{e3} = \sum_{k=1}^{\infty} 2h_{2k}(-1)^k \left\{ \frac{d^{2k-1}}{d[\Psi_{I1}(0)-\Psi_{I2}(0)]^{2k-1}} \left[\frac{1}{\sqrt{2\pi}\,\sigma} e^{-\frac{[\Psi_{I1}(0)-\Psi_{I2}(0)]^2}{2\sigma^2}} \right] \right\}$$

$$= \sum_{k=1}^{\infty} 2h_{2k}(-1)^k G_{2k-1} \qquad \text{(D-45)}$$

The G_{2k-1} in (D-45) can be evaluated by means of the recursive relationship given by (D-37).

Evaluation of the h_{2k} is similar to that for the b_{2n}. From (D-26) and (D-28), it can be seen that

$$\Phi_{sc}(\omega) = \prod_{n=-\infty}^{\infty} \cos\left\{ \left(\frac{B}{A}\right)\left(\frac{T_B}{T_A}\right)\left(\frac{1}{2\pi f_c T_B}\right)[\Psi_{I3}(n)-\Psi_{I4}(n)]\omega \right\}$$

$$= 1 + \sum_{k=1}^{\infty} h_{2k}\,\omega^{2k} \qquad \text{(D-46)}$$

Differentiating the infinite product of (D-46) with respect to ω yields

$$\Phi_{sc}'(\omega) = -\Phi_{sc}(\omega) \sum_{n=-\infty}^{\infty} \left(\frac{B}{A}\right)\left(\frac{T_B}{T_A}\right)\left(\frac{1}{2\pi f_c T_B}\right)[\Psi_{I3}(n)-\Psi_{I4}(n)]$$

$$\cdot \tan\left\{ \left(\frac{B}{A}\right)\left(\frac{T_B}{T_A}\right)\left(\frac{1}{2\pi f_c T_B}\right)[\Psi_{I3}(n)-\Psi_{I4}(n)]\omega \right\} \qquad \text{(D-47)}$$

Substituting the power series expansion given by (D-40) for $\tan z$ into (D-47) yields

$$\Phi'_{S_c}(\omega) = -\Phi_{S_c}(\omega)\sum_{n=-\infty}^{\infty}\left(\frac{B}{A}\right)\left(\frac{T_B}{T_A}\right)\left(\frac{1}{2\pi f_c T_B}\right)\left[\Psi_{I3}(n)-\Psi_{I4}(n)\right]$$

$$\cdot\left\{\sum_{\ell=1}^{\infty}\frac{(-1)^{\ell-1}2^{2\ell}(2^{2\ell}-1)}{(2\ell)!}B_{2\ell}\left\{\left(\frac{B}{A}\right)\left(\frac{T_B}{T_A}\right)\left(\frac{1}{2\pi f_c T_B}\right)\right.\right.$$

$$\left.\left.\cdot\left[\Psi_{I3}(n)-\Psi_{I4}(n)\right]\omega\right\}^{2\ell-1}\right\}$$

$$= -\Phi_{S_c}(\omega)\sum_{\ell=1}^{\infty}\frac{(-1)^{\ell-1}2^{2\ell}(2^{2\ell}-1)}{(2\ell)!}B_{2\ell}\left\{\sum_{n=-\infty}^{\infty}\left\{\left(\frac{B}{A}\right)\left(\frac{T_B}{T_A}\right)\left(\frac{1}{2\pi f_c T_B}\right)\left[\Psi_{I3}(n)-\Psi_{I4}(n)\right]\right\}^{2\ell}\right\}\omega^{2\ell-1}$$

$$= -\Phi_{S_c}(\omega)\sum_{\ell=1}^{\infty}c_{2\ell-1}\,\omega^{2\ell-1} \tag{D-48}$$

where

$$c_{2\ell-1} = \frac{(-1)^{\ell-1}2^{2\ell}(2^{2\ell}-1)}{(2\ell)!}B_{2\ell}\sum_{n=-\infty}^{\infty}\left\{\left(\frac{B}{A}\right)\left(\frac{T_B}{T_A}\right)\left(\frac{1}{2\pi f_c T_B}\right)\cdot\left[\Psi_{I3}(n)-\Psi_{I4}(n)\right]\right\}^{2\ell} \tag{D-49}$$

Differentiating the summation of (D-46) with respect to ω yields an alternate expression for $\Phi'_{S_c}(\omega)$.

$$\Phi'_{S_c}(\omega) = \sum_{k=1}^{\infty}2k\,h_{2k}\,\omega^{2k-1} \tag{D-50}$$

Setting (D-48) and (D-50) equal to each other, solving for h_{2k}, and equating like powers of ω allows the following recursive relationship to be obtained.

$$h_0 = 1$$

$$h_2 = -\frac{1}{2}c_1$$

$$h_4 = -\frac{1}{4}(c_3 + h_2 c_1)$$

$$h_6 = -\frac{1}{6}\left(c_5 + h_4 c_1 + h_2 c_3\right)$$

$$\vdots$$

$$h_{2k} = -\frac{1}{2k}\left[c_{2k-1} + \sum_{\ell=1}^{k-1} h_{2k-2\ell}\, c_{2\ell-1}\right] \qquad \text{(D-51)}$$

EVALUATION OF Q_{e_4}

Referring back to (D-30) it can be observed that the term Q_{e_4} has the same form as the term Q_{e_2}, if $\sum_{i=1}^{\infty} b_{2i}\omega^{2i}$ is replaced by $\sum_{i=1}^{\infty} b_{2i}\omega^{2i} \sum_{k=1}^{\infty} h_{2k}\omega^{2k}$. Evaluating Q_{e_4} in the same manner as Q_{e_2} yields

$$Q_{e4} = \sum_{i=1}^{\infty} \sum_{k=1}^{\infty} 2\, b_{2i}\, h_{2k}\, (-1)^{i+k}\, G_{2i+2k-1} \tag{D-52}$$

The $G_{2i+2k-1}$ in (D-52) can be evaluated by means of the recursive relationship given by (D-37), and the b_{2i} and h_{2k} are exactly as defined earlier in the evaluation of terms Q_{e_2} and Q_{e_3}, respectively.

APPENDIX E

EVALUATION OF SINGLE-POLE BANDPASS FILTER RESPONSE TO QPSK SIGNAL

Chapter IV shows that if the QPSK signal

$$s(t) = \sum_{m=-\infty}^{\infty} a_m(t)\cos(\omega_c t) + \sum_{n=-\infty}^{\infty} b_n(t)\sin(\omega_c t) \tag{E-1}$$

is applied to the input of the single-pole bandpass filter and if an integral number of cycles of the carrier frequency f_c occurs in each bit period T_A of Channel A, the time domain response of the filter to the m^{th} bit of Channel A is

$$s_{1A}(t) = \int_{-\infty}^{0} \frac{A_m f \sin(\pi f T_A)}{\pi(f^2 - f_c^2)} e^{-j\pi f(1+2m)T_A} \left\{ \frac{1}{1+\left[\frac{2(f+f_c)}{B_{IF}}\right]^2} - j\frac{2\left(\frac{f+f_c}{B_{IF}}\right)}{1+\left[\frac{2(f+f_c)}{B_{IF}}\right]^2} \right\} e^{+j2\pi ft}\, df$$

$$+ \int_{0}^{\infty} \frac{A_m f \sin(\pi f T_A)}{\pi(f^2 - f_c^2)} e^{-j\pi f(1+2m)T_A} \left\{ \frac{1}{1+\left[\frac{2(f-f_c)}{B_{IF}}\right]^2} - j\frac{2\left(\frac{f-f_c}{B_{IF}}\right)}{1+\left[\frac{2(f-f_c)}{B_{IF}}\right]^2} \right\} e^{+j2\pi ft}\, df$$

$$= T_1 + T_2 \tag{E-2}$$

The limits of integration for the two terms of (E-2) can be made equal by substituting $f' = -f$ for the first term. Thus

$$T_1 = \frac{A_m}{\pi}\int_{+\infty}^{0} \frac{(-f')\sin(-\pi f' T_A)\, e^{-j2\pi f'\left[t-\left(\frac{1+2m}{2}\right)T_A\right]}}{\left[(-f')^2 - f_c^2\right]\left\{1+\left[\frac{2(-f'+f_c)}{B_{IF}}\right]^2\right\}}(-df')$$

$$-j\frac{2A_m}{\pi B_{IF}}\int_{+\infty}^{0}\frac{(-f')(-f'+f_c)\sin(-\pi f'T_A)\,e^{-j2\pi f'[t-(\frac{1+2m}{2})T_A]}}{[(-f')^2-f_c^2]\left\{1+\left[\frac{2(-f'+f_c)}{B_{IF}}\right]^2\right\}}(-df')$$

$$=\frac{A_m}{\pi}\int_{0}^{\infty}\frac{f'\sin(\pi f'T_A)\,e^{-j2\pi f'[t-(\frac{1+2m}{2})T_A]}}{[(f')^2-f_c^2]\left\{1+\left[2\left(\frac{f'-f_c}{B_{IF}}\right)\right]^2\right\}}df'$$

$$+j\frac{2A_m}{\pi B_{IF}}\int_{0}^{\infty}\frac{f'(f'-f_c)\sin(\pi f'T_A)\,e^{-j2\pi f'[t-(\frac{1+2m}{2})T_A]}}{[(f')^2-f_c^2]\left\{1+\left[2\left(\frac{f-f_c}{B_{IF}}\right)\right]^2\right\}}df' \qquad \text{(E-3)}$$

Letting $f = f'$ in (E-3) and substituting the result into (E-2) yields

$$S_{1A}(t)=\frac{A_m}{\pi}\int_{0}^{\infty}\frac{f\sin(\pi fT_A)\,e^{-j2\pi f[t-(\frac{1+2m}{2})T_A]}}{(f^2-f_c^2)\left\{1+\left[2\left(\frac{f-f_c}{B_{IF}}\right)\right]^2\right\}}df$$

$$+j\frac{2A_m}{\pi B_{IF}}\int_{0}^{\infty}\frac{f(f-f_c)\sin(\pi fT_A)\,e^{-j2\pi f[t-(\frac{1+2m}{2})T_A]}}{(f^2-f_c^2)\left\{1+\left[2\left(\frac{f-f_c}{B_{IF}}\right)\right]^2\right\}}df$$

$$+\frac{A_m}{\pi}\int_{0}^{\infty}\frac{f\sin(\pi fT_A)\,e^{+j2\pi f[t-(\frac{1+2m}{2})T_A]}}{(f^2-f_c^2)\left\{1+\left[2\left(\frac{f-f_c}{B_{IF}}\right)\right]^2\right\}}df$$

$$-j\frac{2A_m}{\pi B_{IF}}\int_{0}^{\infty}\frac{f(f-f_c)\sin(\pi fT_A)\,e^{+j2\pi f[t-(\frac{1+2m}{2})T_A]}}{(f^2-f_c^2)\left\{1+\left[2\left(\frac{f-f_c}{B_{IF}}\right)\right]^2\right\}}df$$

$$=\frac{A_m}{\pi}\int_{0}^{\infty}\frac{f\sin(\pi fT_A)\left\{e^{+j2\pi f[t-(\frac{1+2m}{2})T_A]}+e^{-j2\pi f[t-(\frac{1+2m}{2})T_A]}\right\}}{(f^2-f_c^2)\left\{1+\left[2\left(\frac{f-f_c}{B_{IF}}\right)\right]^2\right\}}df$$

$$-j\frac{2A_m}{\pi B_{IF}}\int_0^{\infty}\frac{f(f-f_c)\sin(\pi f T_A)\left\{e^{+j2\pi f\left[t-\left(\frac{1+2m}{2}\right)T_A\right]}-e^{-j2\pi f\left[t-\left(\frac{1+2m}{2}\right)T_A\right]}\right\}}{(f^2-f_c^2)\left\{1+\left[2\left(\frac{f-f_c}{B_{IF}}\right)\right]^2\right\}}\,df$$

$$=\frac{2A_m}{\pi}\int_0^{\infty}\frac{f\sin(\pi f T_A)\cos\left\{2\pi f\left[t-\left(\frac{1+2m}{2}\right)T_A\right]\right\}}{(f^2-f_c^2)\left\{1+\left[2\left(\frac{f-f_c}{B_{IF}}\right)\right]^2\right\}}\,df$$

$$+\frac{4A_m}{\pi B_{IF}}\int_0^{\infty}\frac{f(f-f_c)\sin(\pi f T_A)\sin\left\{2\pi f\left[t-\left(\frac{1+2m}{2}\right)T_A\right]\right\}}{(f^2-f_c^2)\left\{1+\left[2\left(\frac{f-f_c}{B_{IF}}\right)\right]^2\right\}}\,df \tag{E-4}$$

The above procedure can be repeated to determine a simplified expression for the time domain response of the single-pole filter to the n^{th} bit of Channel B. Chapter IV shows that if f_cT_B is an integer,

$$S_{1B}(t)=\int_{-\infty}^{0}\frac{-jB_nf_c\sin(\pi f T_B)}{\pi(f^2-f_c^2)}e^{-j\pi f(1+2n)T_B}\left\{\frac{1}{1+\left[\frac{2(f+f_c)}{B_{IF}}\right]^2}-j\frac{2\left(\frac{f+f_c}{B_{IF}}\right)}{1+\left[\frac{2(f+f_c)}{B_{IF}}\right]^2}\right\}e^{+j2\pi f t}\,df$$

$$+\int_0^{\infty}\frac{-jB_nf_c\sin(\pi f T_B)}{\pi(f^2-f_c^2)}e^{-j\pi f(1+2n)T_B}\left\{\frac{1}{1+\left[\frac{2(f-f_c)}{B_{IF}}\right]^2}-j\frac{2\left(\frac{f-f_c}{B_{IF}}\right)}{1+\left[\frac{2(f-f_c)}{B_{IF}}\right]^2}\right\}e^{+j2\pi f t}\,df$$

$$=T_3+T_4 \tag{E-5}$$

The limits of integration for the two terms of (E-5) can be made the same by substituting $f' = -f$ for the first term and then interchanging the upper and lower limits. If this is done and if f is then substituted for f' in the resulting expression, (E-5) becomes

$$s_{1B}(t) = \frac{jB_n f_c}{\pi}\int_0^{\infty} \frac{\sin(\pi f T_B)\, e^{-j2\pi f[t-(\frac{1+2n}{2})T_B]}}{(f^2-f_c^2)\{1+[2(\frac{f-f_c}{B_{IF}})]^2\}}\,df$$

$$-\frac{2B_n f_c}{\pi B_{IF}}\int_0^{\infty} \frac{(f-f_c)\sin(\pi f T_B)\, e^{-j2\pi f[t-(\frac{1+2n}{2})T_B]}}{(f^2-f_c^2)\{1+[2(\frac{f-f_c}{B_{IF}})]^2\}}\,df$$

$$-\frac{jB_n f_c}{\pi}\int_0^{\infty} \frac{\sin(\pi f T_B)\, e^{+j2\pi f[t-(\frac{1+2n}{2})T_B]}}{(f^2-f_c^2)\{1+[2(\frac{f-f_c}{B_{IF}})]^2\}}\,df$$

$$-\frac{2B_n f_c}{\pi B_{IF}}\int_0^{\infty} \frac{(f-f_c)\sin(\pi f T_B)\, e^{+j2\pi f[t-(\frac{1+2n}{2})T_B]}}{(f^2-f_c^2)\{1+[2(\frac{f-f_c}{B_{IF}})]^2\}}\,df$$

$$= -\frac{jB_n f_c}{\pi}\int_0^{\infty} \frac{\sin(\pi f T_B)\{e^{+j2\pi f[t-(\frac{1+2n}{2})T_B]} - e^{-j2\pi f[t-(\frac{1+2n}{2})T_B]}\}}{(f^2-f_c^2)\{1+[2(\frac{f-f_c}{B_{IF}})]^2\}}\,df$$

$$-\frac{2B_n f_c}{\pi B_{IF}}\int_0^{\infty} \frac{(f-f_c)\sin(\pi f T_B)\{e^{+j2\pi f[t-(\frac{1+2n}{2})T_B]} + e^{-j2\pi f[t-(\frac{1+2n}{2})T_B]}\}}{(f^2-f_c^2)\{1+[2(\frac{f-f_c}{B_{IF}})^2\}}\,df$$

$$= \frac{2B_n f_c}{\pi}\int_0^{\infty} \frac{\sin(\pi f T_B)\sin\{2\pi f[t-(\frac{1+2n}{2})T_B]\}}{(f^2-f_c^2)\{1+[2(\frac{f-f_c}{B_{IF}})]^2\}}\,df$$

$$-\frac{4B_n f_c}{\pi B_{IF}}\int_0^{\infty} \frac{(f-f_c)\sin(\pi f T_B)\cos\{2\pi f[t-(\frac{1+2n}{2})T_B]\}}{(f^2-f_c^2)\{1+[2(\frac{f-f_c}{B_{IF}})]^2\}}\,df$$

(E-6)

APPENDIX F

EVALUATION OF CHANNEL A NOISE POWER FOR SINGLE-POLE RC FILTERING

Evaluation of the output noise for Channel A of the QPSK receiver is accomplished in much the same manner for practical filtering as for the ideal rectangular filtering case which was treated in Appendix C. A composite frequency response is first obtained for the combination of the bandpass filter with the components of the Channel A detector. Fig. F-1 summarizes the notation to be used for this computation. For an input $X_1(f)$ to the bandpass filter, the filter output can be expressed in the frequency domain as

$$X_2(f) = X_1(f)\,H(f) \tag{F-1}$$

where $H(f)$ is the frequency response of the filter. For single-pole RC filtering, (4-42) shows that the filter frequency response is

$$H(f) = \begin{cases} \dfrac{1}{1+\left[\dfrac{2(f+f_c)}{B_{IF}}\right]^2} - j\,\dfrac{2\left(\dfrac{f+f_c}{B_{IF}}\right)}{1+\left[\dfrac{2(f+f_c)}{B_{IF}}\right]^2} & \text{for } f<0 \\[2ex] \dfrac{1}{1+\left[\dfrac{2(f-f_c)}{B_{IF}}\right]^2} - j\,\dfrac{2\left(\dfrac{f-f_c}{B_{IF}}\right)}{1+\left[\dfrac{2(f-f_c)}{B_{IF}}\right]^2} & \text{for } f>0 \end{cases} \tag{F-2}$$

where $H(f)$ consists of the characteristic of the lowpass equivalent single-pole filter shifted to appear about plus and minus the carrier frequency f_c.

The time domain output of the bandpass filter is given by

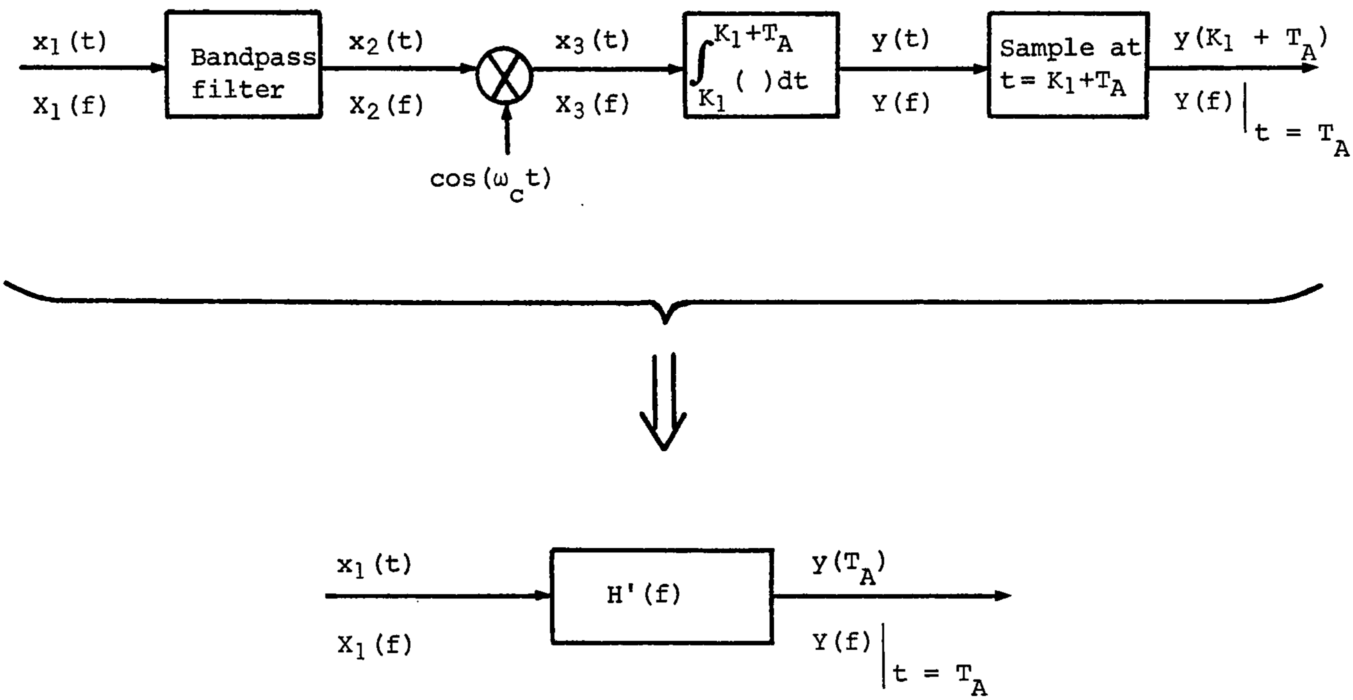

Fig. F.1. - Combination of single-pole filter with Channel A detector components

$$x_2(t) = \mathcal{F}^{-1}\left[X_2(f)\right]$$

$$= \int_{-\infty}^{\infty} X_2(f)\, e^{+j2\pi f t}\, df$$

$$= \int_{-\infty}^{0} \frac{X_1(f)\, e^{+j2\pi f t}}{1+\left[\frac{2(f+f_c)}{B_{IF}}\right]^2}\, df \;-\; j\int_{-\infty}^{0} \frac{X_1(f)\, 2\left(\frac{f+f_c}{B_{IF}}\right) e^{+j2\pi f t}}{1+\left[\frac{2(f+f_c)}{B_{IF}}\right]^2}\, df$$

$$+ \int_{0}^{\infty} \frac{X_1(f)\, e^{+j2\pi f t}}{1+\left[\frac{2(f-f_c)}{B_{IF}}\right]^2}\, df \;-\; j\int_{0}^{\infty} \frac{X_1(f)\, 2\left(\frac{f-f_c}{B_{IF}}\right) e^{+j2\pi f t}}{1+\left[\frac{2(f-f_c)}{B_{IF}}\right]^2}\, df$$

(F-3)

The time domain output of the Channel A multiplier is

$$x_3(t) = x_2(t)\cos(\omega_c t)$$

$$= x_2(t)\left[\frac{e^{+j2\pi f_c t} + e^{-j2\pi f_c t}}{2}\right]$$

$$= \frac{1}{2}\int_{-\infty}^{0} \frac{X_1(f)\left[e^{j2\pi(f+f_c)t} + e^{j2\pi(f-f_c)t}\right]}{1+\left[2\left(\frac{f+f_c}{B_{IF}}\right)\right]^2}\, df$$

$$- \frac{j}{2}\int_{-\infty}^{0} \frac{X_1(f)\, 2\left(\frac{f+f_c}{B_{IF}}\right)\left[e^{j2\pi(f+f_c)t} + e^{j2\pi(f-f_c)t}\right]}{1+\left[2\left(\frac{f+f_c}{B_{IF}}\right)\right]^2}\, df$$

$$+ \frac{1}{2}\int_{0}^{\infty} \frac{X_1(f)\left[e^{j2\pi(f+f_c)t} + e^{j2\pi(f-f_c)t}\right]}{1+\left[2\left(\frac{f-f_c}{B_{IF}}\right)\right]^2}\, df$$

$$- \frac{j}{2} \int_{0}^{\infty} \frac{X_1(f)\, 2\left(\frac{f-f_c}{B_{IF}}\right)\left[e^{j2\pi(f+f_c)t} + e^{j2\pi(f-f_c)t}\right]}{1 + \left[2\left(\frac{f-f_c}{B_{IF}}\right)\right]^2} df \tag{F-4}$$

The time domain output of the integrate-and-dump circuit, at the sampling instant $K_1 + T_A$, is

$$y(K_1 + T_A) = \int_{K_1}^{K_1+T_A} X_3(t)\, dt \tag{F-5}$$

If it is assumed that the input noise is stationary, then the actual limits of integration of (F-5) are not important and any T_A interval could be used for computation of the output noise power. It is convenient to use 0 to T_A as these limits. Therefore

$$y(T_A) = \int_{0}^{T_A} X_3(t)\, dt$$

$$= \frac{1}{2} \int_{-\infty}^{0} \frac{X_1(f)}{1 + \left[2\left(\frac{f+f_c}{B_{IF}}\right)\right]^2} \left\{ \int_{0}^{T_A} \left[e^{j2\pi(f+f_c)t} + e^{j2\pi(f-f_c)t}\right] dt \right\} df$$

$$- \frac{j}{2} \int_{-\infty}^{0} \frac{X_1(f)\, 2\left(\frac{f+f_c}{B_{IF}}\right)}{1 + \left[2\left(\frac{f+f_c}{B_{IF}}\right)\right]^2} \left\{ \int_{0}^{T_A} \left[e^{j2\pi(f+f_c)t} + e^{j2\pi(f-f_c)t}\right] dt \right\} df$$

$$+ \frac{1}{2} \int_{0}^{\infty} \frac{X_1(f)}{1 + \left[\frac{2(f-f_c)}{B_{IF}}\right]^2} \left\{ \int_{0}^{T_A} \left[e^{j2\pi(f+f_c)t} + e^{j2\pi(f-f_c)t}\right] dt \right\} df$$

$$- \frac{j}{2} \int_{0}^{\infty} \frac{X_1(f)\, 2\left(\frac{f-f_c}{B_{IF}}\right)}{1 + \left[\frac{2(f-f_c)}{B_{IF}}\right]^2} \left\{ \int_{0}^{T_A} \left[e^{j2\pi(f+f_c)t} + e^{j2\pi(f-f_c)t}\right] dt \right\} df \tag{F-6}$$

Performing the inner (time domain) integrations in (F-6) and making the simplifications which apply when f_cT_A is an integer, the time domain output of the integrate-and-dump circuit becomes

$$
\begin{aligned}
y(T_A) &= \int_{-\infty}^{0} \frac{X_1(f)\, f \sin(\pi f T_A)\, e^{j\pi f T_A}}{\pi(f^2-f_c^2)\left\{1+\left[2\left(\frac{f+f_c}{B_{IF}}\right)\right]^2\right\}}\, df \\
&\quad - j\int_{-\infty}^{0} \frac{X_1(f)\, f \sin(\pi f T_A)\, 2\left(\frac{f+f_c}{B_{IF}}\right) e^{j\pi f T_A}}{\pi(f^2-f_c^2)\left\{1+\left[2\left(\frac{f+f_c}{B_{IF}}\right)\right]^2\right\}}\, df \\
&\quad + \int_{0}^{\infty} \frac{X_1(f)\, f \sin(\pi f T_A)\, e^{j\pi f T_A}}{\pi(f^2-f_c^2)\left\{1+\left[2\left(\frac{f-f_c}{B_{IF}}\right)\right]^2\right\}}\, df \\
&\quad - j\int_{0}^{\infty} \frac{X_1(f)\, f \sin(\pi f T_A)\, 2\left(\frac{f-f_c}{B_{IF}}\right) e^{j\pi f T_A}}{\pi(f^2-f_c^2)\left\{1+\left[2\left(\frac{f-f_c}{B_{IF}}\right)\right]^2\right\}}\, df \\
&= \int_{-\infty}^{\infty} X_1(f)\, H'(f)\, e^{+j2\pi f T_A}\, df
\end{aligned}
\tag{F-7}
$$

The desired composite frequency response is given by

$$
H'(f) = \begin{cases}
\dfrac{f\sin(\pi f T_A)e^{-j\pi f T_A}}{\pi(f^2-f_c^2)}\left\{\dfrac{1}{1+\left[2\left(\frac{f+f_c}{B_{IF}}\right)\right]^2} - j\,\dfrac{2\left(\frac{f+f_c}{B_{IF}}\right)}{1+\left[2\left(\frac{f+f_c}{B_{IF}}\right)\right]^2}\right\} & \text{for } f<0 \\[2ex]
\dfrac{f\sin(\pi f T_A)e^{-j\pi f T_A}}{\pi(f^2-f_c^2)}\left\{\dfrac{1}{1+\left[2\left(\frac{f-f_c}{B_{IF}}\right)\right]^2} - j\,\dfrac{2\left(\frac{f-f_c}{B_{IF}}\right)}{1+\left[2\left(\frac{f-f_c}{B_{IF}}\right)\right]^2}\right\} & \text{for } f>0
\end{cases}
\tag{F-8}
$$

The magnitude of H'(f) is readily determined by expressing (F-8) in rectangular form and then taking the square root of the sum of the squares of the real and imaginary parts. Squaring this result gives

$$|H'(f)|^2 = \begin{cases} \dfrac{f^2 \sin^2(\pi f T_A)}{\pi^2 (f^2 - f_c^2)^2 \left\{1 + \left[2\left(\frac{f+f_c}{B_{IF}}\right)\right]^2\right\}} & \text{for } f < 0 \\ \\ \dfrac{f^2 \sin^2(\pi f T_A)}{\pi^2 (f^2 - f_c^2)^2 \left\{1 + \left[2\left(\frac{f-f_c}{B_{IF}}\right)\right]^2\right\}} & \text{for } f > 0 \end{cases} \tag{F-9}$$

The power spectral density of the noise at the Channel A output of the QPSK receiver is

$$S_{n,out}(f) = |H'(f)|^2 S_{n,in}(f) \tag{F-10}$$

where $S_{n,in}(f)$ is the power spectral density of the input noise. Substituting (F-9) into (F-10) and using $N_o/2$ as the double-sided power spectral density of the input noise,

$$S_{n,out}(f) = \begin{cases} \dfrac{N_o f^2 \sin^2(\pi f T_A)}{2\pi^2 (f^2 - f_c^2)^2 \left\{1 + \left[2\left(\frac{f+f_c}{B_{IF}}\right)\right]^2\right\}} & \text{for } f < 0 \\ \\ \dfrac{N_o f^2 \sin^2(\pi f T_A)}{2\pi^2 (f^2 - f_c^2)^2 \left\{1 + \left[2\left(\frac{f-f_c}{B_{IF}}\right)\right]^2\right\}} & \text{for } f > 0 \end{cases} \tag{F-11}$$

The variance of the output noise is given by

$$\sigma_n^2 = \int_{-\infty}^{\infty} S_{n,out}(f)\, df$$

$$= \frac{N_0}{2\pi^2} \int_{-\infty}^{0} \frac{f^2 \sin^2(\pi f T_A)}{(f^2 - f_c^2)^2 \left\{1 + \left[2\left(\frac{f+f_c}{B_{IF}}\right)\right]^2\right\}} \, df$$

$$+ \frac{N_0}{2\pi^2} \int_{0}^{\infty} \frac{f^2 \sin^2(\pi f T_A)}{(f^2 - f_c^2)^2 \left\{1 + \left[2\left(\frac{f-f_c}{B_{IF}}\right)\right]^2\right\}} \, df \qquad \text{(F-12)}$$

Equation (F-12) can be simplified somewhat by noting that the two integrands represent a single even function. Thus

$$\sigma_n^2 = \frac{N_0}{\pi^2} \int_{0}^{\infty} \frac{f^2 \sin^2(\pi f T_A)}{(f^2 - f_c^2)^2 \left\{1 + \left[2\left(\frac{f-f_c}{B_{IF}}\right)\right]^2\right\}} \, df \qquad \text{(F-13)}$$

Substituting $z = \pi f T_A$ allows still another simplification and provides the result in a form which is more suitable for numerical evaluation. Thus

$$\sigma_n^2 = \frac{N_0 T_A}{4} \Psi_n \qquad \text{(F-14)}$$

where

$$\Psi_n = \frac{4}{\pi} \int_{0}^{\infty} \frac{z^2 \sin^2(z)}{\left[z^2 - (\pi f_c T_A)^2\right]^2 \left\{1 + \left[\frac{2(z - \pi f_c T_A)}{\pi B_{IF} T_A}\right]^2\right\}} \, dz$$

It is interesting to note that Ψ_n can be obtained from the function $\Psi_{B_1}(m)$ given by (4-56) by letting $m = 0$ and $K_1 = 0$. Thus

$$\Psi_n = \Psi_{B1}(0)\Big|_{K_1 = 0} \qquad \text{(F-15)}$$

This is intuitively satisfying because the corresponding noise variance result given by (C-18) for ideal filtering was expressed in terms of the previously defined function $\Psi_{I_1}(m)$, evaluated for $m = 0$.

As another check on the result given by (F-14), Ψ_n can be evaluated for the limiting case of infinite bandwidth. Thus

$$\lim_{B_{IF}\to\infty} \Psi_n = \frac{4}{\pi}\int_0^\infty \frac{z^2\sin^2(z)}{[z^2-(\pi f_c T_A)^2]^2}\,dz$$

$$= \left(\frac{4}{\pi}\right)\left(\frac{1}{4\pi f_c T_A}\right)\left[\int_0^\infty \frac{z\sin^2(z)}{(z-\pi f_c T_A)^2}\,dz - \int_0^\infty \frac{z\sin^2(z)}{(z+\pi f_c T_A)^2}\,dz\right] \qquad \text{(F-16)}$$

Substituting $y = z - \pi f_c T_A$ into the first integral of (F-16) and $y = z + \pi f_c T_A$ into the second integral, making the simplifications which apply when $f_c T_A$ is an integer, and then combining the results,

$$\lim_{B_{IF}\to\infty} \Psi_n = \frac{1}{\pi^2 f_c T_A}\left[2\pi f_c T_A \int_0^\infty \frac{\sin^2(y)}{y^2}\,dy\right]$$

$$= \frac{2}{\pi}\int_0^\infty \frac{\sin^2(y)}{y^2}\,dy$$

$$= 1 \qquad \text{(F-17)}$$

Substituting (F-17) into (F-14), it can be seen that the output noise power for an infinite IF bandwidth is given by

$$\lim_{B_{IF}\to\infty} \sigma_n^2 = \frac{N_o T_A}{4} \qquad \text{(F-18)}$$

which is the same result as that obtained by letting B_{IF} increase without bound in (C-18) for ideal rectangular filtering.